

**SIMULATIONS OF BORATE ION EXCHANGE AND RADIAL
FLOW FOR REACTOR WATER CLEAN UP SYSTEMS**

By

JIDONG LOU

Bachelor of Engineering

Jiangsu Institute of Chemical Technology


Changzhou, Jiangsu, PRC

1982

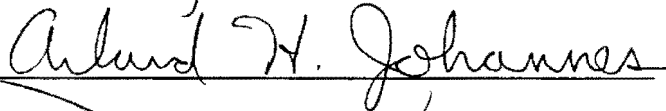
**Submitted to the Faculty of the
Graduate College of the
Oklahoma State University
in partial fulfillment of
the requirements for
the Degree of
MASTER OF SCIENCE
May, 1993**

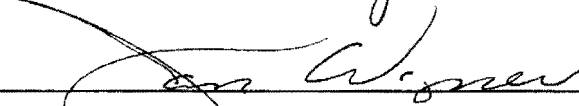
SIMULATIONS OF BORATE ION EXCHANGE AND RADIAL
FLOW FOR REACTOR WATER CLEAN UP SYSTEMS

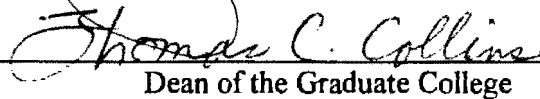
Thesis Approved:



Thesis Adviser







Dean of the Graduate College

PREFACE

Sorption of boric acid solutions and radial flow mixed-bed simulations were studied in this work. Liquid resistance-controlled reactive ion exchange theory at very low concentrations was applied in both simulations. For the sorption of boric acid, the effects of undissociated species and its dissociation on kinetics, as well as the exchange process, must be considered since the boric acid is a weak electrolyte. The influence of the selectivity coefficient and the dissociation equilibrium constant on reversible diffusion was discussed.

Unlike axial flow, radial flow geometry leads to varied superficial velocity and flow fronts within the column. Thus, mass transfer coefficients must be treated as variables. Radial dispersion needs to be considered. These models were developed particularly for application to reactor water clean-up (RWCU) systems. Simulation of boric acid sorption may be modified to treat all weak electrolytes, both acid and base forms.

I wish to express my deepest appreciation to my major adviser, Dr. Gary L. Foutch, for his guidance, inspiration, kind and invaluable helpfulness throughout my master program. I am also grateful to Dr. Jan Wagner and Dr. Arland H. Johannes for serving on the advisory committee and very helpful suggestions.

Particular thanks go to Mr. Vikram Chowdiah for his help and suggestions throughout my study. Special gratitude and appreciation are expressed to my parents for their encouragement and sacrifice. I owe a deep debt of gratitude to my wife, Beilin Chen and my son, Wenhao, for their encouragement, sacrifice and understanding throughout the course of this study.

Financial assistance from the School of Chemical Engineering at Oklahoma State University, and ABB Atom for the completion of this study, are gratefully appreciated.

TABLE OF CONTENTS

Chapter	Page
I. INTRODUCTION	1
Ion Exchange Resin	1
Selectivity	2
Mechanism of Ion Exchange	3
The Removal of Boron by Ion Exchange	4
Radial Flow Packed Bed	5
Objective	6
II. LITERATURE REVIEW	7
Aqueous Boric Acid	7
Kinetics of Ion Exchange Involving Reactions	9
Equilibrium and Rate Theories	12
Equilibrium Theory	13
Rate Theory	15
Radial Flow	17
Numerical Approach	21
III. HOMOGENEOUS ANION EXCHANGE MODELING FOR FILM DIFFUSION CONTROLLED NERTRALIZATION AT VERY LOW CONCENTRATION	23
Introduction	23
Model Development	25
Assumptions	26
Flux Expressions	28
Effective Diffusivities and Exchange Rates	30
Column Material Balance	33
Dimensionless Expressions	34
Numerical Solution	35
Results and Discussion	36
Interface Concentrations	38
Effective Diffusivity	40
Contributions to the Exchange	43
Reversible Diffusion	43
Ratio of Self Diffusivities of Acid Molecule to its Ions	49
Numerical Treatment	50
Conclusion	52

Chapter	Page
IV. SIMULATION OF A MIXED-BED RADIAL FLOW DEMINERALIZER	53
Introduction	53
Model Development	55
Assumptions	55
Flux Expressions	56
Rates and Effective Diffusivities	60
Column Material Balance	62
Numerical Solution	65
Results and Discussion	70
Concentration Distribution	70
Nonionic Mass Transfer Coefficients	70
Effects of Bed Void Fraction	72
Ratio of Exchange Resins	72
Conclusions and Recommendations	78
LITERATURE CITED	79
APPENDIX A - DERIVATION OF ION AND MOLECULAR FLUX EXPRESSIONS FOR INCOMPLETELY DISSOCIATED ACID SORPTION BY A BASE ANIONIC RESIN.....	87
APPENDIX B - DERIVATION OF THE DIMENSIONLESS FORM OF RADIAL FLOW COLUMN MATERIAL BALANCE	94
APPENDIX C - DERIVATION OF DISCRETIZATION EQUATIONS FOR RADIAL FLOW DIFFERENTIAL EQUATIONS.....	99
APPENDIX D - COMPUTER CODE FOR BORON SORPTION	104
APPENDIX E - COMPUTER CODE FOR RADIAL FLOW	114

LIST OF TABLES

Table		Page
I.	Diffusion Coefficients	25
II.	Model Assumptions	27

LIST OF FIGURES

Figure	Page
1. Structure of Radial Flow Unit	18
2. Comparison of Model Calculated Values and Experimental Data	37
3. Variations of Effective Diffusivity D_e with y and K_D^x for Bulk Phase Neutralization	42
4. Effect of Dissociation Equilibrium Constant on Total Mass Transfer Rate.....	44
5. Effect of Selectivity Coefficient K_D^x on the Concentration Distribution Profiles	46
6. Effect of Dissociation Equilibrium Constant on Total Exchange Rate: Concentration Distribution in Column.....	47
7. Effect of Dissociation Equilibrium Constant on Total Exchange Rate: Concentration Fraction in Resin	48
8. Variations of Concentration Distributions in Column with Self-diffusivity Ratios of Boric Acid to its Ions	51
9. Concentration Profiles for Mixed-bed Ion Exchange with Neutralization in the Bulk Phase	59
10. Solution Strategy	66
11. A One Dimensional Uniform Grid	67
12. Concentration Distribution within a Mixed-bed with Inward Radial Flow.....	71
13. Changes of Nonionic Mass Transfer Coefficients along Flow Direction in Inward Radial Flow Column	73
14. Effect of Bed Void Fraction on Nonionic Mass Transfer Coefficients of Sodium in Inward Radial Flow Column	74
15. Effect of Bed Void Fraction on Chloride Breakthrough Curves in Mixed-bed with Inward Radial Flow	75

Figure		Page
16.	Chloride Breakthrough Curves for Simulation of Mixed-bed with Inward Radial Flow with Varying Cation to Total Resin Fraction	76
17.	Sodium Breakthrough Curves for Simulation of Mixed-bed with Inward Radial Flow with Varying Cation to Total Resin Fraction	77

NOMENCLATURE

a_s	interfacial surface area (L^2 / L^3)
C^f	feed concentration (meq/L^3)
C_i	concentration of species i (meq/L^3)
C_i^*	concentration of species i at the surface of the resin (meq/L^3)
C_i^0	concentration of species i in the bulk (meq/L^3)
d_p	particle diameter (L)
D_i	self-diffusivity of species i (L^2/T)
D_{bi}	radial dispersion coefficient of species i (L^2/T)
D_e	effective diffusivity (L^2/T)
F	Faraday's constant
F_v	volumetric flow rate (L^3/T)
h	height of the resin packed in radial flow packed-bed (L)
J_i	flux of species i in the film ($meq/T \cdot L^2$)
k_i	nonionic liquid phase mass transfer coefficient (L/T)
k_i'	ionic liquid phase mass transfer coefficient (L/T)
K	concentration capacity ratio between the resin and bulk phase
K_a	dissociation equilibrium constant of acid
K_A^B	resin selectivity coefficient for ion B in solution compared to A in resin
K_t	dimensionless mass transfer coefficient
K_w	water dissociation equilibrium constant
Pe	Peclet number
Pr	proportional parameter (L/L)

q_i	concentration of species i in the resin (meq/L ³)
Q	capacity of the resin (meq/L ³)
r	radius of radial flow packet-bed
R	universal gas constant
Re	particle Reynolds number
R_i	ratio of mass transfer coefficient
Sc	Schmidt number
T	temperature
t	time (T)
u	superficial velocity in axial flow packed-bed (L/T)
u_r	superficial velocity in radial flow packed-bed (L/T)
V	volume of the packed resin (L ³)
X_i	concentration fraction in liquid phase
Y_i	concentration fraction in the resin phase
Z_i	charge on species i

Greek Letters

α	ratio of exiting to entering ion diffusivities
β	dimensionless proportional coefficient of diffusion rate
δ	the thickness of the film (L)
ϵ	bed void fraction
η	capacity ratio
ϑ	arbitrary proportional coefficient
τ	dimensionless time coordinate
ξ	dimensionless distance coordinate
ϕ	electric potential (ergs/coulomb)
μ	solution viscosity (cp)

Superscripts

bar	refers to resin phase
*	interfacial equilibrium condition
f	column feed condition
o	bulk phase condition
0	previous time value

Subscripts

a	acid molecule
A	ion exiting the resin phase
B	ion entering the resin phase
c	chloride ion
h	hydrogen ion
i	species i
n	sodium ion
o	hydroxide ion
x	borate

CHAPTER I

INTRODUCTION

The industrial applications of ion exchange are extremely widespread, ranging from water purification, bioseparations, and the treatment of precious metals such as gold and uranium. The largest application - in terms of ion exchange resin usage - is water treatment. Water treatment technologies include, softening, deionization for conventional and nuclear boilers, and dealkalation. Although ion exchange processes were developed about ninety years ago, improvements in products, techniques, economics and new applications are continuing. These improvements are driven by the special needs of applications such as pure water, ultrapure water, and waste minimization.

Ion Exchange Resin

The structure of ion exchange materials varies greatly. These include natural minerals, structured inorganic products and polymeric resins. Resins are generally divided into two categories: anion resin which contains mobile ions with negative charge, and cation resin which contains mobile ions with positive charge. The discussions in this thesis will focus on polymeric resins that have either a styrene or an acrylic matrix with fixed ionic groups.

Polystyrene Sulfonic Acid Cation Resins and Anion Resins

Styrene (vinylbenzene) is polymerized readily, using an organic peroxide catalyst, to form linear polystyrene. If divinylbenzene (DVB) is mixed with the styrene, a three-

dimensional polymer network is formed. The DVB crosslinks give a three dimensional structure that renders the polymer insoluble. The characteristic spherical ion-exchange beads therefore are made by suspension polymerization. The exchanger is treated with concentrated sulfuric acid to make a cation resin, while anion resin is treated first with a chloromethyl group and then with an amine group. There are only two acidic groups readily available for cation resins. However, a large number of amines can be used to produce anion-exchange materials for different characteristics. This fact is used to produce special resins for uranium and gold recovery.

Acrylic Cation and Anion Resins

These materials are made usually by copolymerizing acrylic or methacrylic acid with DVB. Polyacrylics, with lower molecular weight and high capacity, have almost replaced the methacrylics entirely. Acrylic exchangers are physically robust materials, with larger capacity and good operating characteristics, and are serious competitors to the polystyrene resins.

Mobile ions in the exchanger (or resin) can be replaced by a stoichiometric equivalent of like charge ions bound within the resin structure. The ability of the exchanger to select certain ionic species in favor of others is used for the following operations:

1. to remove undesirable constituents from solution, and
2. to concentrate or recover valuable components present in trace amounts from solution.

Equipment design for a specific separation depends primarily on the predicted concentration of the effluent solution.

Selectivity

Ion-exchange equilibria in cation- and anion-exchange resins depend largely on the type of functional group and the degree of crosslinking. The degree of crosslinking determines the tightness of the matrix structure and thus its porosity. It cannot be measured directly and is rarely homogeneous.

The most widely employed method for expression of ion-exchange equilibria has been developed from the law of mass action or the Donnan membrane theory (Donnan, 1912; Donnan, 1934; and Donnan and Guggenheim, 1932). Consider the exchange of cations A and B between a resin and a solution containing no other cations. Assume that the ion exchanger is initially in the B form and that the solution contains ions A. The mass action expression for cation exchange can be written:



Here, overbars denote the ionic species in the resin phase, z_A^+ and z_B^+ denote the valency and charge of counterions A and B. We can define the thermodynamic equilibrium constant K_a as follows:

$$K_a = \frac{(\bar{a}_A)^{z_B} (a_B)^{z_A}}{(\bar{a}_B)^{z_A} (a_A)^{z_B}} \quad (1-2)$$

The difficulty in the evaluation of the activity coefficients, and therefore activities, in the resin phase is great. For most practical applications it is usually satisfactory to assume that the solution-phase activity coefficients are almost unity, which is particularly valid in dilute solutions (Michael and Francis, 1985). Therefore, the resin-phase activity coefficients usually are combined into the equilibrium constant K_a , to provide a new pseudoconstant, that is, the selectivity coefficient K . Thus,

$$(K)_B^A = \frac{(\bar{C}_A)^{z_B} (C_B)^{z_A}}{(C_B)^{z_A} (\bar{C}_A)^{z_B}} \quad (1-3)$$

Mechanism of Ion Exchange

The mechanism of ion exchange is essentially a diffusion process to the exchange site followed by chemical reaction of ions. This results in a redistribution of counterions between the resin particle and solution while maintaining electroneutrality. The ion exchange rate process is divided into the following steps:

1. Diffusion of the counterions from the bulk solution through a film outside the resin,
2. Diffusion of the counterions within the resin phase,
3. Chemical reaction between the counterions and the exchange site,
4. Diffusion of the displaced ion out of the resin, and
5. Diffusion of the exchanged ion from the resin surface through the film into the bulk solution.

The overall rate of ion exchange is controlled by the slowest of these steps.

It is well known that ion exchange rates are controlled by diffusion (Boyd et al., 1947; Helfferich, 1962). If diffusion of ions through the film is the slowest step the process is termed film diffusion controlled. Particle diffusion control occurs when the largest rate resistance exists within the resin phase. The diffusional processes are fundamentally described by Fick's first law or Nernst-Planck equation.

Ion exchange processes may be accompanied by chemical reactions such as neutralization and dissociation (Helfferich, 1965). A detailed analysis of various ion exchange processes involving ionic reactions and complex formation was presented by Helfferich (1965).

The Removal of Boron by Ion Exchange in the Power Industry

The ion exchange process plays an important role in the power industry. The needs for extrapure water for the operation of advanced boilers and reactor water clean-up require applications of ion exchange. The power industry is also interested in ion exchange for the removal of boron and silica from reactor water (Foutch, 1992). In nuclear power plants, sodium pentaborate solution is used in the stand-by liquid control system to prevent failure of cold sub-critical conditions of boiling water reactors (Maly and Bosorgmanesh, 1983). On the other hand, the boric acid and silica acid are used directly as a burnable nuclear poison in the coolant of pressurized water reactors. Usually, boron and silica are present in very low concentrations in nuclear reactor boiler water. Boron, as borate, comes from the dissociation of the weak acid, boric acid. Therefore, the dissociation and neutralization reactions are accompanied with the sorption of borate by the ion-exchange resin in the removal process.

Borate separation using strong-base anion-exchange resins has been studied by Yoneda et al.(1959), Rosset et al. (1964), and Christoph et al. (1972). Hirao et al. (1973) found that some boron complexes adsorbed on weak-base anion exchange resins were eluted by distilled water. The advantage of using weak-base exchange resin for borate separation instead of strong-base resin was found to be a reduced need to regenerate the resin (Huang et al., 1990).

Radial Flow Packed Bed

Usually, industrial ion exchange is performed in packed beds. Anionic or cationic resin, or a mixture of the two, is used in a conventional axial-flow deep-bed unit. In recent years, an alternative to traditional deep beds - radial flow ion-exchange units - have been designed and placed in service. This type of unit has been found to be the most

suitable for reactor water clean-up systems as well as for condensate clean-up (Fejes et al., 1989). Compared with conventional axial-flow, radial flow provides the advantages of relatively large volumetric flow rate with low pressure drop. Also in the radial flow configuration flow rate is varied along the radial direction over a broad range (Fejes et al., 1989).

Objective

Ion exchange of weak electrolytes in extremely diluted solutions is particularly interesting in the power industry. Diffusion of ionic species occurs simultaneously with the non-ionic species. This means that dissociation of weak electrolytes may take place in the bulk solution as well as the film during the overall exchange process. The first objective of this thesis is to model the exchange process of weak electrolytes.

Radial flow ion exchange packed beds have potential advantages over axial flow packed beds for water treatment in nuclear power plants, and has the possibility to replace axial flow packed beds in other industrial applications, such as waste-water treatment and purification of biological products. Few references discuss the theory, development, and operation of radial flow ion exchange systems in large scale. The development of a model that describes radial inward flow ion-exchange operation is the second objective of this thesis.

CHAPTER II

LITERATURE REVIEW

An extensive literature review of ion exchange has been carried out by Haub (1984), Yoon (1990) and others. This review concentrates on the objectives of this thesis.

Aqueous Boric Acid

Boron has been used in nuclear-related fields as a neutron absorbing material. The structure, in aqueous solution, of the conjugate base of boric acid has remained a mystery in spite of attempts to obtain a definitive answer to the problem. One can conceive of, at least, three possible structures for a monomeric borate ion of single negative charge, these are BO_2^- , H_2BO_3^- , and $\text{B}(\text{OH})_4^-$. The differences between these structures lie primarily in the coordination number of the boron atom (Edwards et al., 1954). In order to remove boron or borate from aqueous solution by ion exchange, it is necessary to understand the chemistry of aqueous borate and boric acid equilibrium in the system of interest.

The chemistry of aqueous borate is characterized by the existence of a series of polyborate anionic species and by the fact that boric acid undergoes hydration before ionization. In early studies of aqueous boric acid chemistry, several investigators (Kolthoff, 1926; Kolthoff, 1927; and Menzel, 1927) concluded that monoborate ions, BO_4^- , tetraborate ions, $\text{B}_4\text{O}_7^{2-}$, and pentaborate ions, B_5O_8^- , were all present in aqueous borate solutions with the pentaborate $\text{B}_5\text{O}_7^{2-}$ ions being extensively dissociated. Later, Carpeni and Souchay (1945) considered, from a study of neutralization curves of solutions of boric acid between 0.03 and 0.262M, that B_5O_8^- , HB_4O_7^- and BO_2^- ions were formed

successively during the neutralization. They emphasized that condensation of boric acid was affected by the total boron concentration and the pH of the solution, the importance of which had not been fully appreciated by previous workers. Although some other polyborate anionic species have been successively found in aqueous boric acid solution, studies by cryoscopic (Platford, 1971), spectroscopic (Pinchas et al., 1972) and conductivity measurements (Crovetto et al., 1980) confirmed, that in dilute aqueous solutions and without excess boric acid, the monomeric borate ion was the predominant anionic species $B(OH)_4^-$.

With the increasing applications of boron, it is not surprising that the equilibria which occur in various aqueous solutions of boric acid and borate have been extensively studied. Ingri (1962, 1963a,b) carefully studied the equilibria occurring in concentrated boric acid and borate solutions and demonstrated that boric acid in an aqueous medium attains a complex equilibrium with borate and polyborate ions. In dilute aqueous boric acid solutions having a total boric acid concentration of less than 0.01 M, however, the only important equilibrium is:



This conclusion was confirmed by several researchers (Anderson et al., 1964; Momii and Nachtrieb, 1967). Furthermore, by direct determination of the volume of ionization, and from studies of the pressure coefficient of dissociation, the following reaction also exists in dilute solutions:



The two processes are coupled to the water autoprotolytic equilibrium and cannot be distinguished thermodynamically (Corti et al., 1979).

Kinetics of Ion Exchange Involving Reaction

Studies, since World War II, of the kinetic theories of various ion-exchange processes based on different rate controlling steps such as: film diffusion control, particle diffusion control, and different equilibrium relationships (linear and nonlinear) have improved our understanding of the exchange process. It has been well known that chemical reactions, neutralization and dissociation occurring in the ion-exchange process influence the exchange rate. Kinetics of ion exchange involving chemical reaction is much different from that in ordinary ion exchange processes. However, early ion exchange kinetic theories did not consider the effects of chemical reactions (Helfferich, 1965). The first theoretical analysis of ion-exchange kinetics coupled with ionic reactions were presented by Helfferich (1965). Since that time, studies on this subject have been continuing.

Helfferich (1965) classified four types of processes based on the reactions and proposed a theoretical kinetic model, either film-diffusion or particle-diffusion, for each class. He assumed chemical reactions to be very fast and irreversible so that the diffusion process is rate controlling in most cases. He also stated that whenever there is an irreversible sorption on a resin, the dynamics of sorption can be explained on the basis of the shrinking core model. This postulate is generally valid in concentrated solution with the system of strong electrolytes, but cannot be used to describe systems (Helfferich, 1965, Bhandari et al., 1992a):

- where reactions of certain complexes are slow and may become rate-controlling;
and
- where sorption is significantly reversible, especially at low acid concentration and for resin with low basicity.

In such situations the shrinking core model is not expected to be valid (Bhandari et al., 1992a). The neutralization of a weak-acid exchanger, also discussed by Helfferich (1965),

was given as an example for the ionization of undissociated fixed ionogenic groups by reaction with the co-ion. He concluded that such a system should show kinetics governed by diffusion through the resin particle, for which two different particle-diffusion mechanisms can be postulated. One is that the fixed ionogenic groups trap and thus localize most of the free opposite charge ions in the resin, which, often takes place at low solution concentrations, results in slowing the exchange process greatly. The other mechanism, occurring at high solution concentrations, should be determined by the rate of the co-ion diffusion. The second case has been confirmed experimentally by Adams et al. (1969). The four types of ion-exchange processes, however, did not include the case that incompletely dissociated electrolytes (weak electrolytes) are involved in ion exchange.

Blickenstaff and his co-workers were very much interested in Helfferich's study on the kinetics of ion exchange accompanied by chemical reaction. They (1967a,b) carried out a series of experiments and verified Helfferich's hypotheses on the neutralization of strong acid ion exchangers by strong bases. Wagner and Dranoff (1967) noted that Helfferich's model did not consider ion exchange systems involving weak electrolytes, and presented a model for film diffusion controlled neutralization of strong acid resin by a weak base. The effect of the dissociative equilibrium of the weak base was considered in this model. The flux of ions and undissociated species were described by the Nernst-Planck equation and Fick's law, respectively.

Helfferich and Hwang (1985) developed a rate controlling ion model describing the kinetics of acid uptake by weak base resins. Based on the principle of Donnan exclusion of co-ions by the ionized shell of resin, they assumed that the rate controlling species during the sorption of weak monobasic acids is the undissociated acid species, which indicated that the contribution of the ionic species to the total diffusional flux is negligibly small.

Bhandari et al. (1992a,b) consider that both the shrinking core model and the rate controlling ion model are valid only for the case when irreversible reaction is involved.

They presented a model to correlate the sorption equilibria and dynamics for both irreversible and reversible reaction. With their model, they consider the existence of a charged double layer at the resin pore wall where the counterions are concentrated in a double layer. As a result, the core of a pore is relatively dilute with respect to the counterions. The core region therefore offers only a weak Donnan potential, and hence the extent of exclusion of the co-ion from the pore is considerably reduced. Based on this postulate, the sorption equilibrium at ionogenic sites of resin must be taken into account. Their studies reveal that the contributions of both the ionic and the undissociated molecular species are important in determining the total diffusion flux of the weak acid in the pores of the resin.

Meichik et al. (1989) carried out a comparative study of the kinetics of a system in which a weak acid and weak base resin are involved. They concluded that the chemical reaction occurs in the region with comparable contributions from internal diffusion and chemical reaction. In this case, concentrations of all species involved in the reaction were no longer assumed to be negligible at the resin-film interface.

Kataoka et al. (1976) carried out kinetic studies of ion-exchange accompanied by irreversible reaction with film control. They applied the hydraulic-radius model and derived equations for liquid-phase effective diffusivity and the ratio of exchange rate with or without reaction. Later, Kataoka et al. (1977) presented a model for intraparticle ion exchange mass transfer accompanied by instantaneous irreversible reaction. Their results indicated that reaction affects the ion exchange rate appreciably. Also, the Nernst-Planck equation was determined to be applicable for the flux of counter-ions and co-ions in the case involving a reaction front moving into the resin phase.

Haub and Foutch (1986) extended the theory of liquid-resistance controlled reactive ion exchange to very low solution concentrations. They developed a model for mixed-bed ion exchange accompanied by neutralization reactions. They stated that the reactions in the mixed-bed ion exchange processes are reversible. And they considered that the

influence of water dissociation on the exchange rate needs to be considered when concentrations were below 1 ppm. The Nernst-Planck theory and hydraulic radius model were applied in the study. Their work has shown that neutralization reactions are encountered in the treatment of salts by a mixed bed of hydrogen form and hydroxide form resins. They considered the neutralization reactions at the resin-film interface, and within the film or in the bulk fluid.

Zecchini and Foutch (1991) presented a model for the operation of a mixed-bed ion exchange column in the amine cycle at low concentrations. The model considers film diffusion, limited exchange with bulk-phase neutralization and correction for amine and hydroxide concentrations. The effects of dissociation of ammonia on bulk phase concentrations were also considered.

Equilibrium and Rate Theories

Most ion exchange operations are carried out in columns. Unfortunately there are no universal theories for column performance because column kinetics are complex (Helfferich, 1962). Theories commonly applied to describe column performance are equilibrium theory and rate theory. Equilibrium theory is widely used in the studies of multicomponent ion exchange (Dranoff and Lapidus, 1957 and 1961; Klein et al. 1967; Helfferich, 1967 and 1984; Kataoka and Yoshida, 1980; Shallcross, Herrmann and McCoy, 1988; others). Equilibrium is also used in the design of ion-exchange processes (i.e., Tondeur and Bailly, 1986). Rate theory is used to define most ion exchange processes because local equilibrium is not usually attained (Helfferich, 1962). Material balances, equilibrium isotherms, and kinetic or rate laws are generally considered in rate theory. Different equilibrium isotherms and kinetic law expressions give different rate theories. However, they are basically derived by applying the diffusion equations to ion-exchange systems for certain limiting cases (Helfferich, 1962).

Equilibrium Theory:

In equilibrium theory, local equilibrium between the mobile phase and resin phase is assumed to occur at all points. It implies that the rate of boundary motion is slow, so that there is enough time left for ion exchange to occur. Mass-transfer resistance between the two phases is not considered in equilibrium theory. Axial dispersion is frequently neglected (Tondeur and Bailly, 1986).

It has been shown (Kunin, 1958, Kitchener, 1959) that in most cases the equilibria may be described in terms of either Donnan membrane equilibrium theory or standard mass action chemical equilibrium. When rigorously applied to include resin swelling and solution nonideality these two approaches lead to different equilibrium expressions (Kitchener, 1959). However if ideal solutions are assumed, as well as negligible effect due to resin swelling and hydration, they yield the same relationships. In particular, for a binary system with ionic species A and B of the form:



where a, b -- ionic valences; the bar indicates resin phase.

The equilibrium distribution of ions in the resin and solution phases is described by a selectivity coefficient given by:

$$K_{AB} = \frac{(C_A)^b (q_B)^a}{(q_A)^b (C_B)^a} \quad (2-4)$$

The selectivity coefficient K_{AB} is not constant and varies from ions in system as well as resin loading and solution concentration. But it is possible to take selectivity coefficient as constant in certain cases for engineering purposes (Pieroni and Dranoff, 1963).

Dranoff and Lapidus (1957) first introduced equilibrium theory into the analysis of ternary ion exchange systems. Equilibrium between the two phases is characterized by

mass action equilibrium constants. Later, Dranoff and Lapidus (1961) proposed equations as given below:



$$\frac{d(A^+)}{d\theta} = k_f[\bar{A}^+][B^+] - k_b[A^+][\bar{B}^+] \quad (2-6)$$

This reaction corresponds to second order reversible kinetics for a single exchange reaction, and was used to describe a ternary system. Their theory was validated by experimental data.

A general analytical solution for multicomponent ion exchange in fixed beds by applying local equilibrium was presented by Helfferich (1967). The ideal conditions of constant separation factors and uniform presaturation were required to obtain a solution. Axial diffusion and dispersion were neglected.

Kataoka and Yoshida (1980) proposed a model that considered nonidealities in the liquid phase, but assumed that the solid phase was ideal. In their model, a selectivity coefficient corrected by the activity coefficients of different species in the liquid phase, K'_{AB} was used (as given below):

$$K'_{AB} = \left(\frac{q_A}{C_A}\right)^b \left(\frac{C_B}{q_B}\right)^a \frac{\gamma_B^a}{\gamma_A^b} \quad (2-7)$$

where γ_i ($i = A, B$) is the activity coefficient of species i in the liquid phase, 'a, b' are ionic valences.

Many investigators (Bajpai, et al., 1973; Elprince and Babcock, 1975; Smith and Woodburn, 1978; Vazquez et al., 1985; Shallcross et al., 1988; others) considered nonidealities in both the liquid and the solid phase. The solid phase activity coefficients are estimated by applying the well known Gibbs-Duhem equation and Wilson equation (Wilson, 1964).

The Gibbs-Duhem equation is:

$$\sum_i^M y_{mi} (d \ln \gamma_i)_{T,P} = 0 \quad (2-8)$$

The Wilson equation is:

$$\frac{\Delta G^E}{RT} = \sum_{i=1}^M y_{mi} \ln \left[\sum_{j=1}^M \Lambda_{ij} y_{mj} \right] \quad (2-9)$$

where M is the number of counterion species in solid phase, y_{mi} is the Wilson binary interaction parameter defined such that $\Lambda_{ij} = 1$, when $i = j$, and $\Lambda_{ij} > 0$, when $i \neq j$.

Rate Theory:

The film diffusion control and particle diffusion control models are two popular models in rate theory. The linear driving force approximation and Nernst-Planck model are useful in developing rate theory models.

Thomas (1944) developed the most general calculation method using rate theory for the column performance under nonequilibrium conditions. His method was based on the assumption of reversible second order reaction kinetics as an approximation to the actual diffusional process. This presents an obvious problem in Thomas' method for ion exchange calculations since ionic diffusion is controlling rather than chemical reaction. Amundson (1950) extended Thomas' method to obtain an algebraic framework for

numerical integration of the binary case. In this case, the initial solid phase concentrations varied with position in the column, and the feed concentrations varied with time. But Amundson's method is not easy to use, even in the simplest case of linear equilibrium (Vermeulen and Hiester, 1954). For this reason, the linear driving force approximation, first suggested by Glueckauf (1947), is often used in later ion exchange rate model developments. In this method, the rate of ion exchange by the resin is written as the product of surface area, an effective mass-transfer coefficient, k_e and a driving force (consisting of the difference between the bulk average concentration in the resin, \bar{q} , and the surface concentration q_s) (given below).

$$\frac{dq}{dt} = \frac{3k_e}{a}(q_s - \bar{q}) \quad (2-10)$$

If a linear isotherm is assumed, $q=kC$, the general expression for the above equation is:

$$\frac{dq}{dt} = k'a'(C - C_i) \quad (2-11)$$

where k' is the mass transfer coefficient of the ionic species, a' is the specific surface, C is the bulk fluid concentration, and C_i is the interfacial concentration. This ordinary differential equation is easy to handle and obtain an analytical solution.

Based on Thomas' method, Vermeulen and Hiester (1952, 1954) proposed a model in which a linear driving force approximation was assumed to give the exchange rate instead of the second order reaction approximation. The linear driving force model greatly simplifies Thomas' method and is a more practical approach for the actual ion-exchange process. The generalized plots of column and breakthrough profiles presented in their model is used widely for sorption column design and evaluation (Perry, 1973).

Omatete et al. (1980a,b) developed a more comprehensive approach to non-equilibrium multicomponent ion exchange using rate theory. A linear driving force approximation was used for ionic flux equations in their model. From different approximations of irreversible thermodynamics, Nernst-Planck model and Fick's law, they derived the same algebraic form with different definition of the diffusion coefficients. This described the complete multi-component ion-exchange diffusion equations. The diffusion flux equations, mass transfer coefficients and, the column material balance equations can be solved numerically.

Haub and Foutch (1986a,b), and Zecchini (1990) expanded these basic approximations of rate theory to multicomponent mixed-bed ion exchange at low solution concentrations. Their work confirmed that a linear driving force and the Nernst-Planck model approximations are applicable in their case. Simultaneous cation and anion exchange were handled in their model. The results of their models are consistent with industrial data. The effects of a finite exchange rate, dissociation of water molecules, and reversible exchange were considered in their models.

Radial Flow

Ion exchange is the most suitable unit operation for reactor water clean-up (RWCU) purpose (Fejes et al., 1989). A problem, however, existing in ion exchange operating experience of RWCU with conventional axial flow fixed bed, is a fast build-up of the pressure drop during operation. As a result, the resin has to be replaced due to high pressure drop long before the exchange capacity of the resin has been exhausted (Fejes et al., 1989). Hence mixed bed ion exchangers with radial flow are desired for reactor water clean-up systems. The reason is because radial flow units, as shown in Figure II-1, have a relatively large flow area and short flow path.

Therefore, the advantages of radial flow shallow bed ion exchangers are:

- little tendency for pressure drop build-up,
- little risk for resin leakage into the reactor, and
- higher efficiency in the removal of impurities of reactor water.

so that plant safety, plant radiology and plant economics are improved (Fejes et al., 1990).

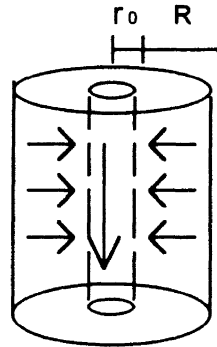


Fig. II-1 The structure of radial flow unit (inward flow)

The performance of radial flow cylindrical packed bed ion-exchange is different from that of axial flow. For radial flow, a specific feature is that the interstitial velocity of the mobile phase can be varied in a very broad range, therefore, the dispersion term needs to be considered in the material balance. The general material balance for radial flow beds, under some assumptions, leads to the expression:

$$\frac{\partial C}{\partial t} + \frac{(1-\epsilon)}{\epsilon} \frac{\partial q}{\partial t} \pm \frac{v}{\epsilon} \frac{\partial C}{\partial r} - \frac{1}{r} \frac{\partial}{\partial r} (Dr \frac{\partial C}{\partial r}) = 0 \quad (2-12)$$

The last left-side term reflects the influence of radial dispersion. The negative sign before the convection term indicates inward flow, while a positive sign is used for outward flow.

So far, most application and theoretical studies of radial flow are on chromatography. Radial flow associated with mixed bed ion exchange, both theoretical approaches and applications in industry, has been sparsely reported.

Lapidus and Amundson (1950) were the first to give general theoretical descriptions for radial flow chromatography. They obtained analytical solutions - equivalent to those of Thomas for axial chromatography - for radial flow chromatography. The dispersion effect was not considered in their model. Later, several researchers (Rachinskii, 1968; Rachinskii and Inchin, 1968,1970; Inchin and Rachinskii, 1968,1973a) put forth the theoretical work on dynamics of radial flow chromatography for negligible radial diffusion.

Models which took molecular dispersion into account were first investigated by Inchin and Rachinskii (1973b). They presented a functional dependence for radial diffusion coefficient, D , which was expressed as follows:

$$D = D_o + D_i = D_o + au_r^n \quad (2-13)$$

where D_o is the coefficient of longitudinal molecular diffusion, and D_i , eddy diffusion coefficient (dependent on the rate of flow), is the other longitudinal effect of material transport. a is an empirical coefficient, u_r is the rate of flow, and n is an empirical power.

The simplest relation

$$D \approx D_o \quad (2-14)$$

was suggested in their work in the case of dormant molecular dispersion ($D_i \ll D_o$). As a result, the radial diffusion coefficient, D , can be treated as constant for a given system because the molecular dispersion coefficient, D_o , is independent of flow rate.

However, the molecular diffusivity is often quite small compared to the diffusivity caused by turbulent eddy mixing, and is often negligible so that the relation in Eq. II-14 cannot be expected to be valid in most practical radial flow system. Following the simplicity of Eq. II-13, Ruthven (1984) and Jonsson (1987) presented another simple linear approximation for radial diffusivity for a single component system, this is:

$$D = \gamma_1 D_0 + \gamma_2 d_p u_r \quad (2-15)$$

where γ_1 and γ_2 are constants which normally have values of about 0.7 and 0.5, respectively. The d_p is the particle diameter. Eq. II-15 can be simplified as

$$D \approx \gamma_2 d_p u_r \quad (2-16)$$

even at low Reynolds numbers (Ruthven, 1984).

A more rigorous mathematical model for radial flow chromatography was presented by Huang et al. (1988). The influences of a variety of parameters were discussed by using a numerical method. Their work shortened the difference between theoretical descriptions and practical applications in radial flow chromatography.

A theoretical study of radial flow chromatography, based on a general nonlinear multicomponent rate model, was investigated by Gu et al. (1991). In their model, the radial dispersion, external mass transfer, intraparticle diffusion, and nonlinear multicomponent isotherms are considered. The model was solved numerically by using the finite element and orthogonal collocation methods for the discretizations of bulk fluid and particle phase partial differential equations, respectively. Comparing radial inward flow to radial outward flow, they concluded the operation under inward flow is generally better than outward flow by providing sharper concentration profiles.

The application of radial chromatography theory to process scale was first described by Hou and Mandaro (1986). The system used a radial flow ion-exchange chromatographic cartridge that eliminated cumbersome procedures and operating problems encountered in conventional axial ion exchange chromatography. The performance of the cartridge was tested with human plasma with a flow rate of almost 100 times that for typical axial flow ion exchange chromatography. More recent papers in scaling-up separation of various biological products have been prepared by Huang, et al. (1988); Plaigin et al. (1989); and Lee et al. (1990).

Numerical Approach

Numerical methods are alternatives when the analytical solutions are not available or impractical, which is often encountered because of complex rate equations or equilibrium relations, irregular boundary conditions and multicomponent systems.

There are some numerical methods available for solving ion exchange systems. An explicit method -- the method of characteristics technique -- reduces first order hyperbolic partial differential equations to an equal sized system of ordinary differential equations was first applied by Acrivos (1956) to adsorption packed columns. Then, Helfferich (1962); Omatete et al. (1980); and Dranoff and Lapidus (1958 and 1961) used this method to solve material balance equations in binary and multicomponent ion-exchange columns. Haub and Foutch (1986) used this technique for cation and anion resins in mixed beds.

For an optimal design of an industrial ion exchange process, it is important to have accurate modeling and simulation of the dynamic behavior of the column. Numerical methods are an alternative to analytical solutions when complex rate equations, equilibrium relations and irregular boundary conditions are encountered in ion exchange column performance. The solution of convective diffusion equations, and modeling of the coupling between different individual components, is a major difficulty in the simulation of ion exchange dynamics.

The method of characteristics technique reduces first order hyperbolic partial differential equations to an equal sized system of ordinary differential equations (Costa et al., 1986). Many investigators have applied the method to adsorption packed columns (Acrivos, 1956) to solve material balance equation in binary and multicomponent ion exchange columns (Helfferich, 1962; Omatete et al., 1980; Dranoff and Lapidus, 1958, and Dranoff and Lapidus, 1961), and for cation and anion resins in mixed beds (Haub and Foutch, 1986).

The orthogonal collocation method of solving partial differential equations -- an implicit method -- is particularly useful for the solution of boundary values problems (Raghavan and Ruthven, 1983). This method was previously applied to the simulation of fixed-bed reactors (Hansen, 1971; Karanth and Hughes, 1974) and later to the simulation of adsorption columns (Liapis and Rippin, 1978, Raghavan and Ruthven, 1983). Recently, Sun and Meunier (1991) proposed an improved finite difference method for fixed-bed multicomponent sorption in which the solution adaptive gridding (SAG) and the quadratic upstream differencing scheme (QUDS) technique were used to reduce oscillations. This technique makes it possible to describe sharp transitions very well with less computational grids than used by uniform schemes. Gu et al. (1991) applied the finite element method and the orthogonal collocation method for the discretization differential equations, and Gear's stiff method for the solution of the resulting ordinary differential equations for simulations of multicomponent radial flow chromatographic operations.

CHAPTER III

HOMOGENEOUS ANION EXCHANGE MODELING FOR FILM DIFFUSION CONTROLLED NEUTRALIZATION AT VERY LOW CONCENTRATIONS

Introduction

Boiling water reactors in nuclear power plants encounter the problem of weak electrolytes, particularly silica acid and boric acid. The favorite unit operation for their removal is ion exchange. Both strong and weak base ion exchange resins can serve this purpose. However, weak base ion exchange resins are preferable since it is easy to be regeneration (Huang, et al., 1991).

The sorption behavior of weak acid anions on weak base resins is complicated because of incomplete dissociation of the acids and reversible reactions in the bulk fluid, the stagnant film around the resin, and within the exchange particles. The most general treatment of acid sorption kinetics on weak base resins is the rate controlled ion model presented by Helfferich and Hwang (1985). According to these authors, acid sorption can be modeled as an irreversible process under most conditions. However, the experimental work of Kunin (1958) and Bhandari et al. (1992) indicates that sorption is significantly reversible, not only at low acid concentrations, but also in concentrated solutions.

In such systems, the exchange of ionic species is accompanied by migration of the undissociated acid. Normally, the mechanism of acid sorption involves the protonation of the fixed ionogenic groups on the resin. In monomeric systems the protonation is very rapid compared to ionic diffusional transport (Helfferich and Hwang, 1985). If a concentrated solution is involved, resistances of diffusional mass transfer, occurring both

in the stagnant liquid film outside of the resins (external diffusion) and the liquid phase within the resin particle (internal diffusion) are significant. The resistance caused by the interaction of weak acid with the functional groups of amine- and hydroxyl-containing ion exchange resins may also be an important factor (Meichik and Leikin, 1989). In this situation, particle diffusion can appreciably affect the rate of exchange or even be the major rate-controlling step.

For the case of very low inlet acid concentration ($< 10^{-4}$ M), however, it is well known that film diffusion is typically the rate controlling step for ion exchange in a packed bed (Haub and Foutch, 1986a,b). The resistance of mass transfer within the resin particle may be neglected due to the low concentration and instantaneous chemical reactions compared to the rate of film diffusion. The exchanging ionic species and undissociated acid diffuse through a stagnant film around the particle (Zecchini and Foutch, 1991). The relationship between ionic and undissociated species in the bulk liquid and the film can be described by equilibrium relation of acid dissociation, which implies that reversible sorption may take place dependent on concentrations in the mobile phase as well as in the resin phase. In order to model this situation, the transport of undissociated acid, water dissociation, reversible chemical reactions and reversible sorption need to be considered.

The objective of this work is to develop a film controlled neutralization model for weak base ion exchange at very low concentration. The diffusion coefficients (given in Table III-1) for the ionic species use the limiting mobilities given by Robinson and Stokes (1959), while the value for undissociated boric acid is estimated by the Nakanishi correlation (Nakanishi, 1978). A static film hydrodynamic model and nonionic mass transfer coefficient correlations for packed beds are applied in this work. Available experimental results, from ABB Atom, of the ion exchange column operation at concentrations near 10^{-3} M boric acid is compared with simulated performance of the laboratory column as predicted by the model.

Table I
DIFFUSION COEFFICIENTS

$$D_{\text{OH}^-} = (RT/F^2)(104.74113 + 3.807544T)$$

$$D_{\text{B(OH)}_4^-} = 35.3^\circ RT/F^2$$

$$D_{\text{H}^+} = (RT/F^2)$$

$$D_{\text{Am}^+} = (RT/F^2)(1.40549T + 39.1537)$$

$$D_{\text{B(OH)}_3\text{-H}_2\text{O}} = \left[(9.97 \times 10^{-8}) / (I_{\text{B(OH)}_3} V_{\text{B(OH)}_3})^{1/3} \right. \\ \left. + (2.4 \times 10^{-8} A_{\text{H}_2\text{O}} S_{\text{H}_2\text{O}} V_{\text{H}_2\text{O}}) / (A_{\text{B(OH)}_3} S_{\text{B(OH)}_3} V_{\text{B(OH)}_3}) \right] (T/\mu_{\text{H}_2\text{O}})^\circ$$

° Corti et al. (1980)

* Nakanishi correlation

where I_i and S_i are unity.

$$V_{\text{B(OH)}_3} = 44.17 \text{ cm}^3 \text{ mol}^{-1} \quad (\text{molar volume of boric acid at } 25^\circ\text{C})$$

$$V_{\text{H}_2\text{O}} = 18.0 \text{ cm}^3 \text{ mol}^{-1} \quad (\text{molar volume of water at } 25^\circ\text{C})$$

$$A_{\text{H}_2\text{O}} = 2.8$$

Model Development

The sorption of dilute boric acid in a homogeneous anion exchange bed is addressed in this model. As discussed in Chapter II, for total boric acid concentrations less than 0.01 M, polyborate ions are not significant in the solution and only monoborate ion, B(OH)_4^- , exists. Therefore, for solutions with concentrations much lower than 0.01 M, it is reasonable to consider that the ions affecting the exchange process are NH_4^+ , H^+ , OH^- , and B(OH)_4^- . The undissociated species involved in the exchange process is boric acid, B(OH)_3 . For derivation of the model equations, Fick's first law is considered for the

undissociated species and the Nernst-Planck equation is used for exchanging ionic fluxes. The equations derived are solved numerically. A computer program is given in Appendix D.

Assumptions

Reasonable assumptions are based on the process conditions of the system. In dilute boron solutions monoborate, $B(OH)_4^-$, and boric acid, $B(OH)_3$, are both involved in the sorption process. Their removal or release affects the concentrations of the other constituents in the bulk liquid and the stagnant film. This effect can be evaluated by the boric acid dissociation equilibrium relationship

$$K_a = \frac{C_{B(OH)_4^-} \cdot C_{H^+}}{C_{B(OH)_3}} \quad (3-1)$$

where K_a is the dissociation equilibrium constant of boric acid. At 25°C, the value of K_a is 5.8×10^{-10} (Owen, 1934). Therefore, the concentration of $B(OH)_4^-$ is much lower than that of boric acid. For instance, in the solution of total boron concentration 10^{-3} M, the concentrations of borate and boric acid are approximately 10^{-7} M and 10^{-3} M, respectively. Based on this point, the ionic flux which will be determined by the Nernst-Planck equation may have less importance in this case.

The migrating boron compounds react with the functional groups of anion resin containing amine and hydroxyl groups to form amine-borate complexes. The boric acid, $B(OH)_3$, within the resin phase may first react with the mobile ions $(OH)^-$ according to the following reaction



Table II

MODEL ASSUMPTIONS

-
1. Film diffusion control
 2. The Nernst-Planck equation incorporates all interactions among diffusing ionic species and Fick's first law applied to undissociated molecule species
 3. Dissociation equilibrium is valid in both liquid phase and particle phase
 4. Neutralization occurs not only in bulk but also within the stagnant film surrounding resin particle
 5. Pseudo steady state exchange
 6. Local equilibrium at solid-film interface
 7. No coion flux across the particle surface
 8. No net coion flux within the film
 9. No net current flow
 10. Reactions are instantaneous when compared with the rate of exchange
 11. Ionic species are all univalent exchange
 12. Curvature of the film is negligible
 13. Uniform bulk and surface compositions
 14. Activity coefficients are constant and unity
 15. Plug flow
 16. Negligible axial dispersion
 17. Isothermal, isobaric operation
 18. Negligible particle diffusion resistance
-

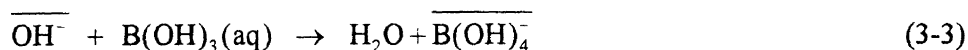
The reaction above is most likely toward the right hand side due to the consumption of B(OH)_4^- through the amine-borate reaction within the resin phase. Although the formation of amine-borate varies with different conditions (concentration of boron, functional groups of the resin and structures, temperature, etc.), the rates of the reactions may be considered to have no influence on the diffusional process.

The boron sorption process, at very low concentrations, can be treated assuming film diffusion control. This leads to other appropriate assumptions. Table III-2 lists all the assumptions that have been applied to develop a practical model.

In an ion exchange packed column, some assumptions listed in Table III-2 may not be totally accurate. Mass transfer obviously varies with time and space. However, for a practical ion exchange process, the variations of concentration with space are much more important than with time. Therefore, it is reasonable to assume pseudo steady state exchange. The concentration may not be uniform since the concentration gradients exist near each particle and nonideal flow situation. It is very difficult to handle this situation in a practical model at present stage.

Flux Expression

Consider the sorption of dilute aqueous boric acid on a weak base resin. The overall reaction is indicated in Equation 3-3, where the barred quantities refer to species in the resin phase.



As discussed in Chapter II, for boron concentrations below 10^{-3} , only monoborate exists in solution from the dissociation of boric acid. The concentrations of ions B(OH)_4^- , H^+ , OH^- , and molecular B(OH)_3 are to an extent characterized by the boric acid dissociation equilibrium relation expressed as Eq. 3-1 and the water dissociation equilibrium constant K_w ,

$$K_w = \frac{(\text{OH}^-)(\text{H}^+)}{\text{H}_2\text{O}} = 10^{-14} \quad (3-4)$$

$\text{B}(\text{OH})_4^-$ diffuses from the bulk solutions through the stagnant film surrounding the resin to the particle surface. At the surface, $\text{B}(\text{OH})_4^-$ ions disappear into the resin phase, releasing OH^- ions that react with the H^+ ions present within the film. For convenience, the following abbreviations are used in the flux equations: 'x' for $\text{B}(\text{OH})_4^-$, 'a' for $\text{B}(\text{OH})_3$, 'o' for OH^- and 'h' for H^+ .

The characteristic conditions in ion exchange require no coion flux into the resin; i.e.

$$J_h = 0 \quad (3-5)$$

no net current flow,

$$J_o + J_x = 0 \quad (3-6)$$

and electrical neutrality to give

$$C_h = C_x + C_o \quad (3-7)$$

The Nernst-Planck equation is used to describe the fluxes of the ionic species in the dilute solution, and Fick's first law for diffusion of undissociated acid. Thus

$$J_h = -D_h \left\{ \frac{\partial C_h}{\partial r} + \frac{FC_h}{RT} \frac{\partial \phi}{\partial r} \right\} \quad (3-8)$$

$$J_o = -D_o \left\{ \frac{\partial C_o}{\partial r} - \frac{FC_o}{RT} \frac{\partial \phi}{\partial r} \right\} \quad (3-9)$$

$$J_x = -D_x \left\{ \frac{\partial C_x}{\partial r} - \frac{FC_x}{RT} \frac{\partial \phi}{\partial r} \right\} \quad (3-10)$$

$$J_a = -D_a \frac{\partial C_a}{\partial r} \quad (3-11)$$

From Equations 3-5 to 3-11 with the pseudo steady state assumption, the fluxes of borate ion and hydroxide ion are described as follows:

$$J_x = - \left[\frac{2D_o D_x (C_o + C_x)}{2D_o C_o + D_o C_x + D_x C_x} \right] \frac{dC_x}{dr} \quad (3-12)$$

$$J_o = - \left[\frac{2D_o D_x (C_o + C_x)}{2D_x C_x + D_x C_o + D_o C_o} \right] \frac{dC_o}{dr} \quad (3-13)$$

Eliminating 'C_o' from Equation 3-12 by Equation A-22 and intergrating with the boundary conditions shown in Equations A-26 and A-27, borate, undissociated boric acid and the total boron flux expressions in terms of diffusing ion concentrations can be obtained. The detailed derivation of the flux expressions are given in Appendix A. The resulting flux expressions for these species through the stagnant film surrounding the resin are:

$$J_x = - \frac{2D_o D_x}{\delta(D_o - D_x)} [C_o^\circ + C_x^\circ - C_x^* - C_o^*] \quad (3-14)$$

$$J_a = - \frac{D_a}{\delta K_a} [C_x^\circ (C_x^\circ + C_o^\circ) - C_x^* (C_x^* + C_o^*)] \quad (3-15)$$

The total boron flux may be expressed by summation of Equations 3-14 and 3-15.

$$J_T = J_x + J_a = - \frac{2D_o D_x}{\delta(D_o - D_x)} [C_o^\circ + C_x^\circ - C_x^* - C_o^*] - \frac{D_a}{\delta K_a} [C_x^\circ (C_x^\circ + C_o^\circ) - C_x^* (C_x^* + C_o^*)] \quad (3-16)$$

Effective Diffusivities and Exchange Rate

The derivation of effective diffusivities is based on the hydraulic radius model. If the concentration of borate within the resin is expressed as 'q_x,' with the static film model and linear driving force assumption, the rate of change of the borate ion concentration within the resin can be given as follows:

$$\frac{dq_x}{dt} = k'_x a_s (C_x^\circ - C_x^*) \quad (3-17)$$

where k'_x is the liquid phase mass transfer coefficient for borate ions. Applying the assumption of pseudo steady state, the borate concentration can be related to its flux across the film as:

$$\frac{dq_x}{dt} = -J_x a_s \quad (3-18)$$

From Equations 3-17 and 3-18, the following expression can be readily obtained.

$$J_x = -k'_x (C_x^o - C_x^*) \quad (3-19)$$

As defined by Kataoka et al. (1973), the relationship of effective diffusivity and mass transfer coefficient is given by Equation 3-20.

$$k' = \frac{D_e}{\delta} \quad (3-20)$$

where δ is the thickness of the static film. Now the explicit expression of effective diffusivity for borate ions can be obtained. Substituting Equation 3-20 into Equation 3-19 to get Equation 3-21.

$$J_x = -\frac{D_e}{\delta} (C_x^o - C_x^*) \quad (3-21)$$

Comparing Equation 3-21 with Equation 3-14, the resulting effective diffusivity for borate ion is obtained as:

$$D_e = -\frac{2D_o D_x}{(D_o - D_x)(C_x^o - C_x^*)} [C_o^o + C_x^o - C_o^* - C_x^*] \quad (3-22)$$

In the hydraulic radius model, fluid flow effects are incorporated in the non-ionic mass transfer coefficients, which depend on the particle Reynolds number as calculated by either Carberry's (1960) or Kataoka's (Kataoka et al., 1973) correlations. They are:
Carberry's correlation (for $Re > 20$)

$$k = 1.15 \frac{u}{\epsilon} (\text{Sc})^{2/3} (\text{Re})^{-1/2} \quad (3-23)$$

Kataoka's correlation (for $\text{Re} < 20$)

$$k = 1.85 \frac{u}{\epsilon} \left(\frac{\epsilon}{1-\epsilon} \right)^{1/3} (\text{ScRe})^{-2/3} \quad (3-24)$$

From the comparison of the hydraulic radius model and the Nernst film model (Kataoka et al., 1973) the effective diffusivity can be related to the non-ionic mass transfer coefficient for the borate ion, by:

$$\left(\frac{D_e}{D_x} \right)^{2/3} = \frac{k'_x}{k_x} \quad (3-25)$$

The influence of ions with different mobilities is indicated by the ratio of ionic to non-ionic mass transfer coefficient, R_x . For borate ions, this may be written:

$$R_x = \frac{k'_x}{k_x} \quad (3-26)$$

Comparing Equations 3-21 and 3-22, the following relationship can be obtained.

$$R_x = \left(\frac{D_e}{D_x} \right)^{2/3} \quad (3-27)$$

Therefore, the particle rate equation for borate ions may be expressed as:

$$\frac{dq_x}{dt} = k_x R_x a_s (C_x^o - C_x^*) \quad (3-28)$$

This expression has more physical meaning than Equation 3-17 since it incorporates fluid flow effects and different ion mobilities on the exchange rate.

With the same assumptions, the rate expression for boric acid is expressed as:

$$\frac{dq_a}{dt} = k a_s (C_a^o - C_a^*) \quad (3-29)$$

The concentrations of boric acid in Equation 3-29 can be eliminated by the substitution of the dissociation equilibrium relation, Eq. 3-1. Therefore, the rate expression for boric acid in terms of diffusing ions may be written:

$$\frac{dq_a}{dt} = \frac{ka_s}{K_a} [C_x^o (C_x^o + C_o^o) - C_x^* (C_x^* + C_o^*)] \quad (3-30)$$

The resulting total diffusion rate in the resin phase, in terms of boron, is:

$$\begin{aligned} \frac{dq_T}{dt} &= \frac{dq_a}{dt} + \frac{dq_x}{dt} \\ &= \frac{ka_s}{K_a} [C_x^o (C_x^o + C_o^o) - C_x^* (C_x^* + C_o^*)] + k_x R_x a_s (C_x^o - C_x^*) \end{aligned} \quad (3-31)$$

The interfacial concentration, in the expressions of the effective diffusivities and rate equations, can be eliminated by the use of the selectivity coefficient, K_o^x , which will be discussed later.

Column Material Balance

The concentration profile within the column and its effluent concentration history are determined by the overall column material balance obtained from the equation of continuity under the assumptions made for a given system. As mentioned above, plug flow is assumed and the effects of axial dispersion are neglected in the derivation of this column material balance. Based on these assumptions, for a steady state flow system, the column material balance for each species may be written as:

$$\frac{\partial C_i}{\partial t} + \frac{(1-\epsilon)}{\epsilon} \frac{\partial q_i}{\partial t} + \frac{u}{\epsilon} \frac{\partial C_i}{\partial z} = 0 \quad (3-32)$$

where z is the distance from the column inlet, in cm. The term $\frac{\partial q_i}{\partial t}$ is given by the particle rate expressions above. The corresponding initial and boundary conditions are:

$$C_x^o(z, t = 0) = 0 \quad (3-33)$$

$$C_x^o(z = 0, t) = C_x^f \quad (3-34)$$

where C_x^f is the concentration of borate at the column inlet. The material balance is a partial differential equation, which, after some change of variables, is readily solved by the method of characteristics.

Dimensionless Expressions and Solution

The differential Equations 3-28, 3-30 to 3-32 may be solved by both analytical and numerical methods with the corresponding initial and boundary conditions. However, with the advent of high speed computers, numerical methods have become ever more powerful in solving differential equations. The use of a dimensionless approach is more convenient in solving these equations. For this purpose, Equations 3-28, 3-30 to 3-32 can be rewritten using the following dimensionless terms:

Dimensionless mobile phase concentration

$$X_i = \frac{C_i}{C_T} \quad (3-35)$$

Dimensionless stationary phase concentration

$$Y_i = \frac{q_i}{Q} \quad (3-36)$$

Dimensionless distance coordinate

$$\xi = \frac{k(1-\epsilon)}{ud_p} z \quad (3-37)$$

Dimensionless time coordinate

$$\tau = \frac{kC_T^f}{d_p Q} \left(t - \frac{\varepsilon z}{u} \right) \quad (3-38)$$

After changing to these dimensionless variables and rearrangement, Equations 3-28, 3-30 to 3-32 become:

$$\frac{dY_x}{d\tau} = 6R_x (X_x^o - X_x^*) \quad (3-39)$$

$$\frac{dY_a}{d\tau} = \frac{6}{K_a} \frac{D_a}{D_{ex}} R_x [X_x^o (X_x^o + X_o^o) - X_x^* (X_x^* + X_o^o)] \quad (3-40)$$

$$\begin{aligned} \frac{dY}{d\tau} &= \frac{dY_a}{d\tau} + \frac{dY_x}{d\tau} \\ &= \frac{6}{K_a} \frac{D_a}{D_{ex}} R_x [X_x^o (X_x^o + X_o^o) - X_x^* (X_x^* + X_o^o)] + 6R_x (X_x^o - X_x^*) \end{aligned} \quad (3-41)$$

$$\frac{\partial X_i}{\partial \xi} = - \frac{\partial Y_i}{\partial \tau} \quad (3-42)$$

Likewise, the initial and boundary conditions can be rewritten as:

$$X_x(\xi, \tau = 0) = 0 \quad (3-43)$$

$$X_x(\xi = 0, \tau) = X_x^f \quad (3-44)$$

Numerical Solution

Equations 3-41 and 3-42, which describe the total exchange rate and column material balance in a dimensionless form, are coupled first order ODE. Once the interface concentration and effective diffusivities are obtained, these equations are easy to be solved numerically with the initial and boundary conditions shown in Equations 3-43 and 3-44.

The interface concentration in terms of bulk concentrations and self diffusivities can be obtained by integrating Equation A-19 and introducing selectivity coefficient expression. The detail will be given in the following section.

Euler and Adam's-Bashforth explicit methods were applied in this work for solving the ODEs. Runge-Kutta fourth order was combined to improve the accuracy to the third order in the dimensionless distance increment. The details will be discussed in later section of this chapter. In addition, water dissociation equilibrium was considered as a factor of determining ionic species concentration in bulk. Newton-Raphson method was used to determine hydrogen ion concentration based on water dissociation equilibrium, acid dissociation equilibrium, mass balance and charge balance. A computer code for solving this model is given in Appendix D.

Results and Discussion

This model is developed to handle the ion exchange of extremely dilute weak acid solutions with incomplete dissociated acid species by a base form anion resin. For the system with incomplete dissociated base, for example, ammonia or morpholine treated by an acid form cation resin, this model can also be acceptable with a little modification. Since the process was assumed to be film diffusion controlled, it can be applied to the system having fast reaction in the resin phase with negligible particle resistance.

Experimental data from ABB Atom for sorption of boric acid was used to evaluate this model. The comparison of values calculated by the model and experimental data is given in Figure III-1. The left concentration profile was obtained after a process run of 115 minutes with feed flow rate of 2 ml/sec. After 22 hours, the right concentration profile was obtained by the calculation of this model. This is compared with 24 hours obtained by experiment. This model is a relatively good to fit of experimental results, especially the tendency of the data. With this model, the effects of major parameters, such

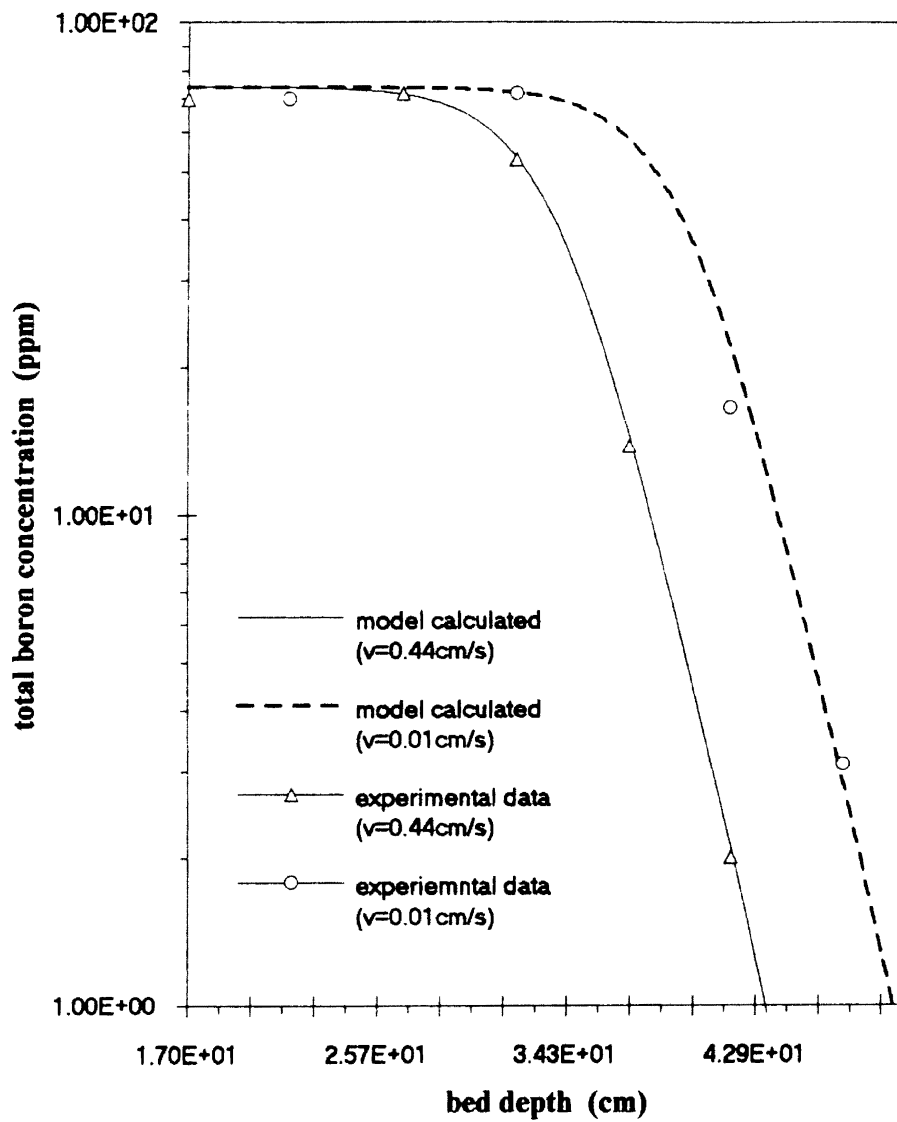


Figure III-1 Comparison of model calculated values and experimental data

as selectivity coefficient and dissociation equilibrium constant, are studied. The reversible diffusion and different contributions of ionic and undissociated species in sorption of weak electrolytes are discussed.

Interface Concentration

Consider the exchange of counter ions A and B between an exchange resin and a solution containing no other counter ions. Suppose that the ion exchanger is initially in the A form and that the solution contains ions B. Applying the mass action law to the equilibrium relationship in ion exchange, the expression for counter ion exchange can be written:



In the situation of counter ions of equal valence, the corresponding selectivity coefficient can, in molar concentration, be expressed as:

$$K_A^B = \frac{\bar{C}_B C_A}{\bar{C}_A C_B} \quad (3-46)$$

Applied to this work with consistent nomenclature, and assuming that the film-resin interface concentration is taken to be that in equilibrium with the instantaneous resin composition, rearrangement in a convenient form yields,

$$K_o^x = \frac{C_o^*/C_T y_x}{C_x^*/C_T 1-y_x} \quad (3-47)$$

Equation 3-47 gives the relation of interface counter ions concentrations. The explicit expression is:

$$C_o^* = C_x^* \left(K_o^x \frac{1-y_x}{y_x} \right) \quad (3-48)$$

The interface and bulk liquid concentration relationship given in Equation 3-49 may be obtained from the integration of Equation A-19.

$$[D_o C_o^* + D_x C_x^*] [C_o^* + C_x^*] = [D_o C_o^o + D_x C_x^o] [C_o^o + C_x^o] \quad (3-49)$$

Substituting Equation 3-48 in Equation 3-49 and rearranging, the following expression for the interface concentration of borate ion is obtained:

$$C_x^* = \sqrt{\frac{(D_o C_o^o + D_x C_x^o)(C_o^o + C_x^o)}{(D_o K_o^x \frac{1-y_x}{y_x} + D_x)(K_o^x \frac{1-y_x}{y_x} + 1)}} \quad (3-50)$$

The convenient expression for analysis is given in Equation 3-51

$$\frac{C_x^*}{C_x^o} = \sqrt{\frac{(\alpha Y + 1)(Y + 1)}{(\alpha S + 1)(S + 1)}} \quad (3-51)$$

where

$$S = K_o^x \frac{1-y_x}{y_x} \quad (3-52)$$

$$Y = \frac{C_o^o}{C_x^o} \quad (3-53)$$

$$\alpha = \frac{D_o}{D_x} \quad (3-54)$$

Equation 3-51 shows that the ratio of the interface to bulk concentrations depends on:

1. the ratio of bulk concentrations of exchanging ions;
2. the ratio of interface concentrations of exchanging ions; and
3. the ratio of self-diffusivities of exchanging ions.

Since the concentrations of exchanging ions both in the bulk and at the interface are determined by the acid dissociation equilibrium relationship and water dissociation relationship, the degree of acid dissociation greatly influences the ratio of the interface to bulk concentration. The selectivity coefficient is, of course, also one of the major effects on the ratio of the interface to bulk concentrations. These effects will be discussed in later sections.

Effective Diffusivity

Combining Equations 3-24, 3-48 and 3-50, the interface concentrations can be eliminated from the expression of effective diffusivity. The resulting expression of effective diffusivity, D_e , for borate ions can be rewritten in terms of the ratio of the bulk concentrations of counter ions and their self diffusivities, selectivity coefficient, and borate ion concentration fraction in resin phase.

$$D_e = \frac{2\alpha D_x}{(1-\alpha)(1-X)} [SX + X - Y - 1] \quad (3-55)$$

where

$$X = \frac{C_x^*}{C_x^o} = \sqrt{\frac{(\alpha Y + 1)(Y + 1)}{(\alpha S + 1)(S + 1)}} \quad (3-56)$$

This was the expected expression for ion species effective diffusivity analogous to that derived by Haub (1984).

Equation 3-55 reveals that effective diffusivity depends on α , D_x , K_o^* , y_x and the bulk concentration ratio of exchanging ions C_o^o/C_x^o . The α , D_x , and K_o^* are the system variables and are fixed for a given system. But these values vary from one system to another and have a large impact upon the effective diffusivity and the rate of exchange. Generally, the effective diffusivity increases as $\alpha > 1$, and decreases as $\alpha < 1$ with progression of ion exchange.

The resin selectivity coefficient has a strong influence on the effective diffusivity. Figure III-2 shows the effect of selectivity coefficient on the effective diffusivity under $\alpha = 5.7$ and $K_o^* = 10$ to 0.1 in the case of monovalent ion exchange system. As this figure shows clearly, the effective diffusivity increases with y_x but the degree of this increase is changed by the different values of the selectivity coefficient. Namely, for large values, $K_o^* > 1$, $D_e - y_x$ curves tend to concave, and in the early stage of exchange except at the very beginning, the values of the effective diffusivity increase more slowly but sharply in the final period of exchange. On the contrary, for small values, $K_o^* < 1$, the curve increases sharply from the start of exchange and the values of the effective diffusivity are approximately constant as the concentration fraction in resin approaches unity.

These different phenomena reflect the complexity of influence of the selectivity coefficient on the effective diffusivity. For the former, it may be the reason that under favorable equilibrium, film diffusion resistance is much greater in the early stage of exchange, and the resistance in the resin phase is negligibly small. For the later, it may be that diffusion resistance in the resin phase is much larger than that in the liquid phase in the final stage of exchange.

The existence of undissociated acid also influences the effective diffusivity through dissociation in the bulk and the acid-base reaction within the resin phase. The fact is

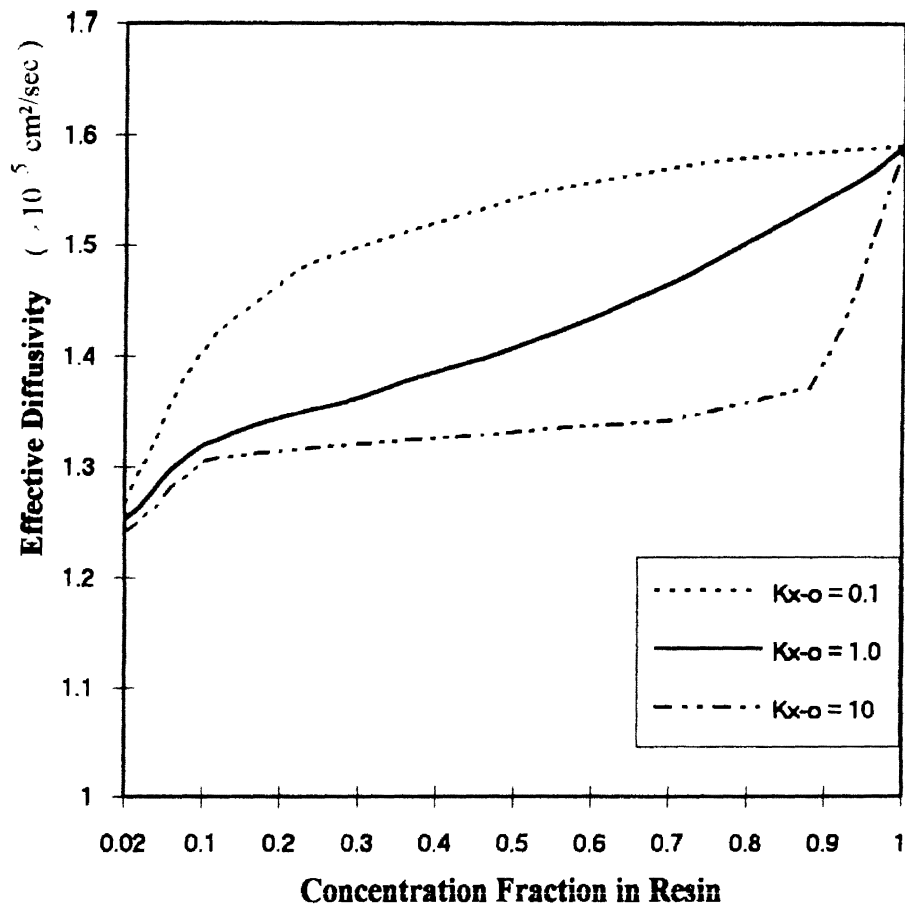


Figure III-2 Variation of effective diffusivity D_e with y and K_0^x for bulk phase neutralization

contributed by the factors of changing the bulk and interface concentrations of exchanging ion species and changing the value of y_x . The unexpected degree of increase of the effective diffusivity at the beginning of exchange is the result of the diffusion of undissociated acid.

Contributions to the Exchange

According to the rate controlling ion model of Helfferich and Hwang (1985), for weak acids, the only species contribution to the diffusion flux is the undissociated acid molecule. This is valid only if the degree of dissociation of weak acid is very low. In this case the ionic flux is much smaller than the flux of undissociated molecular species. Equation 3-15 shows that the flux of undissociated species is proportional to $1/K_a$. With the increase of the dissociation equilibrium constant, the contribution of undissociated acid molecules to the total diffusion decreases. The plots of different contributions to the total exchange by the migration of acid molecule are shown in Figure III-3. It is clear from these plots and Equations 3-18 and 3-29 that the contribution of ionic species diffusion to the total exchange increases with the values of dissociation equilibrium constant. In the case of low acid concentration with large dissociation equilibrium constant, the contribution of ionic species diffusion is significant, even dominant.

Reversible Diffusion

Once the concentration of exchanging ions at the resin surface is higher than that in the bulk, reversible diffusion takes place. As discussed above, the undissociated boric acid entering the resin phase will react to produce borate ions. Thus, the concentration of borate within the resin phase increases much faster than in the case of ionic species diffusion alone. The concentration of borate at the resin surface consequently increases

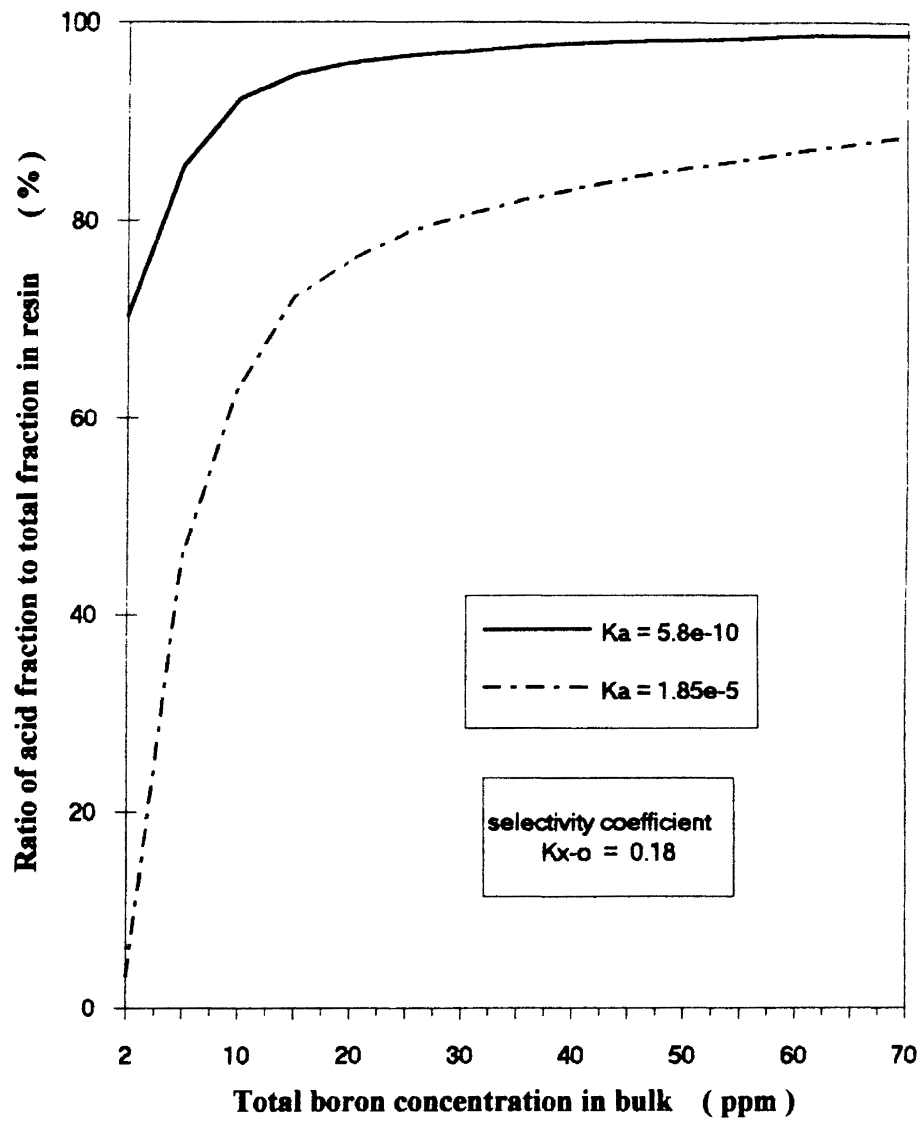


Figure III-3 Effect of dissociation equilibrium constant on total mass transfer rate

rapidly. As a result, it is not difficult to make the conclusion that the ion exchange of weak electrolytes often accompanies reversible diffusion.

The degree of reversible diffusion during the exchange process varies with the selectivity coefficient and the dissociation equilibrium constant. It is hard to obtain the direct relationship or explicit expression between these. Figure III-4 shows the effects of selectivity coefficient on the exchange process. These concentration distributions were obtained with the region of selectivity coefficient from 0.1 to 10 and with the same operating time. Experimental results, shown as black dots and obtained with selectivity coefficient 0.18, are given for comparing. With increase of selectivity coefficient greater than unity, the profile moves from left to right. This phenomena indicates that the exchange process slows down since reversible diffusion occurs. The degree of reversible diffusion increases with increase of selectivity coefficient. The same results were obtained with a decrease of selectivity coefficient less than unity. The effects of dissociation on the exchange process is shown in Figure III-5. The concentration distribution profiles moves from left to right with increasing dissociation equilibrium constant. Reversible diffusion occurs significantly in the case of higher dissociation. The two left profiles also imply that reversible diffusion may take place only within certain regions of bulk concentrations. Figure III-6 shows the effect of dissociation on the utilization of resin capacity. The results reflect that the utilization of resin capacity, in sorption of weak electrolytes, decreases with an increase in dissociation. This phenomena may result from the equilibrium relation between the interface and resin concentrations of exchanging ionic species. With lower values of the dissociation equilibrium constant, the migration of undissociated species gives the major contribution to total diffusion. In this case, resin capacity use is higher since that equilibrium relation has little influence on the diffusion of undissociation species.

Generally, reversible diffusion can be related to larger selectivity coefficient and a higher degree of dissociation or lower acid concentration. With a large selectivity

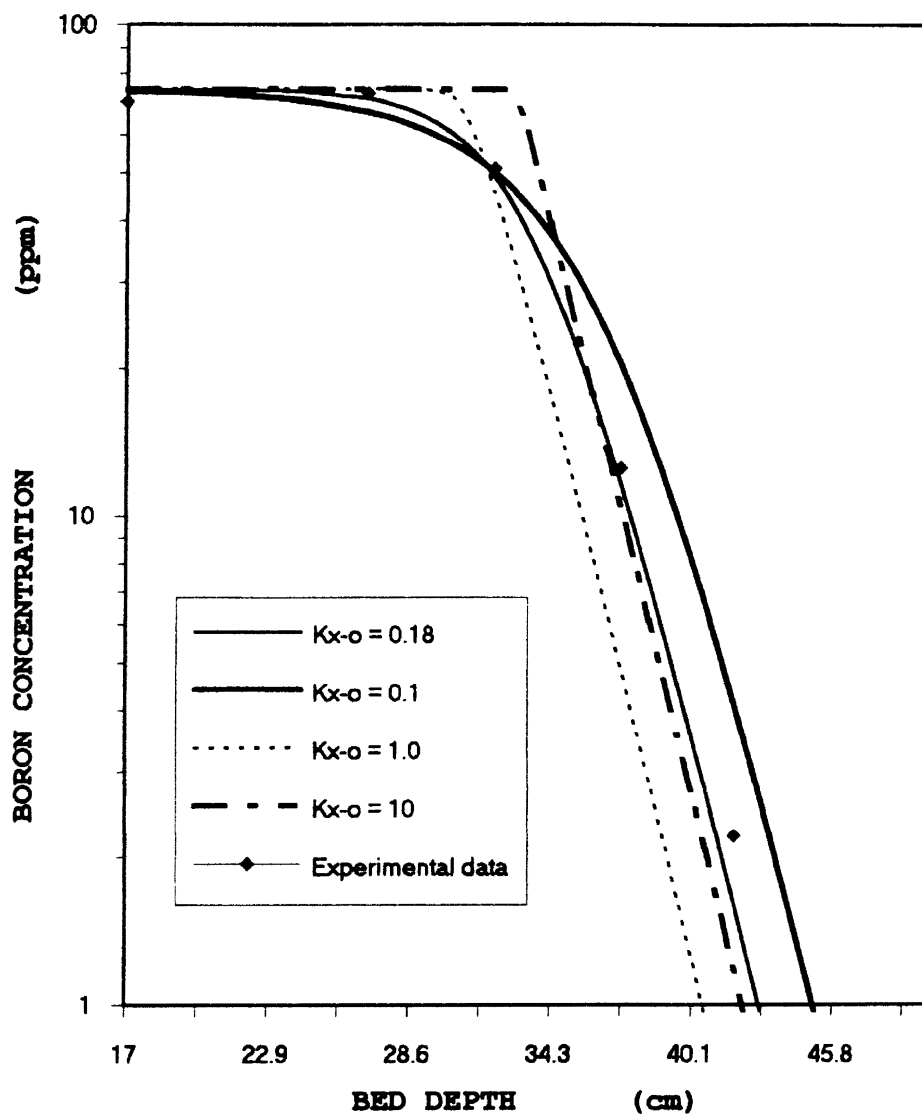


Figure III-4 Effect of selectivity coefficient K_{O}^{X} on the concentration distribution profiles (Experimental data obtained at the value of $K_{O}^{X} = 0.18$)

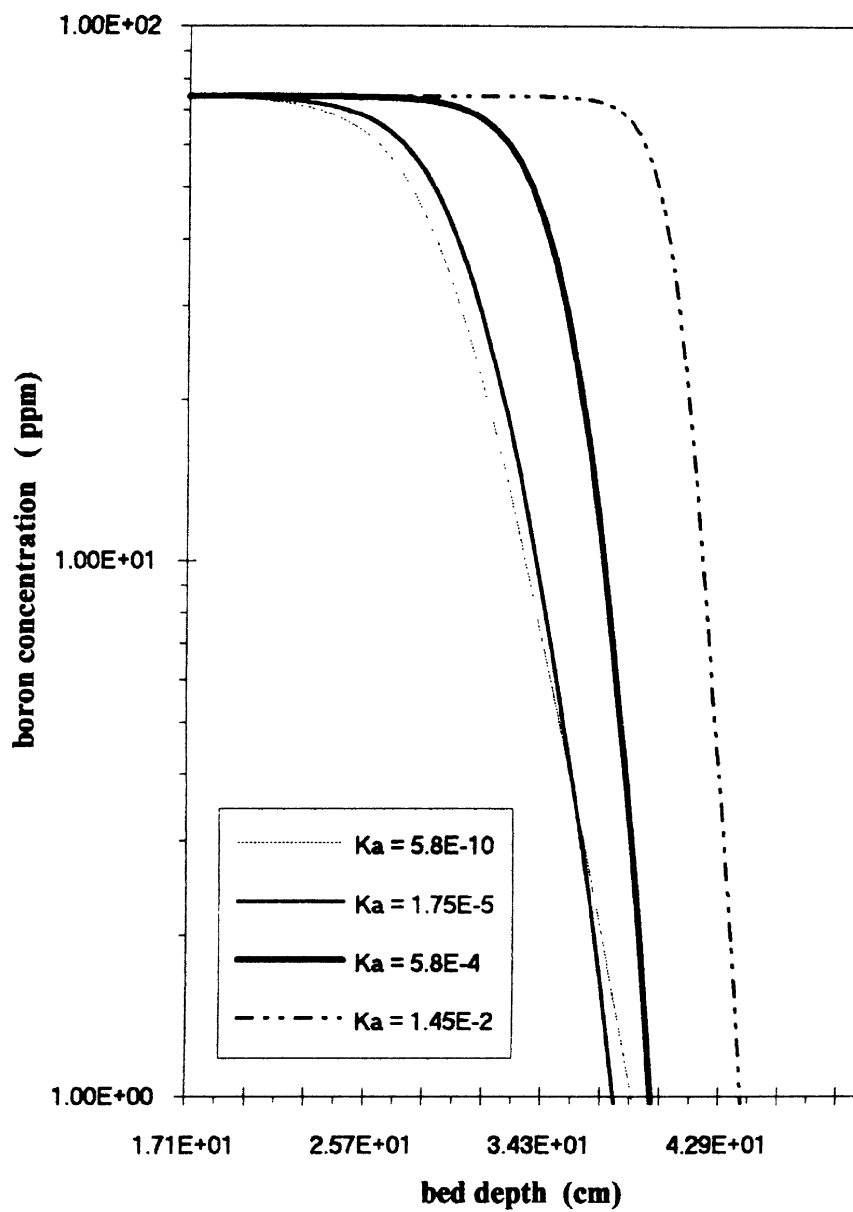


Figure III-5 Effect of dissociation equilibrium constant on total exchange rate:
Concentration distribution in column

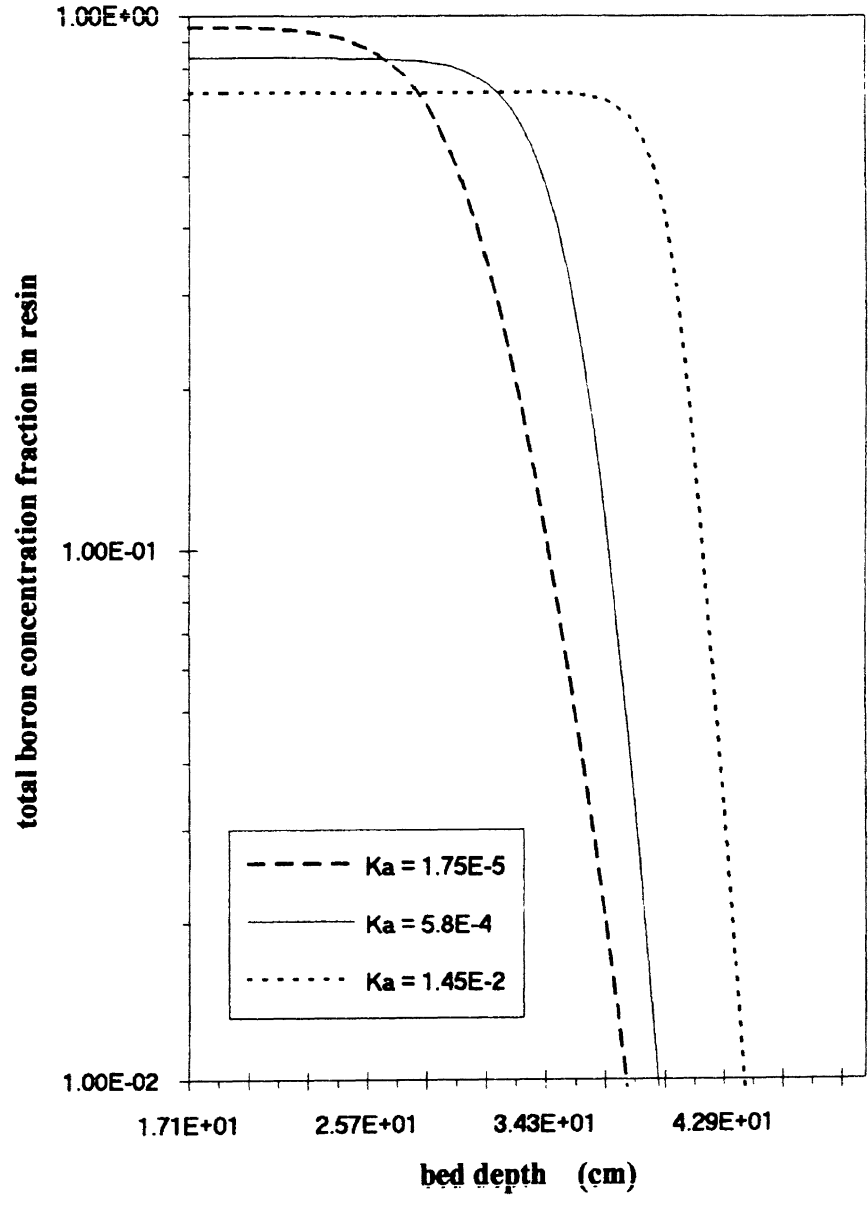


Figure III-6 Effect of dissociation equilibrium constant on total exchange rate:
Concentration fraction in resin

coefficient, $K_o^x > 1$, the diffusion of counter ions existing initially in the bulk liquid is favorable. The film diffusion resistance is dominant at the beginning of the exchange, and the particle diffusion resistance becomes a major factor of the diffusion resistance in the final stage of exchange. The situation is just opposite if the system of interest has a small value of the resin selectivity coefficient, $K_o^x < 1$. Thus, the interface concentration increases rapidly in the final stage of exchange for strong favorable exchange, $K_o^x > 1$, and at the beginning of exchange for less favorable exchange, $K_o^x < 1$. From Equation 3-50, the interface concentration of borate ion will be greater than its concentration in the bulk, if the value of the concentration ratio Y of exchanging ions in the bulk is greater than the value of the interface concentration ratio S of exchanging ions. Therefore, a system with a large selectivity coefficient is subject to the reversible diffusion in the ion exchange of weak electrolyte solutions. In the case of a higher degree of dissociation, the driving force for ionic species is much larger because of higher bulk concentrations. This results in the interface concentrations increasing very rapidly. The diffusion of undissociated species accelerates the increase of the interface concentrations due to the dissociation and reaction to increase ionic species concentrations within the resin phase and at the resin surface as well. Under this situation, it is easy to make the interface concentrations greater than the bulk concentrations in the lower bulk acid concentration region.

Ratio of Self Diffusivities of Acid Molecule to its Ion

Weak electrolytes usually dissociate more than one kind of ionic groups at different concentrations. As mentioned in Chapter II, boric acid may dissociate to more than three kinds of different ion groups at concentrations higher than 0.01 M. For different ion groups, the mobility is not the same. The diffusion rate, thus, varies with different ratio of self diffusivities of the weak electrolyte molecule to its ions due to the different contributions to total diffusion, different mobilities and dissociation degree in the exchange

process. Figure III-7 shows the effect of self-diffusivity ratios of the acid molecule to its ions on exchange process. The results indicate that the total exchange rate varies with the different ratios and imply that the contribution of acid molecule diffusion to total exchange rate is dominant in the conditions with dissociation equilibrium constant value 5.8×10^{-10} and selectivity coefficient 0.18. Generally, exchange rate increases with increase of the ratios. The largest ratio, however, does not correspond to the sharpest concentration distribution profile because the reversible diffusion is more significant in this situation. Generally speaking, the total exchange rate in sorption of weak electrolyte by ion exchange varies with feed concentration conditions if more than one kind of ion group, resulted from dissociation of weak electrolytes in such feed concentration conditions, may be present in solution.

Numerical Treatment

The rate and material balance equations derived here consist of a system of differential equations. It is preferable to solve these equations by a numerical method. The rate equations are ordinary differential equations and are expressed explicitly in concentration. Some of the single step methods, for instance Euler method (either explicit or modified), Runge-Kutta fourth order method, and Adam's-Bashforth explicit method, may be applied for their solution. Haub and Foutch (1986a,b) employed the explicit Euler method to solve the rate equation for mixed bed ion exchange. The error was on the order of the step size (global). To improve the accuracy, it is necessary to use very small time step size which increases the calculation time. Omatete (1980) compared the Euler explicit method, modified Euler method and Runge-Kutta-Fehlberg method and implied that the modified Euler method was the best one for this application, since it needs the least computer time to converge to the same solution. The Adam's-Bashforth explicit method can be combined with Euler's methods and Runge-Kutta fourth order method to

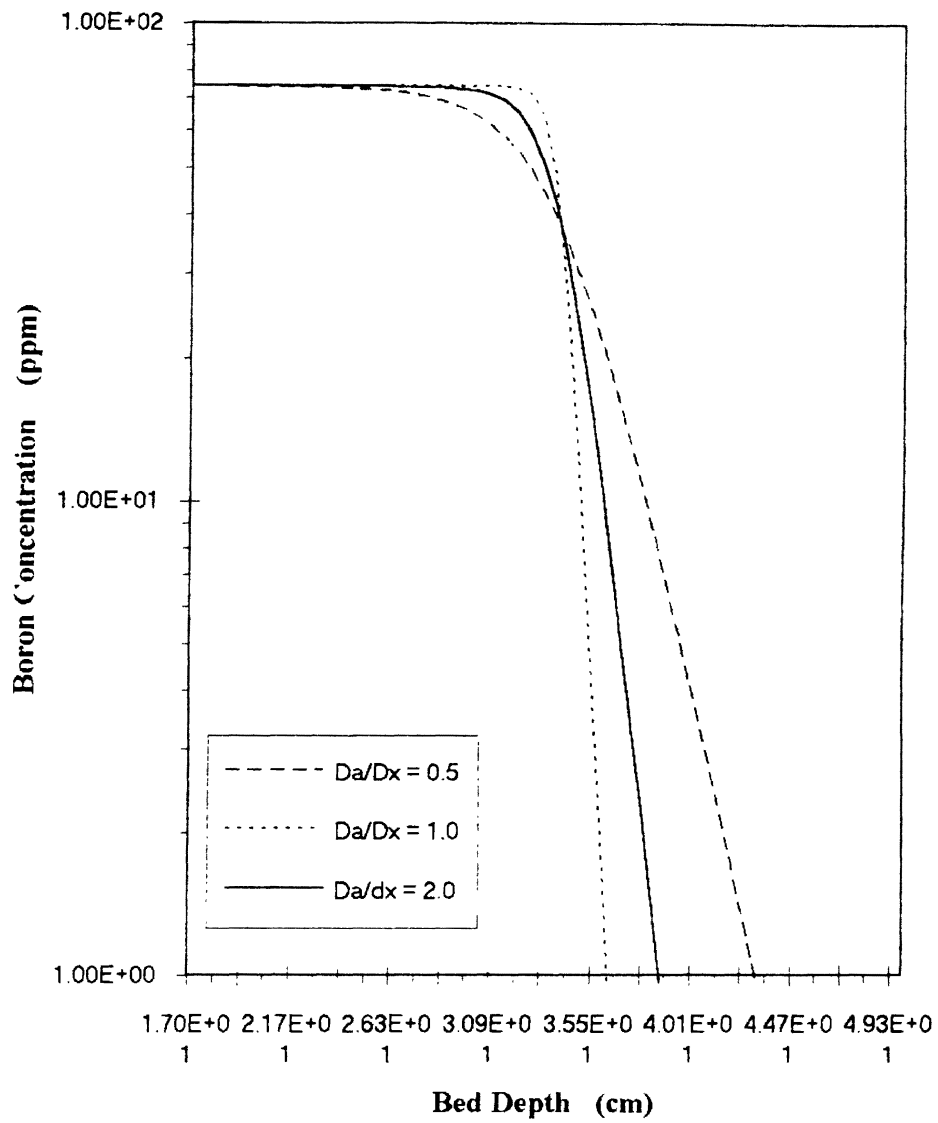


Figure III-7 Variations of concentration distributions in column with self-diffusivity ratios of boric acid to its ions
 Da -- acid molecular self-diffusivity
 Dx -- ionic group self-diffusivity

solve the material balance equation to improve the accuracy to the third order in the dimensionless distance increment. The Adam's-Bashforth method requires only one evaluation per step once the initial four steps have been completed. So it considerably improves the accuracy without increasing calculation time significantly.

Conclusion

The model developed here can be used to treat the sorption of extremely dilute solution of weak acid on base form anion resin. It may be adapted for the sorption of extremely dilute solutions of weak base on a acid form cation resin.

The effects of the migration of undissociated acid molecules, dissociation equilibrium constant, and selectivity coefficient on the ion exchange process were studied. These results indicated that the process of the sorption of weak electrolyte solutions in ion exchange is more complicated. The reversible diffusion is significant under large values of the selectivity coefficient and the dissociation equilibrium constant. The contribution of ionic diffusion is significant and even dominant in the system with a high degree of dissociation.

CHAPTER IV

SIMULATION OF A MIXED-BED RADIAL FLOW DEMINERALIZER

Introduction

Removal of both suspended and dissolved impurities from reactor water is an important problem in modern nuclear power plants. The reactor water clean-up (RWCU) system is designed for this task. The most fundamental questions for the selection of clean-up processes are related to the chemistry of the impurities in the condensate in the make-up water and in the main recirculation system of the reactor (Ljungberg and Hallden, 1984). Based on the practical experience of reactor water circulation in nuclear power plants, the principal sources of impurities in the feed water and condensate are the corrosion of the structural materials and input of different chemical compounds by the make-up water and by condenser leakage (Fejes et al., 1989). Considering the particularities of the reactor operation process, the removal of suspended impurities is much more likely to be performed by the heat transfer core surfaces than by the clean-up itself (Fejes et al., 1989). Subsequently, the main purpose of the RWCU system will be the removal of the dissolved impurities. Thus, ion exchange is the most suitable unit operation for this purpose.

For boiling water reactors, most operating experience shows that mixed-bed ion exchange has great advantages, and is the most economic and effective means for meeting the requirement of RWCU. The problem with conventional axial flow mixed-bed ion exchange is, however, the unavoidable fast build-up of the pressure drop during operation.

Because of high pressure drop, the mixed-bed resin often has to be replaced long before the exchange capacity of the resin has been exhausted.

Mixed-bed ion exchange in radial flow with larger flow area and shorter flow path has little tendency for pressure drop build-up. The operating practices of radial flow demineralizers of the RWCU system in some ABB Atom power plants have satisfactorily shown this advantage (Fejes et al., 1989).

As shown in Fig. II-1, the feed water flows radially through the packed-bed in a cylindrical unit. In general, the essential features of kinetics of different mixed-bed ion exchange processes may be applied for mixed-bed radial flow deionization systems. Because of the radial flow geometry, however, some complications arise in mathematical modeling. Since the radial flow rate in the cylindrical column varies in a broad range along the radial coordinate of the column, radial dispersion and external mass transfer coefficients are no longer constants as in axial flow ion exchange. This feature is rarely considered in modeling column performance of axial flow ion exchange.

As indicated in Chapter II, no theoretical study for multi-component mixed-bed ion exchange in cylindrical radial flow geometry has been found. The purpose of this work is to develop a practical model which approximates such a system. The current theory of liquid resistance-controlled reactive mixed-bed ion exchange to very low solution concentrations, developed by Haub and Foutch (1986a), is applied in this model. Since the dispersion term is included in the governing equation under consideration, it has higher order partial differential equations that must be solved to obtain the concentration history as well as the concentration distribution in the column for each species. Therefore, in this work a numerical approach to the solution of this model was preferable to analytical solution. To avoid possible diversion from solution, the model was solved by applying the 'Control-volume method' developed by Patankar (1991). The solution of this model enables us to address several important issues, such as specific surface area of the bed material and the flow rate, which concern the characteristics and performance of ion

exchange packed-bed with cylindrical radial flow geometry and its differences with axial flow units.

Model Development

This model was developed for cylindrical radial flow packed-bed for mixed-bed ion exchange with very low solution concentrations (below 1 ppm). Depending on the ratio of cation to anion resins and other optimum operating conditions, a mixed bed ion exchange unit may produce a neutral, or slightly acidic or basic effluent. Within a mixed-bed, the neutralization may take place in the bulk solution, Nernst film, or film-resin interface due to the variation in the solution ionic composition. For ion exchange at very low concentrations, the water dissociation needs to be taken into account. Since the cylindrical radial flow mixed bed for reactor water clean-up often operates under high flow rate with solutions at very low concentrations, it is reasonable to assume that the process is film diffusion controlled. Therefore, this model development is based on the kinetics of liquid phase diffusion control mixed-bed ion exchange. The effluent concentrations are determined by using the column material balance differential equations which are solved numerically.

Assumptions

Some assumptions are the same as those discussed in the previous chapter, which are: film diffusion control, instantaneous neutralization reactions compared to the rate of diffusion, pseudo steady state mass transfer across the Nernst film, uniform bulk and surface compositions for a given exchange particle, local equilibrium for each component at the solid-film interface, isothermal system, and activity coefficients of unity for the concentrations studied. The characteristics of ion exchange require no net coion flux, no

net current flow and no coion flux across the particle surface. For the application of mixed-bed ion exchange at very low concentrations, the above assumptions are valid and necessary in this work.

Consider an ion exchange packed-bed with cylindrical radial flow geometry which is filled with uniform spherical porous and homogeneously packed solid resin. The flow pattern is plug type and uniform in radial direction. Compared with radial dispersion, molecular dispersion in the axial direction may be neglected. The assumptions of plug flow, uniform flow and negligible axial dispersion lead to a negligible vertical concentration gradient in the radial flow column. Unlike axial flow, the self-stabilizing effect does not exist in a radial flow column because the flow pattern is radially symmetrical and cannot be aligned with gravity. Any defects in the packing may cause a non-uniform flow pattern, even channeling. Although it can be a problem in some practical cases, the possible maldistribution of flow streams is ignored in this model development.

Flux Expressions

As in the previous work, the ion flux expressions used to determine the effective diffusivity are based on the Nernst-Planck model. Since the cation and anion resin may be treated separately, the derivation of flux expressions for each ion species is similar to the derivation of ion flux expressions in earlier work (Chapter III and Appendix A of this thesis). For simplicity in mathematical equations and consistency with previous expressions, ion species are abbreviated as follows: 'n' for Sodium; 'h' for Hydrogen; 'c' for Chloride and 'o' for Hydroxide.

In mixed-bed ion exchange the typical concentration profiles under the conditions of bulk phase neutralization are exaggeratedly shown in Figure 4-1. The following equations can be obtained by applying model assumptions and mixed-bed ion exchange conditions.

No net current flow

$$J_o + J_c = J_h + J_n \quad (4-1)$$

Local electroneutrality

$$C_n + C_h = C_c + C_o \quad \text{in } r_o + \delta \geq r \geq r_o \quad (4-2)$$

No net flux of coion

$$J_h = -J_n = 0 \quad (4-3)$$

$$J_o = -J_c = 0 \quad (4-4)$$

The Nernst-Planck equation for each ion species is

$$J_h = -D_h \left\{ \frac{\partial C_h}{\partial r} + \frac{FC_h}{RT} \frac{\partial \phi}{\partial r} \right\} \quad (4-5)$$

$$J_n = -D_n \left\{ \frac{\partial C_n}{\partial r} + \frac{FC_n}{RT} \frac{\partial \phi}{\partial r} \right\} \quad (4-6)$$

$$J_o = -D_o \left\{ \frac{\partial C_o}{\partial r} - \frac{FC_o}{RT} \frac{\partial \phi}{\partial r} \right\} \quad (4-7)$$

$$J_c = -D_c \left\{ \frac{\partial C_c}{\partial r} - \frac{FC_c}{RT} \frac{\partial \phi}{\partial r} \right\} \quad (4-8)$$

By using Equations 4-1 to 4-4 and introducing the assumption of pseudo steady state exchange, the potential terms can be eliminated from Equations 4-5 to 4-8 and rearrange to yield,

$$J_h = -\left\{ \frac{2D_h D_n (C_h + C_n)}{D_n C_h + D_h C_n + 2D_n C_n} \right\} \frac{dC_h}{dr} \quad (4-9)$$

$$J_n = -\left\{ \frac{2D_h D_n (C_h + C_n)}{D_n C_h + D_h C_n + 2D_h C_h} \right\} \frac{dC_n}{dr} \quad (4-10)$$

$$J_o = -\left\{ \frac{2D_o D_c (C_o + C_c)}{D_c C_o + D_o C_c + 2D_c C_c} \right\} \frac{dC_o}{dr} \quad (4-11)$$

$$J_c = -\left\{ \frac{2D_o D_c (C_o + C_c)}{D_c C_o + D_o C_c + 2D_o C_o} \right\} \frac{dC_c}{dr} \quad (4-12)$$

For a shallow bed, the boundary conditions as shown in Figure 4-1 are

$$C_h = C_h^* \quad \text{and} \quad C_n = C_n^* \quad \text{at} \quad r = r_o \quad (4-13)$$

$$C_h = C_h^\circ \quad \text{and} \quad C_n = C_n^\circ \quad \text{at} \quad r = r_o + \delta \quad (4-14)$$

$$C_o = C_o^* \quad \text{and} \quad C_c = C_c^* \quad \text{at} \quad r = r_o \quad (4-15)$$

$$C_o = C_o^\circ \quad \text{and} \quad C_c = C_c^\circ \quad \text{at} \quad r = r_o + \delta \quad (4-16)$$

and within the film layer, the concentration conditions are

$$C_h = C_h \quad \text{and} \quad C_n = C_n \quad \text{in} \quad r_o \leq r \leq r_o + \delta \quad (4-17)$$

$$C_o = C_o \quad \text{and} \quad C_c = C_c \quad \text{in} \quad r_o \leq r \leq r_o + \delta \quad (4-18)$$

where δ is the thickness of the film layer.

If Equations 4-9 and 4-10 are substituted into Equation 4-3, and the resulting equation is integrated with the boundary conditions given in Equations 4-14 and 4-17, the concentration relationship between sodium and hydrogen ions can be obtained as Equation 4-19.

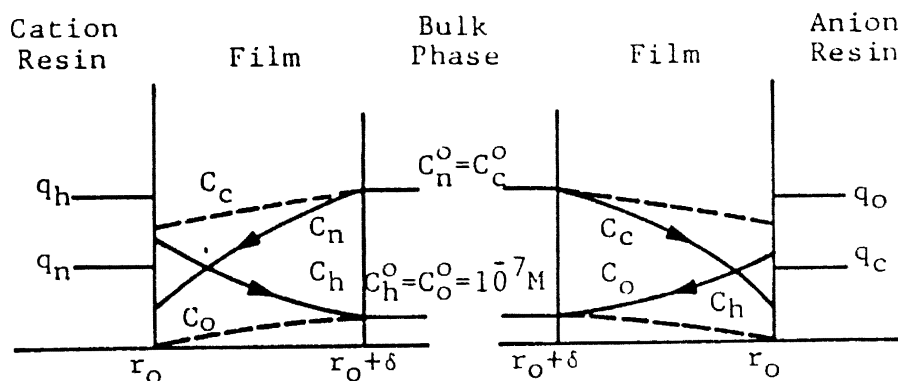


Figure IV-1 Concentration profiles for mixed-bed ion exchange with neutralization in the bulk phase (Haub, 1984)
(— Diffusing Counterions, ---- Nondiffusing Coions)

$$[D_h C_h + D_n C_n][C_h + C_n] = [D_h C_h^o + D_n C_n^o][C_h^o + C_n^o] = \text{RHS1} \quad (4-19)$$

or

$$C_h = \frac{-C_n(D_h + D_n) + [C_n^2(D_h + D_n)^2 - 4D_h(D_n C_n^2 - \text{RHS1})]^{1/2}}{2D_h} \quad (4-20)$$

Similarly, substituting Equations 4-11 and 4-12 into Equation 4-4 and integrating the resulting equation with the boundary condition Equations 4-16 and 4-18, yields the following concentration relationship between chloride and hydroxide ions in the film surrounding anion resins.

$$[D_o C_o + D_c C_c][C_o + C_c] = [D_o C_o^o + D_c C_c^o][C_o^o + C_c^o] = \text{RHS2} \quad (4-21)$$

or

$$C_o = \frac{-C_c(D_o + D_c) + [C_c^2(D_o + D_c)^2 - 4D_o(D_c C_c^2 - \text{RHS2})]^{1/2}}{2D_o} \quad (4-22)$$

'RHS1' and 'RHS2' are used to represent the quantity on the right hand side of Equations 4-19 and 4-21, respectively. Equations 4-20 and 4-22 can be used to eliminate the concentrations of hydrogen ion and hydroxide ion in the film from Equations 4-10 and 4-12, respectively. The resulting equations are integrated from bulk to the film-resin interface with the boundary conditions shown in Equations 4-13 to 4-16. The final flux expressions of sodium and chloride ions are given in Equations 4-23 and 4-24, respectively.

$$J_n = -\frac{2D_h D_n}{\delta(D_h - D_n)} [C_h^o + C_n^o - C_h^* - C_n^*] \quad (4-23)$$

$$J_c = -\frac{2D_o D_c}{\delta(D_o - D_c)} [C_o^o + C_c^o - C_o^* - C_c^*] \quad (4-24)$$

Rate Expressions and Effective Diffusivities

Based on the linear driving force assumption and static film model, the rate expression is given for species 'i':

$$\frac{dq_i}{dt} = k_i' a_s (C_i^o - C_i^*) = -J_i a_s \quad (4-25)$$

where ' k_i' ' is the ionic mass transfer coefficient for species 'i' with a dependence on effective diffusivity defined in Equation 3-18. Applying the relation into Equation 4-25, substituting Equation 4-23 for J_i , and solving the resulting equation for D_e , the effective diffusivity for sodium is obtained as:

$$D_e = \frac{2\alpha_1 D_n}{(\alpha_1 - 1)(C_n^o - C_n^*)} [C_n^o + C_h^o - C_n^* - C_h^*] \quad (4-26)$$

where $\alpha_1 (= D_h/D_n)$ is the ratio of self-diffusivities of hydrogen and sodium. Similarly using Equation 4-24 instead Equation 4-23, the effective diffusivity for chloride is given in Equation 4-27.

$$D_e = \frac{2\alpha_2 D_c}{(\alpha_2 - 1)(C_c^o - C_c^*)} [C_c^o + C_o^o - C_c^* - C_o^*] \quad (4-27)$$

where $\alpha_2 (= D_o/D_c)$ is the ratio of self-diffusivities of hydroxide and chloride.

Since the thickness of the stagnant film depends on fluid flow conditions, the fluid flow effects need to be taken into account in the rate expression. Based on this description in the previous chapter, the rate expression in which the fluid flow effects are under consideration can be given as

$$\frac{dq_i}{dt} = k_i R_i a_s (C_i^o - C_i^*) \quad (4-28)$$

where k_i is the nonionic mass transfer coefficient for species 'i'. Carberry's (1960) correlation in Equation 3-21 and Kataoka's (1973) correlation in Equation 3-22 can be applied to determine k_i with corresponding flow region. The ratio of ionic to nonionic mass transfer coefficient, R_i is defined as

$$R_i = \left(\frac{D_e}{D_i} \right)^{2/3} \quad (4-29)$$

If the interface concentrations and bulk concentrations are known, the exchange rate for each transferred ion species can be solved by combining Equations 4-26 or 4-27, 4-29

and 4-28. The relationship of the bulk concentrations and particle concentrations can be obtained from a column material balance. To solve the interface concentrations, the definition of selectivity coefficient of ion exchange, as given in the Chapter III of this thesis, must be introduced. The expressions for the interface concentrations can be obtained by procedures similar to the derivation of Equations 4-20 and 4-22. The resulting equations are given as:

$$C_n^* = \sqrt{\frac{(D_h C_h^o + D_n C_n^o)(C_h^o + C_n^o)}{\left(D_h K_h^n \frac{1-y_n}{y_n} + D_n\right) \left(K_h^n \frac{1-y_n}{y_n} + 1\right)}} \quad (4-30)$$

$$C_c^* = \sqrt{\frac{(D_o C_o^o + D_c C_c^o)(C_o^o + C_c^o)}{\left(D_o K_o^c \frac{1-y_c}{y_c} + D_c\right) \left(K_o^c \frac{1-y_c}{y_c} + 1\right)}} \quad (4-31)$$

In the derivation of the interface concentrations, the boundary conditions shown in Equations 4-13 to 4-16 are used. Now we need one additional equation to solve this system.

Column Material Balance

For ion exchange in a radial flow packed-bed, considering dispersion in the radial direction, the fundamental differential equation may be given by making a material balance for each species in cylindrical coordinates:

$$\frac{\partial C_i}{\partial t} + \left(\frac{1-\varepsilon}{\varepsilon}\right) \frac{\partial q_i}{\partial t} \pm \frac{u}{\varepsilon} \frac{\partial C_i}{\partial r} - \frac{1}{r} \frac{\partial}{\partial r} \left(D_{i,r} \frac{\partial C_i}{\partial r}\right) = 0 \quad (4-32)$$

where u is the superficial velocity, and is dependent on position. The positive sign before the convection term is for outward flow and the minus sign for inward flow. The radial dispersion coefficient of component 'i' is a variable in this equation.

Equations 4-32 and 4-28 are coupled partial differential equations, which describe the performance of ion exchange in a radial flow column, and must be solved simultaneously.

The initial and boundary conditions for inward flow are:

$$C_i(t = 0, r) = 0 \quad (4-33)$$

$$q_i(t = 0, r) = 0 \quad (4-34)$$

$$C_i(r = R, t > 0) = C_i^f \quad (4-35)$$

$$\left. \frac{dC_i}{dr} \right|_{r=R_0} = 0 \quad (4-36)$$

Equations 4-28 and 4-32 to 4-36 can be reduced to a dimensionless forms by introducing the following variables.

$$X = \frac{C}{C^f} \quad (4-37)$$

$$Y = \frac{q}{C^f} \quad (4-38)$$

$$\tau = \frac{tF}{V\varepsilon} \quad (4-39)$$

$$\xi = \frac{r^2 - R_0^2}{R_1^2 - R_0^2} \quad (4-40)$$

$$P_e = \frac{u(R_1 - R_0)}{\varepsilon D} \quad (4-41)$$

where

$$V = \pi h(R_1^2 - R_0^2) \quad (4-42)$$

$$u = \frac{F}{2\pi r h} \quad (4-43)$$

Therefore, the dimensionless forms of Equations 4-28 and 4-32 to 4-36 are:

$$\frac{\partial X_i}{\partial \tau} + \left(\frac{K}{\eta} \right) \frac{\partial Y_i}{\partial \tau} \pm \frac{\partial X}{\partial \xi} - \frac{1}{P_e P_r} \frac{\partial X_i}{\partial \xi} - \frac{1}{P_e P_r} \frac{\partial^2 X_i}{\partial \xi^2} = 0 \quad (4-44)$$

$$\frac{\partial Y_i}{\partial \tau} = \mathfrak{S} R_i (X_i^o - X_i^*) \quad (4-45)$$

$$X_i(\tau = 0, \xi) = 0 \quad (4-46)$$

$$Y_i(\tau = 0, \xi) = 0 \quad (4-47)$$

$$X_i(\xi = 1, \tau > 0) = 1 \quad (4-48)$$

$$\frac{\partial X_i}{\partial \xi} \Big|_{\xi=0} = 0 \quad (4-49)$$

where

$$\mathfrak{S} = K_i d_p a_s \quad (4-50)$$

$$K = \frac{Q}{C^r} \quad (4-51)$$

$$K_t = \frac{kV\varepsilon}{Fd_p} \quad (4-52)$$

$$\eta = \frac{\varepsilon}{1-\varepsilon} \quad (4-53)$$

$$P_r = \frac{r}{(R_1 - R_0)} \quad (4-54)$$

The dimensionless variable ' ϑ ' depends on position in the radial direction. It reflects the effects of flow patterns and resins and column geometry on the ion exchange rate. The dimensionless mass transfer coefficient ' K_t ' defined by Equation 4-52. The capacity ratio ' η ' is expressed in Equation 4-53.

Equations 4-44 and 4-45 are the dimensionless coupled differential equations and are easily solved by numerical methods. The detailed derivation for these equations is given in Appendix B.

Numerical Solution

Numerical treatment is an alternative way to solve the coupled partial differential equations 4-44 and 4-45. Both finite difference and finite element methods may be applied to reduce the equations to first-order ordinary differential equations, which are readily solved by standard software, such as, subroutine DGEAR of the International Mathematical and Statistical Library. In this work, Patankar's control volume method is modified to solve these equations. The solution strategy is shown in Figure IV-2.

After substituting Equation 4-45 into Equation 4-44 and rearranging, the following equation is obtained.

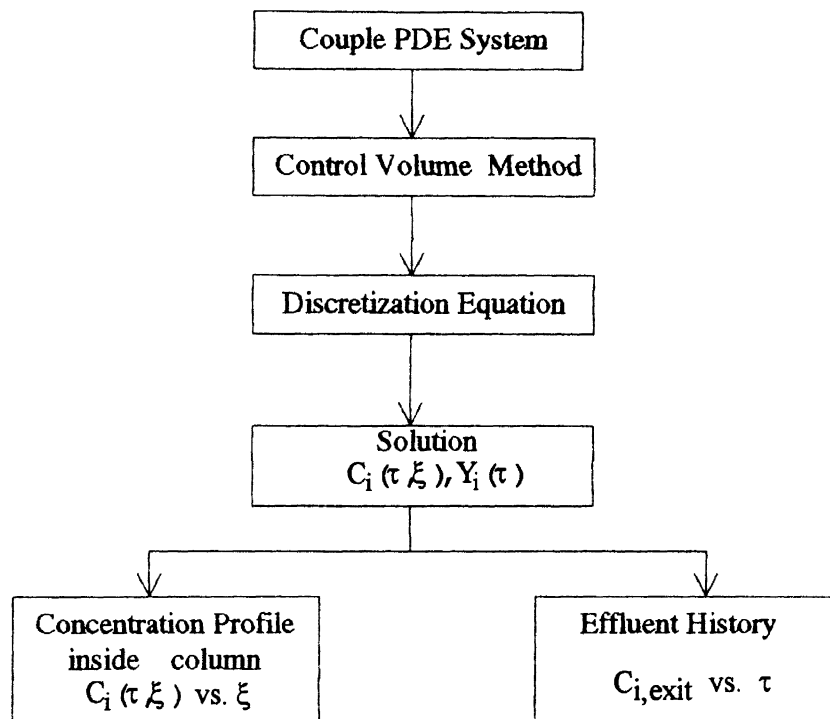


Figure IV-2. Solution strategy

$$\frac{\partial X}{\partial \tau} = \mp \frac{\partial X}{\partial \xi} + \frac{1}{P_e P_r} \frac{\partial X}{\partial \xi} + \frac{1}{P_e P_r} \frac{\partial^2 X}{\partial \xi^2} - \beta(X - X^*) \quad (4-55)$$

where

$$\beta = \frac{K \theta R_i}{\eta} \quad (4-56)$$

In obtaining a numerical solution of Equation 4-55, we choose a number of locations (grid points) along the ξ direction and seek the discrete values of concentration at these points in both bulk and resin phase. Based on the control volume method, the region of interest is divided into a number of subdomains, or control volumes. Each subdomain is bounded by the location $i-1/2$ and $i+1/2$ (shown by dashed lines in Figure IV-3) and uniform conditions in each subdomain are assumed.

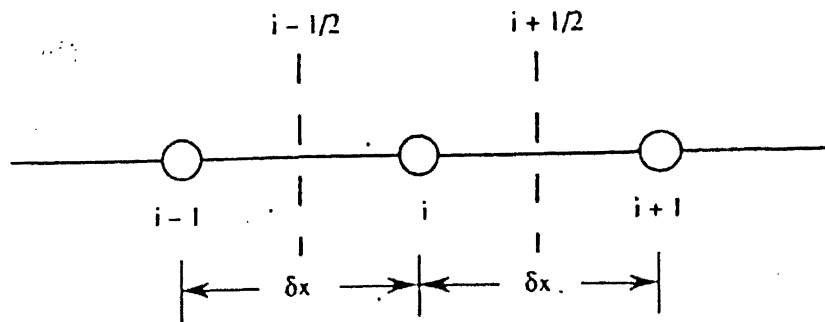


Figure IV-3 A one dimensional uniform grid

A nonsteady state diffusion with reference to the subdomain should be the balance among the concentrations at previous time, at the two faces of the control volume and the amount of ion exchange by resins within the control volume. Therefore, under inward

radial flow the corresponding derived discretization equation of Equation 4-55, for each internal grid point, may be expressed as:

$$A_i X_i = A_{i-1} X_{i-1} + A_{i+1} X_{i+1} + b_i \quad (4-57)$$

where

$$A_{i-1} = \left(1 + \frac{1}{P_e P_r}\right) + \frac{2}{P_e P_r \Delta \xi} \quad (4-58)$$

$$A_{i+1} = \frac{2}{P_e P_r \Delta \xi} \quad (4-59)$$

$$A_i^0 = \frac{\Delta \xi}{\Delta \tau} \quad (4-60)$$

$$b_i = -S_i X_i^* + A_i^0 X_i^0 \quad (4-61)$$

$$S_i = -\Delta \xi \cdot \beta \quad (4-62)$$

$$A_i = A_{i-1} + A_{i+1} + A_i^0 - S_i \quad (4-63)$$

The discretization equation (Eq. 4-57) is easily adapted by introducing boundary conditions.

At $\xi = 1$

$$A_1 X_1 = A_2 X_2 + b_1 \quad (4-64)$$

At $\xi = 0$ (effluent point, noted by the subscript 'B')

$$A_B X_B = A_{B-1} X_{B-1} + b_B \quad (4-65)$$

The detailed derivation of discretization equations is given in Appendix C.

The discretization equations of the form 4-57 for internal grid points and of the forms 4-64 and 4-65 for boundary points can be solved as a set of simultaneous linear equations. The coefficient matrix of these equations is the tridiagonal matrix, which is readily solved by TriDiagonal-Matrix Algorithm or Thomas method.

The recursion relation is:

$$X_i = P_i X_{i+1} + G_i \quad (4-66)$$

where

$$P_i = \frac{A_{i+1}}{A_i - A_{i-1} P_{i-1}} \quad (4-67)$$

$$G_i = \frac{b_i + A_{i-1} G_{i-1}}{A_i - A_{i-1} P_{i-1}} \quad (4-68)$$

and the following relations are determined by boundary conditions.

$$P_1 = \frac{A_2}{A_1} \quad (4-69)$$

$$G_1 = \frac{b_1}{A_1} \quad (4-70)$$

$$X_B = G_B \quad (4-71)$$

In this numerical procedure the mass transfer coefficient, k_i , and radial dispersion coefficient, D , values are treated as variables which are dependent on the variations of u_r , the velocity along the radial coordinate ξ . Meanwhile, dispersion caused by molecular diffusion is neglected and is simplified as the proportional of u_r . Thus, the Peclet number Pe , defined in Equation 4-41, is constant for each component.

Carberry's (1960) correlation or Kataoka's (1973) correlation is employed to calculate the nonionic mass transfer coefficient, k , in the corresponding flow region.

The interface concentrations and effective diffusivities at each control volume are evaluated by Equations 4-30, 4-31 and 4-27, derived from the liquid film resistance-controlled model. The initial guess of bulk concentrations at each control volume is necessary to start the calculation and these values are renewed iteratively by solving Equations 4-57, 4-64 and 4-65.

Results and Discussion

Concentration Distribution

Figure IV-4 shows the simulated breakthrough curves for sodium and chloride system in a inward flow demineralizer. These curves are similar to those obtained from axial flow. The concentration distribution along the flow direction within the column (shown in Figure IV-4) depletes very fast from the saturated front. The sharper concentration profiles are favorable for separation because lower effluent concentrations can be expected from the resins with the same degree of exhaustion of exchange capacity.

Nonionic Mass Transfer Coefficients

In this model, the nonionic mass transfer coefficients are treated as variables with the radial coordinate. For flow system at low Reynolds numbers ($Re < 20$), the nonionic mass transfer coefficient, k , is proportional to $u_r^{1/3}$, which is based on Kataoka's (1973) correlation. For flow system at high Reynolds numbers ($Re > 20$), k values are proportional to $u_r^{1/2}$, which is indicated by Carberry's (1960) equation. Since superficial velocity in radial flow column varies over a broad range, both flow regions may be present within the column. When one flow region changes to the other, k values change

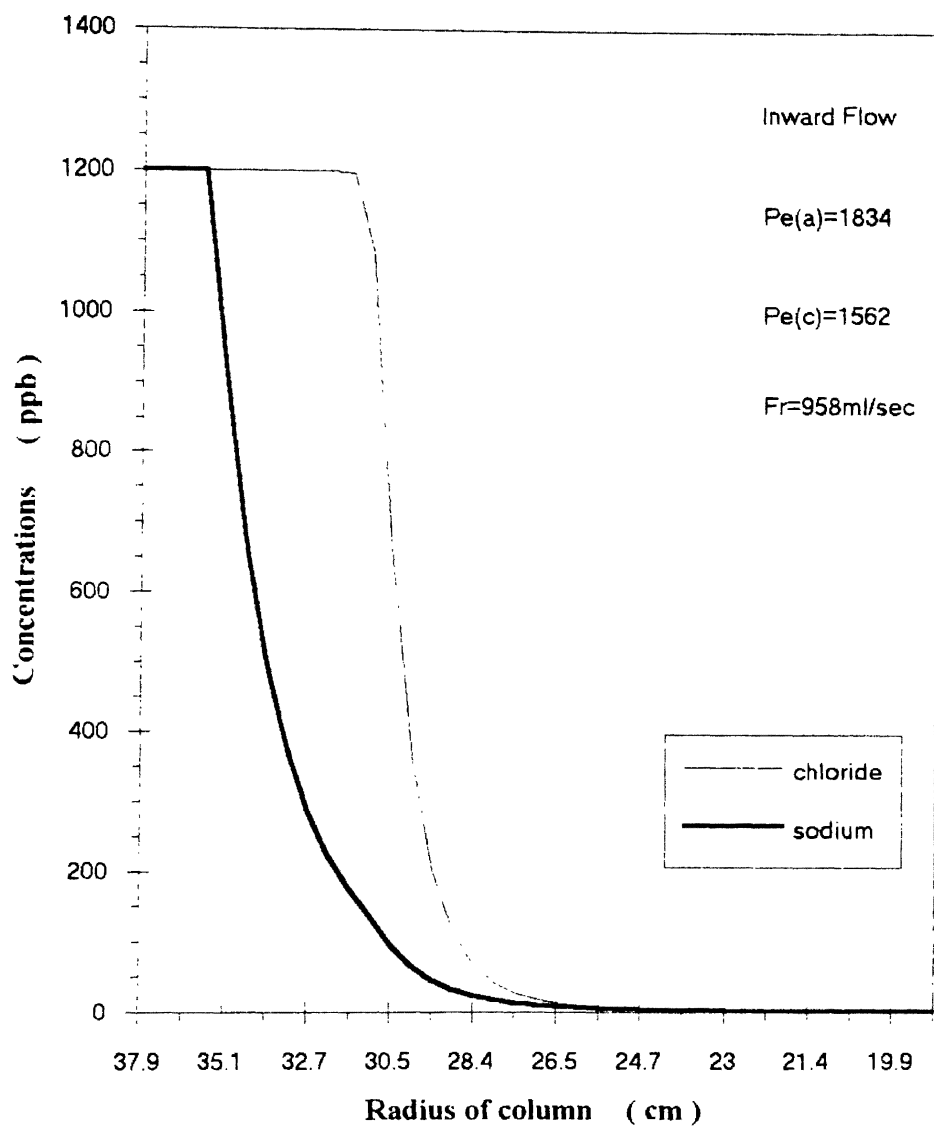


Figure IV-4 Concentraion distribution within a mixed-bed with inward radial flow (the corresponding operation time 300 mins)

sharply (shown in Figure IV-5). Generally speaking, the changes of nonionic mass transfer coefficients are much weaker than velocity. The larger the ionic mobility, the less the effect of variations of radial velocity on k .

Effects of Bed Void Fraction

Figures IV-6 and IV-7 show the influence of bed void fraction. The influence of bed void fraction on breakthrough curves is similar to axial flow. The larger bed void fraction has less exchange resin in a given column volume so that the breakthrough comes earlier (Figure IV-6). The effect of bed void fraction on k results from the change of interfacial velocity with different bed void fraction. Since the change of radial velocity may lead to the change of flow region, the change of k is different with the change of bed void fraction. Figure IV-7 indicates the difference. This fact is also implied in Figure IV-6. The sharper breakthrough curve corresponds to the larger change of k at the value 0.45.

Ratio of Exchange Resins

In mixed-bed ion exchange applications, the ratio of exchange resins is of interest. As shown in Figure III-8 and III-9, the ratio of exchange resins in a column influences the total capacity of the resins and the lower concentration limits in the effluent solution. The capacity for cation and anion resin are 3.0728 meq/cm^3 and 2.4334 meq/cm^3 , respectively. Under these conditions, Figures III-8 and III-9 show that the cation resin fraction of 0.4 gives the sharpest breakthrough curve, which indicates favorable separation and the best use of resin capacity.

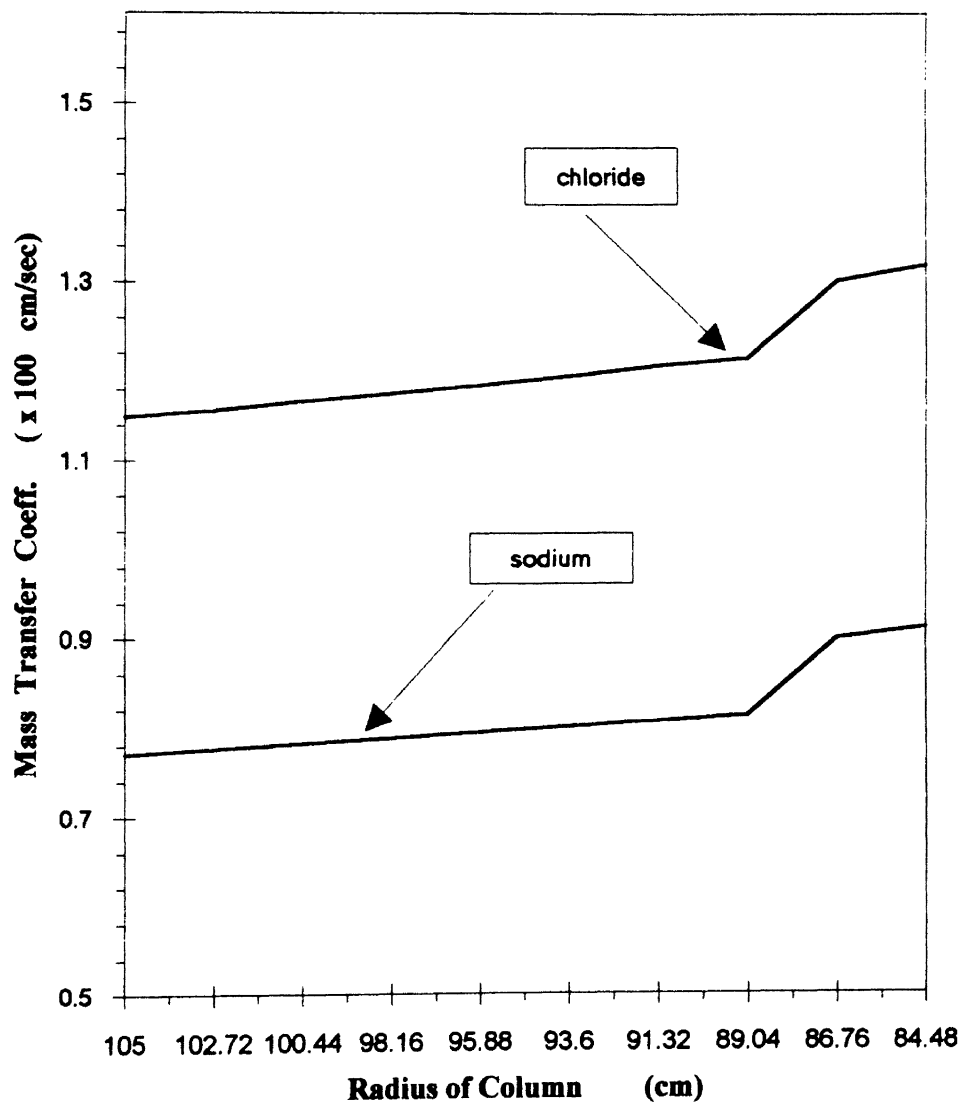


Figure IV-5 Changes of nonionic mass transfer coefficients along the flow direction in inward radial flow column

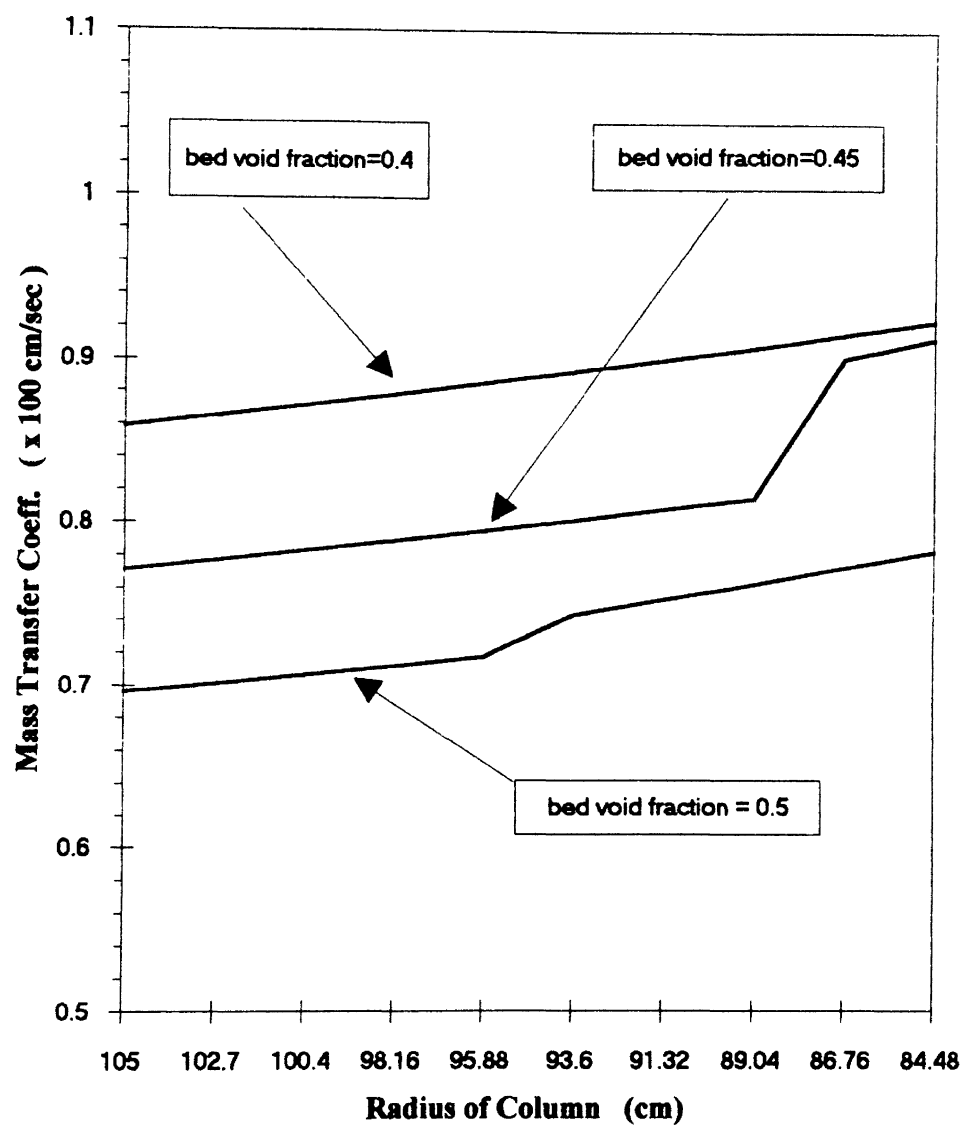


Figure IV-6 Effect of bed void fraction on nonionic mass transfer coefficients of sodium in inward radial flow column

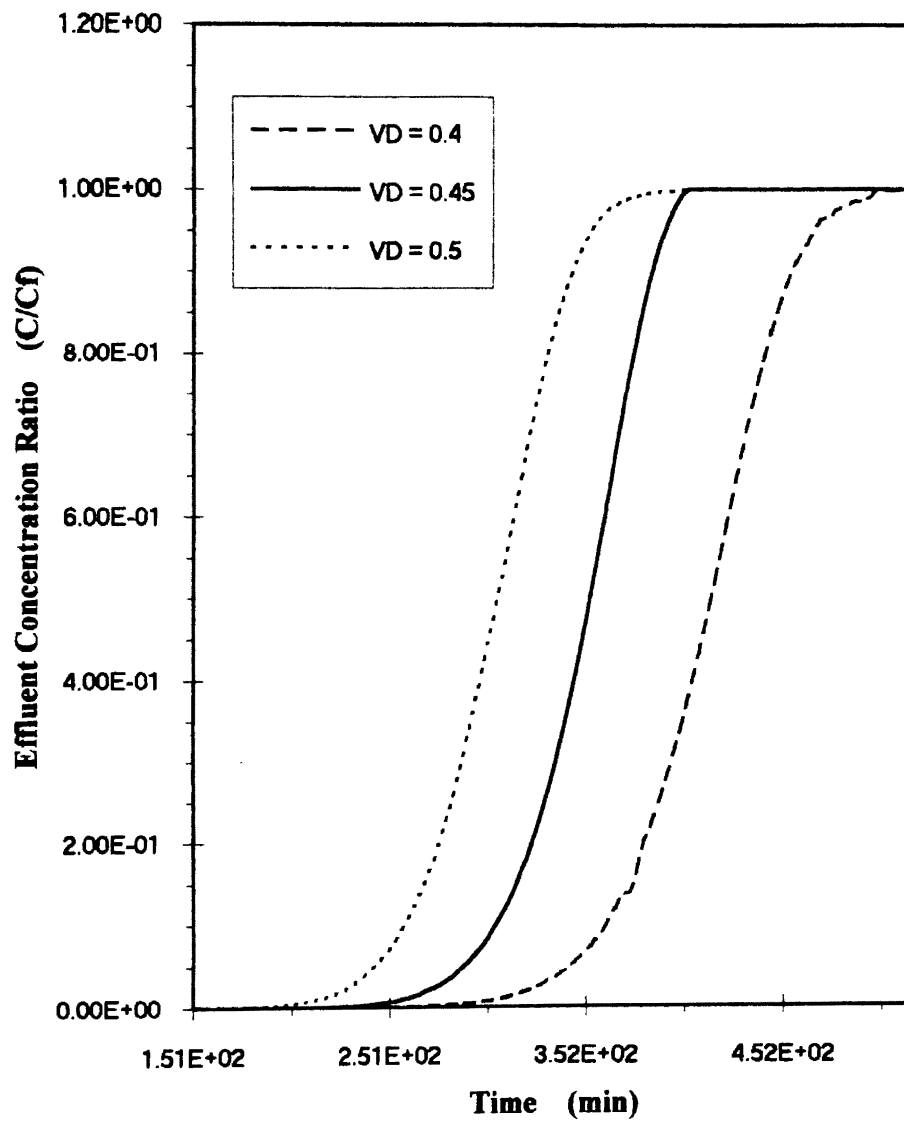


Figure IV-7 Effect of bed void fraction on chloride breakthrough curves in a mixed-bed with inward radial flow

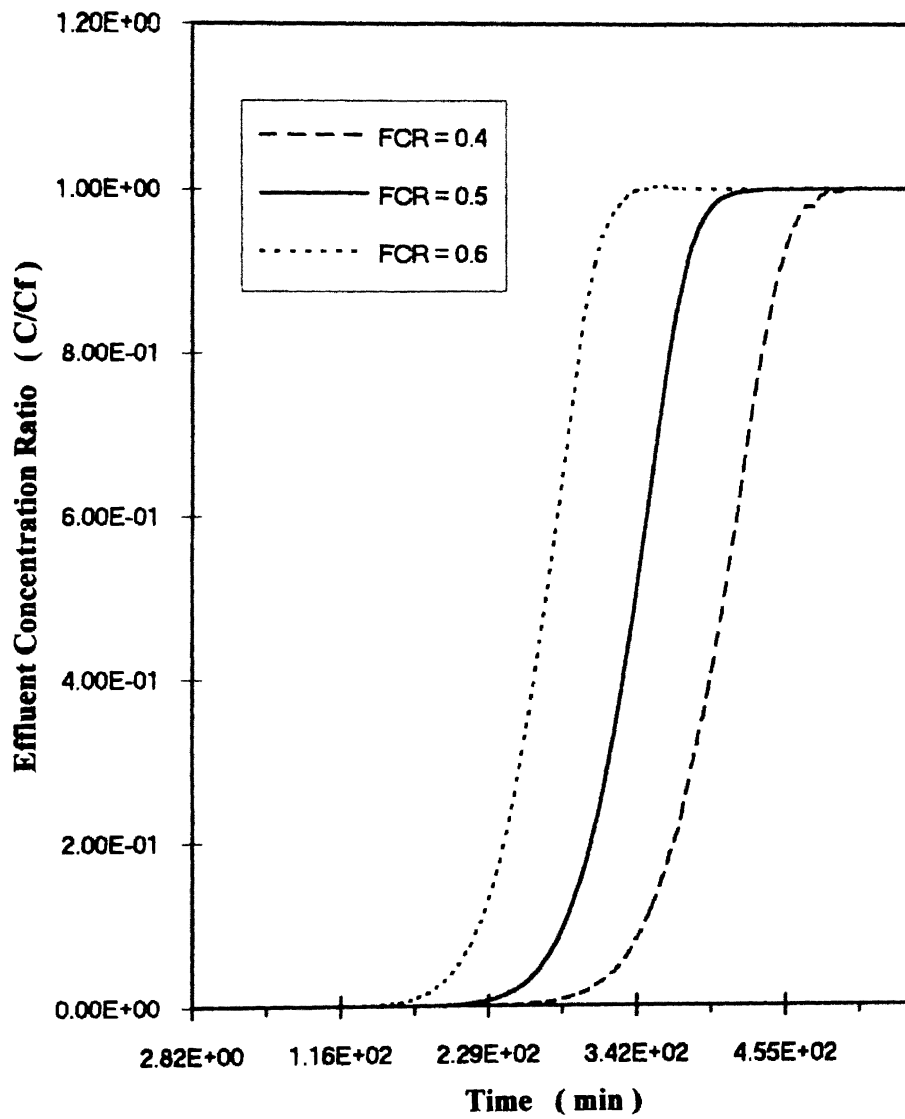


Figure IV-8 Chloride breakthrough curves for simulation of mixed bed with inward radial flow with varying cation to total resin fraction

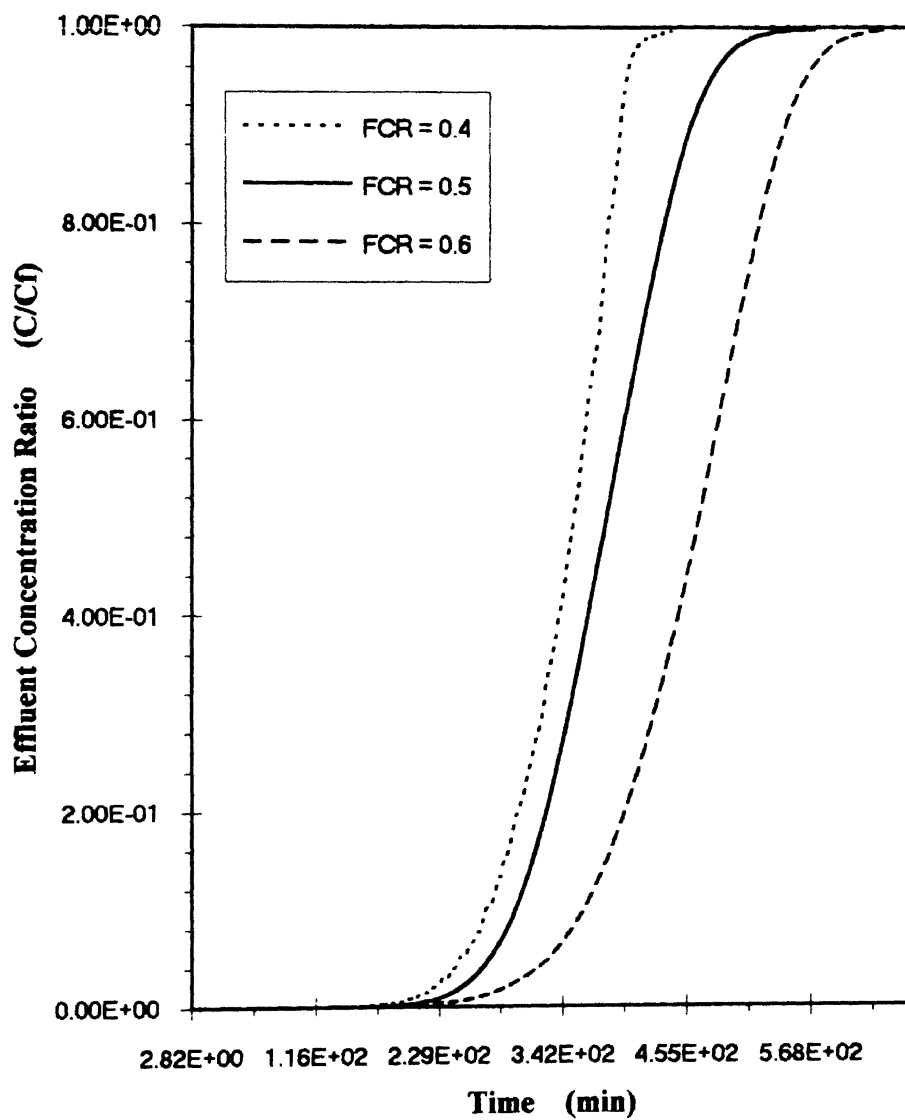


Figure IV-9 Sodium breakthrough curves for simulation of mixed-bed with inward radial flow with varying cation to total resin fraction

Conclusions and Recommendations

A mixed-bed model with radial flow for demineralizers was developed. Radial dispersion and nonionic mass transfer coefficients were treated as variables with the radial coordinate in the model. The model was solved numerically by using Partanka's (1991) control volume method. The concentration distribution within the column, variations of nonionic mass transfer coefficients with radial coordinate, and effects of bed void fraction were studied. The radial flow geometry, especially with inward radial flow, offers sharper profiles, which are favorable for separation and make best use of resin capacity. Clearly, the bed void fraction is the parameter of the most interest. It influences the flow velocity which influences the values of nonionic mass transfer coefficients and pressure drop as well. The most important advantage of radial flow geometry over axial flow geometry is, as mentioned in Chapter II, that radial flow has relatively larger flow area and shorter flow path. Subsequently, the two factors result in less pressure drop.

This work provides some useful information for studying mixed-bed demineralizers with radial flow. However, this model has not been fully tested yet. Effects on column performance caused by some other factors, for example, Peclet number, dispersion coefficient, different flow styles (inward and outward), comparison of operating behaviors resulted from different geometries, have not yet been studied. By the way, the simplified dispersion coefficients, which are proportional to velocity and lead to constant Peclet number, may not be helpful to study the effects caused by Peclet number.

BIBLIOGRAPHY

- Acrivos, A. (1958). Solution of the Laminar boundary layer energy equation at high Prandtl number. *Phys. Fluids*, 3, 657-658.
- Adams, G., Jones, P. M. and Millar, J. R. (1969). Kinetics of acid uptake by weak-base anion exchangers. *J. Chem. Sci. (London)*, A, 2543-2551.
- Anderson, J. L., Eyring, E. M., and Whittaker, M. P. (1964). Temperature jump rate studies of polyborate formation in aqueous boric acid. *J. Phys. Chem.*, 68, 1128-1132.
- Bajpai, R. K., Gupta, A. K., and Rao, M. G. (1973). Single particle studies of binary and ternary cation exchange kinetics. *A.I.Ch.E. J.*, 20, 989
- Bhandari, M. V., Juvekar, V. A., and Patwardhan, S. R. (1992a). Sorption studies on ion exchange resins. 1. Sorption of strong acids on weak base resins. *Ind. Eng. Chem. Res.*, 31, 1060-1073.
- Bhandari, M. V., Juvekar, V. A., and Patwardhan, S. R. (1992b). Sorption studies on ion exchange resins. 2. Sorption of weak acids on weak base resins. *Ind. Eng. Chem. Res.*, 31, 1073-1080.
- Blickenstaff, R. A., Wagner, J. D. and Dranoff, J. S. (1967a). The Kinetics of Ion Exchange Accompanied by Irreversible Reaction. I. Film Diffusion Controlled Neutralization of a Strong Acid Exchanger by Strong Bases, *J. Phys. Chem.*, 71, 1665-1669.
- Blickenstaff, R. A., Wagner, J. D. and Dranoff, J. S. (1967b). The kinetics of ion exchange accompanied by irreversible reaction. II. Intraparticle diffusion controlled neutralization of a strong acid exchanger by strong bases. *J. Phys. Chem.*, 71, 1670-1674.
- Boyd, G. E., Adamson, A. W., and Myers, L. S., Jr. (1947). The exchange adsorption of ions from aqueous solutions by organic zeolites. II. Kinetics. *J. Am. Chem. Soc.*, 69, 2836

- Carberry, J. R. (1960). A boundary-layer model of fluid-particle mass transfer in fixed beds. A.I.Ch.E. J., 6, 460-463.
- Carpeni and Souchay, J.Chim. Phys., 42, 149 (1945).
- Christoph, G., Heybey, J., Schutze, H., Weise, G. and Wetzel K. (1976). Theoretical and experimental investigations for enrichment of boron-10 by ion-exchange chromatography. Isotopenpraxis, 12(1), 17-21.
- Corti, H., Crovetto, R., and Roberto, F. P. (1980). Mobilities and ion-pairing in LiB(OH)_4 and NaB(OH)_4 aqueous solutions. A conductivity study. J. Solution Chem., 9(8), 617-625.
- Costa, J. I. and Gluekauf, E. (1947). Theory of chromatography. III. Experimental separation of two solutes and comparison with theory. J. Chem. Soc. (London), 1308-1314.
- Donnan, F. G. (1912). The Theory of membrane equilibrium in the presence of a non-dialyzable electrolyte. Z. Elektrochem., 17, 572.
- Donnan, F. G. and Guggenheim, E. A. (1932). Exact thermodynamics of membrane equilibrium. Z. physik. Chem., A162, 346-360.
- Donnan, F. G. (1934). The Exact thermodynamics of membrane equilibrium. Z. physik. Chem., A168, 369-380.
- Dranoff, J. S. and Lapidus, L. (1957). Equilibrium in ternary ion exchange systems. Ind. Eng. Chem., 49, 1297-1302.
- Dranoff, J. S. and Lapidus, L. (1958). Multicomponent ion exchange column calculations. Ind. Eng. Chem., 50, 1648-1653.
- Dranoff, J. S. and Lapidus, L. (1961). Ion exchange in ternary systems. Ind. Eng. Chem., 53, 71-76.
- Edwards, J. O. (1954). Rates of substitution reactions in oxyanions. J. Chem. Educ., 31, 270-275.
- Elprince, A. M. and Babcock, K.L. (1975). Prediction of ion-exchange equilibria in aqueous systems with more than two counterions. Soil Sci., 120, 332-338.
- Fejes, P.P., Hedin, G. and Samuelsson, A. (1989). Experiences with clean-up systems at BWRs. Report, (ABB Atom, Sweden).

- Foutch, G. L. and Berg, A. (1992). Modeling of ion exchange processes in ultrapure water. (Present in the Bournemouth conference).
- Glueckauf, E. and Coates, J. I. (1947). Theory of chromatography, IV. The influence of incomplete equilibrium on the front boundary of chromatograms and on the effectiveness of separation. J. Chem. Soc., 1315-1321.
- Gu, T.Y., Tsai, G. J. and Tsao, G. T. (1991). A theoretical study of multicomponent radial flow chromatography. Chem. Eng. Sci., (London), 46, 1279-1289.
- Hansen, K. W. (1971). Analysis of transient models for catalytic tubular reactors by orthogonal collocation. Chem. Eng. Sci., 26, 1555-1569.
- Haub, C. E. (1984). M.S. Thesis, Oklahoma State University, Stillwater, OK.
- Haub, C. E. and Foutch, G. L. (1986a). Mixed-bed ion exchange at concentrations approaching the dissociation of water 1. Model development. Ind. Eng. Chem. Fund., 25, 373-381.
- Haub, C. E. and Foutch, G. L. (1986b). Mixed-bed ion exchange at concentrations approaching the dissociation of water 2. Column model applications. Ind. Eng. Chem. Fund., 25, 381
- Helfferich, F. G. (1962). Ion Exchange. New York: McGraw Hill Book Company.
- Helfferich, F. G. (1965). Ion exchange kinetics. V. Ion exchange accompanied by reactions. J. Phys. Chem., 69, 1178
- Helfferich, F. G. (1967). Multicomponent ion exchange in fixed beds. Ind. Eng. Chem. Fund., 6, 352.
- Helfferich, F. G. (1984). Conceptual view of column behavior in multicomponent adsorption or ion-exchange system. A.I.Ch.E. Symp. Ser., 80(233), 1-13.
- Helfferich, F. G. and Hwang, Y. L. (1985). Kinetics of acid uptake by weak base anion exchangers: Mechanism of proton transfer. A.I.Ch.E. Symp. Ser., 242, 81-97.
- Hirao, T., Kotata, M and Kakihana, H. (1973). Chromatographic separation of isotopes using pure water as eluent. I. Separation of boron isotopes by a strong-base exchange resin in fluoride form. Nippon Kagaku Kaishi, 1477-1481.
- Hiester, N. K. and Vermeulen, T. (1952). Saturation performance of adsorption columns. Chem. Eng. Progr., 48, 505-512.
- Hou, K. C. and Mandaro, R. M., Biotechniques, 4, 358 (1986).

- Huang, H, Hsiang, C. C., Lee, S. C., and Ting, G. (1990). The sorption behavior of boric acid on weak-base anion exchange resin. Solvent Extraction and Ion Exchange, 9(2), 319-335.
- Huang, H. S., Lee, W. C. and Tsao, G. T. (1988). Mathematical models of radial chromatography. Chem. Eng. J., 38, 179-186.
- Inchin, P. A. and Rachinskii, V. V. (1968). Theory of radial-cylindrical sorption dynamics. II. Dynamics of sorption during filtration towards the axis of a cylindrical layer of sorbent. Russ. J. Phys. Chem., 42(2), 278.
- Inchin, P. A. and Rachinskii, V. V. (1973). Theory of radially cylindrical sorption dynamics. IV. Non-equilibrium frontal sorption dynamics for a linear isotherm. Russ. J. Phys. Chem., 47(8), 1159.
- Inchin, P. A. and Rachinskii, V. V. (1973). Theory of radial-cylindrical sorption dynamics. V. Frontal equilibrium sorption dynamics with longitudinal diffusion. Russ. J. Phys. Chem., 47(9), 1331 .
- Ingri, N. (1962). Equilibrium studies of polyanions. VIII. First equilibrium steps in the hydrolysis of boric acid, a comparison between equilibriums in 0.1M and 3.0M NaClO₄. Acta Chem. Scand., 16, 439-448.
- Ingri, N. (1963a). Equilibrium studies of polyanions. X. The first equilibrium steps in the acidification of B(OH)₄⁻, an application of the self-medium method. Acta Chem. Scand., 17, 573-580.
- Ingri, N. (1963b). Equilibrium studies of polyanions. XI. Polyborates in 3.0M NaBr, 3.0M LiBr, and 3.0M KBr, a comparison with data obtained in 3.0M NaClO₄. Acta Chem. Scand., 17, 581-589.
- Jonsson, J. A.(Ed), (1987). Chromatographic Theory and Basic Principles. New York: Marcel Dekker.
- Karant, N. G. and Hughes, R. (1974). Simulation of an adiabatic packed bed reactor. Chem. Eng. Sci., 29, 197-205.
- Kataoka, T., Sato, N. and Ueyama, K. (1968). Effective liquid phase diffusivity in ion exchange. J. Chem. Eng. Japan, 1, 38-42.
- Kataoka, T, Yoshida, H., and Yamada, T. (1973). Liquid phase mass transfer in ion exchange based on the hydraulic radius model. J. Chem. Eng. Jpn., 6, 172-177.
- Kataoka, T., Yoshida, H., and Shibahara, Y. (1976). Liquid phase mass transfer in ion exchange accompanied by chemical reaction. J. Chem. Eng. Jpn., 9, 130.

- Kataoka, T., Yoshida, H., and Ozasa, Y. (1977). Intraparticle ion exchange mass transfer accompanied by instantaneous irreversible reaction. Chem. Eng. Sci., (London), 32, 1237-1240.
- Kataoka, T. and Yoshida, H. (1980). Ion exchange equilibria in ternary systems. J. Chem. Eng. Jpn., 13, 328-330.
- Kitchener, J. A. (1959). Modern Aspects of Electrochemistry, (J. O'M. Bockris, ed.), No. 2, American, New York.
- Klein, G., Tondeur, D., and Vermeulen, T. (1967). Multicomponent ion exchange in fixed beds. Ind. Eng. Chem. Fund., 6, 339-351.
- Kolthoff, I. M. (1926). The change of the dissociation constant of boric acid with the concentration of this acid. Rec. Trav. Chim., 45, 501-507.
- Kolthoff, I. M. and Bosch, W. The abnormal change in pH in boric acid-sodium hydroxide mixtures at different concentrations and temperatures. Rec. Trav. Chim., 46, 180-188.
- Kunin, R. (1958). Ion Exchange Resins. London: Wiley.
- Lapidus, L. and Amundson, N. R. (1950). Mathematics of adsorption in beds. III. Radial flow. J. Phys. Colloid Chem., 54, 821-829.
- Lee, W. C., Tsai, G. J., and Tsao, G. T. (1990). Radial-flow affinity chromatography for trypsin purification. ACS Symp. Ser. 427, 104-117.
- Liapis, A. I. and Rippin, D. W. T. (1978). The simulation of binary adsorption in activated carbon columns using estimates of diffusional resistance within the carbon particles derived from batch experiments. Chem. Eng. Sci., 33, 593.
- Ljungberg, L.G. and Hallden, E. (1984). BWR water chemistry impurity studies. Literature review of effects on SCC. EPRI NP-3663, (Sweden).
- Maly, J. and Bozorgmanesh, H. (1983). BWR neutron-absorption standards. Report, EPRI-NP-2731 (Sci. Appl., Inc.).
- Meichik, N. R. and Leikin, Y. A. (1989). Acid-base equilibria and sorption properties of nitrogen- and hydroxy-containing ion exchangers. Russ. J. Phys. Chem., 63(2), 543-546.

- Meichik, N. R., Leikin, Y. A., Galitskaya, N. B., and Kosaeva, A. E., (1989). Kinetics of the sorption of boron by anion-exchange resins. Russ. J. Phys. Chem., 63(3), 1871.
- Menzel, J. (1927). Boric acids and alkali borates. I. The free boric acids. II. The alkali borates in H₂O solution. Z. Anorg. Chem., 164, 22
- Momii, R. K. and Nachtrieb, N. H. (1967). Nuclear magnetic resonance study of borate-polyborate equilibria in aqueous solution. Inorg. Chem., 6, 1189-1192.
- Nakanishi, K. (1978). Prediction of diffusion coefficient of nonelectrolytes in dilute solution based on generalized Hammond-Stokes plot. Ind. Eng. Chem. Fund., 17, 253-256.
- Omatete, O. O., Clazie, R. N., and Vermeulen, T. (1980a). (1980). Column dynamics of ternary ion exchange Part I: Diffusional and mass transfer relations. Chem. Eng. J., 19, 229-240.
- Omatete, O. O., Clazie, R. N., and Vermeulen, T. (1980). Column dynamics of ternary ion exchange Part II: Solution mass transfer controlling. Chem. Eng. J., 19, 241-250.
- Owen, B. B. (1934). The dissociation constant of boric acid from 10 to 50°. J. Phys. Chem., 56, 1695-1697.
- Patanka, S.V. (1991). Computation of conduction and duct flow heat transfer. Maple Grove, MN: Innovative Research, Inc.
- Perry, R. H. and Chilton, C. H.(Ed.,1973). Chem. Engineer's Handbook, New York: McGraw-Hill.
- Pieroni, L. J. and Dranoff, J. S. (1963). Ion exchange equilibria in a ternary system. A.I.Ch.E. J., 9, 42-45.
- Pinchas, S. and Shamir, J. (1972). Anomalous behavior of ¹⁸O-Labeled compounds. VI. The vibrational spectra of isotopic metaborates. J. Chem. Phys., 56, 2017-2019.
- Plaigin, M., Lacoste-Bourgeacq, J. F., Mandaro, R. and Lemay, C. (1989). Purification of plasma fractions by radial flow chromatography cartridges. Colloque INSERM, 175, 169-175.
- Platford, R. F. (1971). Osmotic and activity coefficients of some simple borate solutions at the freezing point. Can. J. Chem., 49(5), 709-711.

- Rachinskii, V.V. (1968). Basic principles of radial chromatography. J. Chromatogr., 33, 234-241.
- Rachinskii, V. V. and Inchin, P. A. (1968). Theory of radial-cylindrical sorption dynamics. I. fundamental laws. Russ. J. Phys. Chem., 42(4), 497.
- Rachinskii, V. V. and Inchin, P. A. (1970). Theory of radial-cylindrical sorption dynamics. III. Steady-state conditions in frontal sorption dynamics. Russ. J. Phys. Chem., 44(3), 415.
- Raghavan, N. S. and Ruthven, D. M. (1983). Numerical simulation of a fixed-bed adsorption column by the method of orthogonal collocation. A.I.Ch.E. J., 29, 922-925.
- Robinson, R. A. and Stokes, R. H. (1959). Electrolyte Solutions. England: Butterworths.
- Rosset, R., Fould, H., Chemla, M., Labrousse, H., Hure, J. and Tremillon, B. (1964). Separation of boron isotopes with use of anion exchange resins. Bull. Soc. Chim. Fr., 607-616.
- Ruthven, D. M. (1984). Principles of Adsorption and Adsorption Processes. New York: Wiley.
- Shallcross, D. C., Herrmann, C. C., and McCoy, B. J. (1988). An improved model for the prediction of multicomponent ion exchange equilibria. Chem. Eng. Sci., (London), 43, 279-288.
- Smith, R. P. and Woodburn, E. T. (1978) Prediction of multicomponent ion exchange equilibria for the ternary system $\text{SO}_4^{2-} - \text{NO}_3^- - \text{Cl}^-$ from data of binary systems. A.I.Ch.E. J., 24, 577-587.
- Sun, L. M. and Meunier, F. (1991). An improved finite difference method for fixed-bed multicomponent sorption A.I.Ch.E. J., 37, 244-254.
- Tondeur, D. and Bailly, M. (1986). Design methods for ion-exchange processes based on the 'equilibrium theory'. NATO ASI Ser., Ser. E 107, 147-197.
- Vazquez Una, G. V., Pampin, R. M., and Caeiro, R. B. (1985). Prediccion del equilibrio en sistemas ternarios de intercambio ionico. Anales Quimica Ser., A 81, 141-145.
- Vermeulen, T. and Hiester, N. K. (1954). Ion-exchange and adsorption column kinetics with uniform partial presaturation. J. Chem. Phys., 22, 96-101.

- Wagner, J. D. and Dranoff, J. S. (1967). The kinetics of ion exchange accompanied by irreversible reaction. III. Film diffusion controlled neutralization of a strong acid exchanger by a weak base. J. Phys. Chem., 71, 4551-4553.
- Wilson, G. M. (1964). Vapor-liquid equilibrium XI. A new expression for the excess energy of mixing. Am. Chem. Soc. J., 86, 127 (1964).
- Yoneda, Y., Uchijima, T., and Makishima, S. (1959). Separation of boron isotopes by ion exchange. J. Phys. Chem., 63, 2057
- Yoon, T. (1990). Ph.D. Dissertation, Oklahoma State University, Stillwater, OK.
- Zecchini, E. J. (1990). Ph.D. Dissertation, Oklahoma State University, Stillwater, OK.
- Zecchini, E. J. and Foutch, G.L. (1991). Mixed-bed ion-exchange modeling with amine form cation resins. Ind. Eng. Chem. Res., 30, 1886-1892.

APPENDIX A

DERIVATION OF ION AND MOLECULAR FLUX EXPRESSIONS FOR INCOMPLETELY DISSOCIATED ACID SORPTION BY A BASE ANIONIC RESIN

The following derivation results from the Nernst-Planck treatment of the ionic species combined with Fick's first law for non-dissociated molecules. Much effort is devoted to a general form solution of the flux expressions for this film diffusion controlled ion exchange process.

In addressing ultrapure water concentrations, the ion flux expressions for film diffusion controlled binary ion exchange was addressed in detail by Haub (1984) for mixed-bed ion-exchange applications. Zecchini (1990) developed general form ion flux expressions for ternary ion exchange. This work will be consistent with their work in nomenclatures and logical structure. Some modifications are made, as necessary, to deal with undissociated species. Since it is assumed that the exchange process is the film diffusion controlled ion exchange, the static film model is inherent in the derivation of the flux expressions.

Consider in a monovalent system. Applying the Nernst-Planck equation for the diffusion of each ion and the Fick's first law for the diffusion of the undissociated acid molecule, the following expressions are obtained:

$$J_h = -D_h \left[\frac{\partial C_h}{\partial r} + \frac{FC_h}{RT} \frac{\partial \phi}{\partial r} \right] \quad (\text{A-1})$$

$$J_o = -D_o \left[\frac{\partial C_o}{\partial r} - \frac{FC_o}{RT} \frac{\partial \phi}{\partial r} \right] \quad (\text{A-2})$$

$$J_x = -D_x \left[\frac{\partial C_x}{\partial r} \mp \frac{FC_x}{RT} \frac{\partial \phi}{\partial r} \right] \quad (\text{A-3})$$

$$J_a = -D_a \frac{\partial C_a}{\partial r} \quad (\text{A-4})$$

In Equation A-3, the minus sign before the partial term is for the anion, positive sign for the cation. The following derivation is based on ion exchange in a homogeneous anion bed.

The assumptions of no coion flux, no net current flow and electrical neutrality lead to

$$J_h = 0 \quad (\text{no coion flux}) \quad (\text{A-5})$$

$$J_o + J_x = 0 \quad (\text{no net current flow}) \quad (\text{A-6})$$

$$C_o + C_x = C_h \quad (\text{electrical neutrality}) \quad (\text{A-7})$$

From Eqs. A-1 and A-5 the following equation can be obtained

$$\frac{F}{RT} \frac{\partial \phi}{\partial r} = -\frac{1}{C_h} \frac{\partial C_h}{\partial r} \quad (\text{A-8})$$

To eliminate the potential gradient and coion concentration from the diffusing ion flux expression, substitute eq. A-8 into Eqs. A-2 and A-3, to get

$$J_x = -D_x \left[\frac{\partial C_x}{\partial r} - \frac{C_x}{C_h} \frac{\partial C_h}{\partial r} \right] \quad (\text{A-9})$$

$$J_o = -D_o \left[\frac{\partial C_o}{\partial r} - \frac{C_o}{C_h} \frac{\partial C_h}{\partial r} \right] \quad (\text{A-10})$$

Taking the derivative of Equation A-7 with respect of ' r ' yields Equation A-11

$$\frac{\partial C_o}{\partial r} + \frac{\partial C_x}{\partial r} = \frac{\partial C_h}{\partial r} \quad (\text{A-11})$$

Combining Equations A-7, A-9, A-10 and A-11, the flux equations in terms of diffusing ion concentrations and concentration gradients are expressed as follows:

$$J_x = -D_x \left\{ \frac{\partial C_x}{\partial r} + \frac{C_x}{C_o + C_x} \left(\frac{\partial C_x}{\partial r} + \frac{\partial C_o}{\partial r} \right) \right\} \quad (\text{A-12})$$

$$J_o = -D_o \left\{ \frac{\partial C_o}{\partial r} + \frac{C_o}{C_o + C_x} \left(\frac{\partial C_x}{\partial r} + \frac{\partial C_o}{\partial r} \right) \right\} \quad (\text{A-13})$$

These expressions are not convenient for practical use. In order to obtain the flux expression for each ion species in terms of diffusing ion concentrations and its concentration gradient only, the terms $\frac{\partial C_o}{\partial r}$ and $\frac{\partial C_x}{\partial r}$ need to be eliminated from Equations A-13 and A-14, respectively.

According to the assumption of no net current flow, Equations A-13 and A-14 can be combined to yield the following expression

$$D_x \left[\frac{\partial C_x}{\partial r} + \frac{C_x}{C_o + C_x} \left(\frac{\partial C_x}{\partial r} + \frac{\partial C_o}{\partial r} \right) \right] + D_o \left[\frac{\partial C_o}{\partial r} + \frac{C_o}{C_o + C_x} \left(\frac{\partial C_x}{\partial r} + \frac{\partial C_o}{\partial r} \right) \right] = 0 \quad (\text{A-14})$$

Making use of pseudo steady state assumption, the partial derivatives in Equation A-15 can be replaced by ordinary derivatives. After collecting terms and multiplying through by $(C_x + C_o)$, the Equation A-14 may be rewritten in this way,

$$(2D_o C_o + D_o C_x + D_x C_x) \frac{dC_o}{dr} + (2D_x C_x + D_o C_o + D_x C_o) \frac{dC_x}{dr} = 0 \quad (\text{A-15})$$

Thus,

$$\frac{dC_o}{dr} = -\frac{dC_x}{dr} \left[\frac{2D_x C_x + D_o C_o + D_x C_o}{2D_o C_o + D_o C_x + D_x C_x} \right] \quad (\text{A-16})$$

and

$$\frac{dC_o}{dC_x} = - \left[\frac{2D_x C_x + D_o C_o + D_x C_o}{2D_o C_o + D_o C_x + D_x C_x} \right] \quad (\text{A-17})$$

Equation A-18 reflects the relationship of hydroxide and borate concentration gradients and allows the expression of the hydroxide concentration gradient in terms of the borate concentration gradient, the diffusivities and concentrations of diffusing ions in the flux expression. The relation of borate and hydroxide concentrations can be obtained by integrating Equation A-17.

According to the definition of a derivative, Equation A-18 can also be obtained from Equation A-15.

$$\frac{d}{dr} [(D_o C_o + D_x C_x) (C_x + C_o)] = 0 \quad (\text{A-18})$$

This expression can be used conveniently to determine the relationship between the film concentrations and the bulk phase concentrations since the term enclosed in the parenthesis is a constant.

Therefore, integrating equation A-18 from bulk to the film gives:

$$[D_o C_o + D_x C_x] [C_o + C_x] = [D_o C_o^o + D_x C_x^o] [C_o^o + C_x^o] = \text{RHS} \quad (\text{A-19})$$

where the superscript ' o ' devotes the bulk phase. The quantity on the right hand side will be abbreviated as RHS for convenience. Rewriting equation A-19 in a quadratic form and

solving to obtain the expression of hydroxide concentration in terms of the borate concentration yields,

$$D_o C_o^2 + (D_o C_x + D_x C_x) C_o + (D_x C_x^2 - \text{RHS}) = 0 \quad (\text{A-20})$$

$$C_o = \frac{-C_x(D_o + D_x) + [C_x^2(D_o + D_x)^2 - 4D_o(D_x C_x^2 - \text{RHS})]^{1/2}}{2D_o} \quad (\text{A-21})$$

The positive square root is used since the concentration of a species can never be less than zero.

Now we are ready to obtain the expression for borate flux. Substituting Eq. A-16 and Eq. A-19 into Eq. A-12 and rearranging yields,

$$J_x = -\frac{dC_x}{dr} \left\{ D_x + \frac{D_x C_x (D_o - D_x)}{[C_x^2 (D_o - D_x)^2 + 4D_o \text{RHS}]^{1/2}} \right\} \quad (\text{A-22})$$

Applying the assumption of pseudo steady state results in:

$$\frac{dJ_x}{dr} = 0 \quad (\text{A-23})$$

or

$$J_x = \text{constant} \quad (\text{A-24})$$

Thus the flux expression, Eq. A-23, can be separated and integrated with the boundary conditions:

$$C_x = C_x^o \quad \text{at } r = r_o + \delta \quad (\text{A-25})$$

and

$$C_x = C_x^* \quad \text{at } r = r_o \quad (\text{A-26})$$

The final flux expression for borate is given as:

$$J_x = -\frac{2D_o D_x}{\delta(D_o - D_x)} [C_o^\circ + C_x^\circ - C_o^* - C_x^*] \quad (\text{A-27})$$

Equation A-27 is the expected result similar to that derived by Haub (1984) and Zecchini (1990).

For the undissociated boric acid, the boundary conditions are:

$$C_a = C_a^\circ \quad \text{at } r = r_o + \delta \quad (\text{A-28})$$

and

$$C_a = C_a^* \quad \text{at } r = r_o \quad (\text{A-29})$$

Integrating Equation A-4 with these boundary conditions above gives

$$J_a = -\frac{D_a}{\delta} (C_a^\circ - C_a^*) \quad (\text{A-30})$$

The boric acid concentrations in Equation A-30 can be expressed in terms of borate and hydrogen concentrations since their relation is constrained by the dissociation equilibrium relation. This is:

$$C_a = \frac{C_x C_h}{K_a} \quad (\text{A-31})$$

It is necessary to replace hydrogen concentration by diffusing ion concentrations - boric acid and hydroxide as demonstrated in Equation A-7.

So

$$C_a = \frac{C_x(C_x + C_o)}{K_a} \quad (\text{A-32})$$

Substituting this relation into Equation A-30 yields the undissociated acid species flux expression in terms of diffusing ion concentrations:

$$J_a = -\frac{D_a}{\delta K_a} [C_x^o(C_x^o + C_o^o) - C_x^*(C_x^* + C_o^*)] \quad (\text{A-33})$$

Combining Eq. A-33 with Eq. A-27, we can obtain the total boron flux expression in terms of diffusing ion concentrations.

$$J = J_a + J_x = -\frac{D_a}{\delta K_a} [C_x^o(C_x^o + C_o^o) - C_x^*(C_x^* + C_o^*)] \\ - \frac{2D_o D_x}{\delta(D_o - D_x)} [C_o^o + C_x^o - C_o^* - C_x^*] \quad (\text{A-34})$$

APPENDIX B

THE DERIVATION OF THE DIMENSIONLESS FORM RADIAL FLOW COLUMN MATERIAL BALANCE

For diffusion in a cylindrical, packed-bed column with radial flow, a general diffusion model is obtained by making a material balance in cylindrical coordinates:

$$\frac{\partial C}{\partial t} \pm \left(\frac{u_r}{\epsilon} \frac{\partial C}{\partial r} + \frac{u_\theta}{r\epsilon} \frac{\partial C}{\partial \theta} + \frac{u_z}{\epsilon} \frac{\partial C}{\partial z} \right) = \frac{1}{r} \frac{\partial}{\partial r} \left(D r \frac{\partial C}{\partial r} \right) + \frac{D}{r^2 \epsilon} \frac{\partial^2 C}{\partial \theta^2} + \frac{D}{\epsilon} \frac{\partial^2 C}{\partial z^2} + R \quad (\text{B-1})$$

where the signs before the second term of left side indicate the radial flow direction, '+' is outward flow and '-' is inward flow. 'R' is the ion exchange rate expressed as:

$$R = - \frac{\partial q}{\partial t} \quad (\text{B-2})$$

The assumptions of uniform and symmetrical fluid flow in the θ direction, negligible end effects in the 'z' direction, uniform concentration distribution in the 'z' direction and negligible dispersion in vertical direction lead to the simplifying form of Equation (B-1).

$$\frac{\partial C}{\partial t} + \frac{\partial q}{\partial t} \pm \frac{u_r}{\epsilon} \frac{\partial C}{\partial r} - \frac{1}{r} \frac{\partial}{\partial r} \left(D r \frac{\partial C}{\partial r} \right) = 0 \quad (\text{B-3})$$

The 'R' in Equation (B-1) is replaced by the expression in Equation (B-2).

The rate expression is given by the assumption of the linear driving force in the static film model.

$$\frac{\partial q}{\partial t} = k' a_s (C^o - C^*) \quad (\text{B-4})$$

Equations B-3 and B-4 are coupled partial differential equations and need to be solved simultaneously. The initial and boundary conditions for the two equations are

$$C(t = 0, r) = 0 \quad (\text{B-5})$$

$$q(t = 0, r) = 0 \quad (\text{for primary cycle}) \quad (\text{B-6})$$

$$C(r = R_1, t > 0) = C^f \quad (\text{B-7})$$

$$\left. \frac{\partial C}{\partial r} \right|_{r=R_0} = 0 \quad (\text{B-8})$$

Equations B-3 to B-8 can be reduced to dimensionless form by introducing the following variables:

Dimensionless mobile phase concentration

$$X = \frac{C}{C^f} \quad (\text{B-9})$$

Dimensionless resin phase concentration

$$Y = \frac{q}{Q} \quad (\text{B-10})$$

Dimensionless time coordinate

$$\tau = \frac{tF}{V\varepsilon} \quad (\text{B-11})$$

Dimensionless distance coordinate

$$\xi = \frac{r^2 - R_0^2}{R_1^2 - R_0^2} \quad (\text{B-12})$$

Capacity ratio

$$\eta = \frac{\varepsilon}{1-\varepsilon} \quad (\text{B-13})$$

Dimensionless mass transfer coefficient

$$K_t = \frac{kV\varepsilon}{Fd_p} \quad (\text{B-14})$$

Concentration capacity ratio between resin and bulk phases

$$K = \frac{Q}{C^f} \quad (\text{B-15})$$

Peclet number

$$P_e = \frac{u_r(R_1 - R_0)}{\varepsilon D} \quad (\text{B-16})$$

and relative position

$$P_r = \frac{r}{R_1 - R_0} \quad (\text{B-17})$$

Derived Equations B-11 and B-12, the following expressions can be obtained:

$$\partial \alpha = \frac{V\varepsilon}{F} \partial \tau \quad (\text{B-18})$$

$$\partial \xi = \frac{2r}{R_1^2 - R_0^2} \partial r \quad (\text{B-19})$$

and the second derivative of ' ξ ' respected to ' r ' is,

$$\partial \xi^2 = \frac{2}{R_1^2 - R_0^2} \partial r^2 \quad (\text{B-20})$$

With these relationships in Equations B-9 to B-19, each term in Equation B-3 can be expressed as follows:

$$\frac{\partial C}{\partial t} = \frac{FC^f}{V\varepsilon} \frac{\partial X}{\partial \tau} \quad (\text{B-21})$$

$$\frac{1-\varepsilon}{\varepsilon} \frac{\partial q}{\partial t} = \frac{1}{\eta} \frac{FQ}{V\varepsilon} \frac{\partial Y}{\partial \tau} \quad (\text{B-22})$$

$$\frac{u_r}{\varepsilon} \frac{\partial C}{\partial r} = \frac{u_r}{\varepsilon} \frac{2rC^f}{R_1^2 - R_0^2} \frac{\partial X}{\partial \xi} \quad (\text{B-23})$$

$$\frac{1}{r} \frac{\partial}{\partial r} \left(Dr \frac{\partial C}{\partial r} \right) = \frac{2C^f}{R_1^2 - R_0^2} \left[\frac{r^2}{R_1^2 - R_0^2} \frac{\partial D}{\partial \xi} \frac{\partial X}{\partial \xi} + D \frac{\partial X}{\partial \xi} + D \frac{\partial^2 X}{\partial \xi^2} \right] \quad (\text{B-24})$$

Assuming that the dispersion coefficient 'D' is determined by Equation 2-16 and, the Peclet number is approximate constant, substituting Equations B-20 to B-23 and dimensionless relations into Equation B-3, yields,

$$\frac{\partial X}{\partial \tau} + \frac{K}{\eta} \frac{\partial Y}{\partial \tau} \pm \frac{\partial X}{\partial \xi} - \frac{1}{P_e P_r} \frac{\partial X}{\partial \xi} - \frac{1}{P_e P_r} \frac{\partial^2 X}{\partial \xi^2} = 0 \quad (\text{B-25})$$

and the equation B-4 becomes:

$$\frac{\partial Y}{\partial \tau} = \mathfrak{S} R_i (X^\circ - X^*) \quad (\text{B-26})$$

where

$$\mathfrak{S} = K_i d_p a_s \quad (\text{B-27})$$

$$R_i = \frac{k'}{k} = \left(\frac{D_e}{D_i} \right)^{2/3} \quad (\text{B-28})$$

Equations B-24 and B-25 are the final dimensionless forms of Equations B-3 and B-4. These expressions are more conveniently solved by some numerical methods.

APPENDIX C

DERIVATION OF DISCRETIZATION EQUATIONS FROM RADIAL FLOW DIFFERENTIAL EQUATIONS

In the model of mixed bed ion exchange with radial flow, the coupled differential equations [Equations C-1 and C-2] needs to be solved simultaneously.

$$\frac{\partial X}{\partial \tau} + \frac{K}{\eta} \frac{\partial Y}{\partial \tau} \pm \frac{\partial X}{\partial \xi} - \frac{1}{Pe Pr} \frac{\partial X}{\partial \xi} - \frac{1}{Pe Pr} \frac{\partial^2 X}{\partial \xi^2} = 0 \quad (C-1)$$

$$\frac{\partial Y}{\partial \tau} = \theta R_i (X^0 - X^*) \quad (C-2)$$

Substituting Equation C-2 into Equation C-1 and rearranging yields,

$$\frac{\partial X}{\partial \tau} = \pm \frac{\partial X}{\partial \xi} + \frac{1}{Pe Pr} \frac{\partial X}{\partial \xi} + \frac{1}{Pe Pr} \frac{\partial^2 X}{\partial \xi^2} - \beta (X^0 - X^*) \quad (C-3)$$

where

$$\beta = \frac{K \theta R_i}{\eta} \quad (C-4)$$

There are a number of ways in which differential equations such as Eq. C-3 can be converted into its discrete counterpart, namely algebraic equations containing X_{i-1} , X_i , X_{i+1} , etc. as unknowns. Here, the control-volume method proposed by Patankar (1991) is applied for this purpose.

Since Equation C-3 contains derivatives, the discretization equation is obtained by replacing the derivatives by the finite difference approximation.

$$\left. \frac{\partial X}{\partial \tau} \right|_i = \frac{X_i - X_i^0}{\Delta \tau} \quad (\text{C-5})$$

$$\left. \frac{\partial X}{\partial \xi} \right|_i = \frac{X_{i-1} - X_i}{\Delta \xi} \quad (\text{C-6})$$

$$\left. \frac{\partial^2 X}{\partial \xi^2} \right|_i = \frac{1}{\Delta \xi} \left[\left(\frac{\partial X}{\partial \xi} \right)_{i-1/2} - \left(\frac{\partial X}{\partial \xi} \right)_{i+1/2} \right] \quad (\text{C-7})$$

and

$$\left. \frac{\partial X}{\partial \xi} \right|_{i-1/2} = \frac{X_{i-1} - X_i}{1/2 \Delta \xi} = \frac{2(X_{i-1} - X_i)}{\Delta \xi} \quad (\text{C-8})$$

the same procedure as used at the point ' i-1/2 ' for the finite difference expression at the point ' i+1/2 ',

$$\left. \frac{\partial X}{\partial \xi} \right|_{i+1/2} = \frac{2(X_i - X_{i+1})}{\Delta \xi} \quad (\text{C-9})$$

where the superscript ' 0 ' indicates the last time.

Substituting these expressions for half position into Equation C-7, the following finite difference expression for the second derivative term is obtained.

$$\left. \frac{\partial^2 X}{\partial \xi^2} \right|_i = \frac{2}{(\Delta \xi)^2} (X_{i-1} + X_{i+1} - 2X_i) \quad (\text{C-10})$$

Here, we take the inward flow as an example for the derivation of the discretization equation. Now, substituting Equations C-5, C-6 and C-10 into Equation C-3 to obtain the discretization equation as,

$$A_i X_i = A_{i-1} X_{i-1} + A_{i+1} X_{i+1} + b_i \quad (\text{C-11})$$

where

$$A_{i-1} = \left(1 + \frac{1}{P_e P_r}\right) + \frac{2}{(\Delta \xi)^2 P_e P_r} \quad (\text{C-12})$$

$$A_{i+1} = \frac{2}{(\Delta \xi)^2 P_e P_r} \quad (\text{C-13})$$

$$A_i^0 = \frac{\Delta \xi}{\Delta \tau} \quad (\text{C-14})$$

$$b_i = -S_i X_i^* + A_i^0 X_i^0 \quad (\text{C-15})$$

$$S_i = -\Delta \xi \cdot \beta \quad (\text{C-16})$$

$$A_i = A_{i-1} + A_{i+1} + A_i^0 - S_i \quad (\text{C-17})$$

If the domain is divided by n equal parts, there are $n+1$ grid points and n unknowns. Then $n-1$ equations can be derived by the same technique as above for $n-1$ internal grid points. The additional equation will be obtained by applying boundary conditions.

For boundary points:

at $\xi = 1$

$$X(\xi = 1) = 1 \quad (\text{C-18})$$

$$A_{i-1} = 0 \quad (\text{C-19})$$

$$A_{i+1} = 0 \quad (\text{C-20})$$

$$b_i = 1 \quad (C-21)$$

$$A_i = 1 \quad (C-22)$$

at $\xi=0$, here indicated by the subscript ' B '.

$$\left. \frac{\partial X}{\partial \xi} \right|_{\xi=0} = 0 \quad (C-23)$$

then

$$\left. \frac{\partial X}{\partial \tau} \right|_B = \frac{X_B - X_B^0}{\Delta \tau} \quad (C-24)$$

$$\left. \frac{\partial X}{\partial \xi} \right|_B = 0 \quad (C-25)$$

$$\begin{aligned} \left. \frac{\partial^2 X}{\partial \xi^2} \right|_B &= \frac{1}{\Delta \xi} \left[\left(\frac{\partial X}{\partial \xi} \right)_{B-1} - \left(\frac{\partial X}{\partial \xi} \right)_{B+1} \right] \\ &= \frac{1}{\Delta \xi} \left(\frac{X_{B-1} - X_B}{1/2 \Delta \xi} \right) = \frac{2}{(\Delta \xi)^2} (X_{B-1} - X_B) \end{aligned} \quad (C-26)$$

where the point ' B+1 ' is the neighbor point of the effluent boundary point and is out of the domain of interest and

$$\left. \frac{\partial X}{\partial \xi} \right|_{B+1} = \left. \frac{\partial X}{\partial \xi} \right|_B = 0 \quad (C-27)$$

Substituting Equations C-24 to C-26 into equation C-3, then arranging as the same form as Equation C-11, yields,

$$\mathbf{A}_B \mathbf{X}_B = \mathbf{A}_{B-1} \mathbf{X}_{B-1} + \mathbf{A}_{B+1} \mathbf{X}_{B+1} + \mathbf{b}_B \quad (\text{C-28})$$

where

$$\mathbf{A}_{B-1} = \frac{2}{(\Delta\xi)^2 \mathbf{P}_e \mathbf{P}_r} \quad (\text{C-29})$$

$$\mathbf{A}_{B+1} = 0 \quad (\text{C-30})$$

$$\mathbf{A}_B^0 = \frac{\Delta\xi}{\Delta\tau} \quad (\text{C-31})$$

$$\mathbf{b}_B = -\mathbf{S}_B \mathbf{X}_B^* + \mathbf{A}_B^0 \mathbf{X}_B^0 \quad (\text{C-32})$$

$$\mathbf{S}_B = -\Delta\xi \cdot \beta \quad (\text{C-33})$$

$$\mathbf{A}_B = \mathbf{A}_{B-1} + \mathbf{A}_{B+1} + \mathbf{A}_B^0 - \mathbf{S}_B \quad (\text{C-34})$$

Equation C-11 is a general form for each internal grid point. For n-1 internal grid point we may write n-1 equations based on this general form. These equations plus Equation C-28 can be arranged as a tridiagonal matrix with dominant diagonal terms. This is the most important characteristic to guarantee converge and stable.

APPENDIX D

COMPUTER CODE FOR BORON SORPTION

\$debug

```

C      THIS PROGRAM IS TO USE FOR ION EXCHANGE IN ANION BED.
      IMPLICIT REAL*8 (A-H, O-Z)
      REAL*8 KLA, YCA(4,2000), XCA(4,2000), RATC(4,2000)
      REAL*8 XCB(4,2000), RATB(4,2000), YCT(4,2000), YCB(4,2000)
      CHARACTER FILE1*20

C      ***** FUNCTION STATEMENTS *****

C      CARBERRY'S CORRELATION
      F1(R,S) = 1.15*VS/(VD*(S**(2./3.))*(R**.5))
C      KATAOKA'S CORRELATION
      F2(R,S) = 1.85*VS*((VD/(1.-VD))**(1./3.))/
# (VD*(S**(2./3.))*(R**(2./3.)))

C      **** OPEN FILES ****

      WRITE(*,*) ' ENTER THE OUTPUT FILE NAME'
      READ(*,2000)FILE1
2000  FORMAT(A20)
      OPEN (5, FILE=FILE1,ACCESS='APPEND',STATUS='UNKNOWN')

C      ***** INITIALIZATIONS *****

      DATA KPBK, KPPR,TIME1,TIME /0, 1, 115.,500/
      DATA YCO,TKCO/0.0010, 0.18/
      DATA PDA, VD/0.06D0, 0.35D0/
      DATA CF, FR, DIA, CHT/6.845D-3, 2.0D0, 2.4D0, 50.0D0/
      DATA QA/ 0.96D0/
      DATA DH,DN,DO,DC/9.35D-5, 1.38D-5, 5.324D-5, 0.9350D-5/
      DATA XI,DB/0.010D0, 0.486D-5/
      DATA CP, DEN/0.9068D0, 1.0D0/
      DATA DISS,FCR/5.80D-10,1.0/

C      ***** PRINT SYSTEM PARAMETERS *****

      WRITE(*,*) ' ENTER TAU VALUE'
      READ(*,*)TAU
      WRITE (5,10)
      WRITE (5,11)
      WRITE (5,12) YCO
      WRITE (5,13) PDA
      WRITE (5,81) VD
      WRITE (5,14) QA
      WRITE (5,82) TKCO
      WRITE (5,15) CF, FR
      WRITE (5,83) DIA, CHT
      WRITE (5,16) DH,DB
      WRITE (5,84) DO, DC
      WRITE (5,17) CP, DEN

C      ***** THE DISSOCIATED BORATE ION CONCENTRATION *****

      CCO=(-DISS+(DISS**2.+4.*DISS*CF)**.5)/2.

```

```

CHO=DISS*(CF-CCO)/CCO
PH=-LOG10(CHO)
POH=14.-PH
COII=10.**(-POH)
ChII=10.**(-PH)
CBO=CF-CCO
CF1=CCO
CF2=CBO
CFT1=CCO+COII
CFT2=CBO
CfT=CF
CHGBAL=0.
CF=CFT1+CFT2

```

C ***** CALCULATE NONIONIC MASS TRANSFER COEFFICIENTS *****

```

AREA =3.141592*(DIA**2)/4.
VS = FR/AREA
REA = PDA*100.*VS*DEN/((1.-VD)*CP)
SCA = (CP/100.)/(DEN*DC)
IF (REA.LT.20.) THEN
KLA = F2(REA,SCA)
ELSE
KLA = F1(REA,SCA)
ENDIF

```

C ***** SET MATRIX DIMENSIONS BASED ON TAU AND XI *****

```

CHTD = KLA*(1.-VD)*CHT/(VS*PDA)
NT=CHTD/XI
WRITE(*,*) ' NT=',NT
FLOW2=KLA

```

C ***** PRINT CALCULATED PARAMETERS *****

```

WRITE (5,18)
WRITE (5,19)
WRITE (5,20)
WRITE (5,21) TAU, XI, NT
WRITE (5,22) REA
WRITE (5,88) KLA
WRITE (5,23) VS
WRITE (5,99) DB

```

C ***** PRINT BREAKTHROUGH CURVE HEADINGS *****

```

IF (KPBK.NE.1) GO TO 50
WRITE (5,24)
WRITE (5,25)
WRITE (5,26)
WRITE (5,27)
WRITE (5,28)

```

50 CONTINUE

```

C ***** PRINT CONCENTRATION PROFILE HEADINGS *****

  T = 0.
  TAUPR = KLA*CFT*((TIME*60.)-VD*CHT/VS)/(PDA*QA)
  TAUPR1= KLA*CFT*((TIME1*60.)-VD*CHT/VS)/(PDA*QA)
  IF(KPPR.NE.1) GO TO 60
  WRITE (5,30)
  WRITE (5,31) TIME
  WRITE (5,32)
  WRITE (5,33)
  WRITE (5,34)
60 CONTINUE

C ***** SET INITIAL COLUMN CONDITIONS *****

  MT = NT + 1
  DO 100 M = 1,MT
  YCA(1,M) = YCO
  YCT(1,M) =YCA(1,M)
100 CONTINUE

C ***** CALCULATE DIMENSIONLESS PROGRAM TIME LIMIT BASED ON
C   INLET CONDITIONS (Z=0) *****

  TMAXA =QA*3.142*(DIA/2.)**2.*CHT/(FR*CFt*60.)
  TMAX = TMAXA
  TAUMAX = KLA*CFt*(TMAX*60.)/(PDA*QA)
  WRITE (*,222)
  WRITE (*,223) TMAX
  WRITE (*,224)
222 FORMAT(' PROGRAM RUN TIME IS BASED ON TOTAL RESIN CAPACITY')
223 FORMAT(' AND FLOW CONDITIONS. THE PROGRAM WILL RUN FOR',F9.1)
224 FORMAT(' MINUTES OF COLUMN OPERATION FOR CURRENT CONDITIONS.')
```

```

C ***** INITIALIZE VALUES *****

  J = 1
  JK = 1
  TAUTOT = 0.
  JFLAG = 0
  XCA(JK,NT) = 0.
  KK = 1
  KPRINT = 1
  TAUFLOW = FLOW2*CFT*(TIME1*60.-(VD*CHT)/VS)/(PDA*QA)

C ***** LOOP TO INCREMENT TIME AND CHECK PROGRAM RESTRAINTS *****

1 CONTINUE
  IF(TAUTOT.GT.GAUFLOW) THEN
  TIME2 = TIME - TIME1
  CALL FLOW(NT,CHT,PDA,VD,DEN,DC,CP,XI,CFT,TIME2,QA,TAUC)
  TAUPR=TAUC+TAUPR1
  ENDIF
  IF (TAUTOT.GT.TAUMAX) GO TO 138
```

```

      IF(J.EQ.4) THEN
      JD = 1
      ELSE
      JD = J + 1
      ENDIF

C ***** SET COLUMN INLET CONDITIONS *****

      XCA(J,1) = CF1/CF
      XCB(J,1) = CF2/CF
      COO=COII
      CHO =CHII
      CCT =CFT
      IF(JD.EQ.1) THEN
      WRITE(*,555)
      WRITE(*,556)COO,ChO,C1,Y1,Y2,B1
555  FORMAT(' COO',9X,'CHO',8X,'CCO',9X,'YCA',8X,'YCB',9X,'CBO')
556  FORMAT(",5(2X,E9.3),2X,E10.4)
      ELSE
      GOTO 540
      ENDIF
540  CONTINUE

C ***** LOOP TO INCREMENT DISTANCE *****

      DO 400 K=1,NT

C ***** DEFINE BULK PHASE CONCENTRATIONS FOR SUBROUTINES *****

      CCO = XCA(J,K)*CF
      CBO = XCB(J,K)*CF
      CCT1=CCT
      CO1=COO
      CC1=CCO
      CB1=CBO
      ch1=cho
      YT = YCT(J,K)
      Y1=YCA(J,590)
      Y2=YCB(J,590)
      C1=XCA(J,590)*CF
      B1=XCB(J,590)*CF

C ***** INTEGRATE X *****

      XCL = XCA(J,K)
      XCBL= XCB(J,K)

C ***** CALL ROUTINES TO CALCULATE 'RIA,XCI,RIC, AND XNI' *****

      IF(YT.LT.1.0) THEN
      CALL BULK(TKCO,COO,CCO,YT,DO,DC,RIA,RIB,CCI,CCBI,
1 DE,DISS, CCT,dB)
      XCI=CCI/CF
      XCBI=CCBI/CF

```

```

ELSE
XCI=XCL
XCBI=XCBL
YT = 1.0
ENDIF

```

C ** CHANGE CALCULATED INTERFACE CONCENTRATIONS TO FEED BASIS **

```

RATC(J,K) = 6.*RIA*(XCL - XCI)
RATB(J,K) = 6.*RIB*(XCBL-XCBI)
YCA(JD,K) = YCA(J,K)+TAU*RATC(J,K)
YCB(JD,K) = YCB(J,K)+TAU*RATB(J,K)
YCT(JD,K) = YCT(J,K)+TAU*(RATC(J,K)+RATB(J,K))
YCTT=YCT(JD,K)
IF(YCTT.GT.1.0) THEN
YTT=YCT(J,K)
CALL MB(YTT,DISS,CHO,XCL,XCBL,XI,TAU,XCLN,XCBLN,TRATE)
XCB(J,K+1)=XCBLN
XCA(J,K+1)=XCLN
RATC(J,K)=RATC(J,K)*TRATE/(RATC(J,K)+RATB(J,K))
RATB(J,K)=RATB(J,K)*TRATE/(RATC(J,K)+RATB(J,K))
YCA(JD,K) = YCA(J,K)+TAU*RATC(J,K)
YCB(JD,K) = YCB(J,K)+TAU*RATB(J,K)
YCT(JD,K)=1.0
GOTO 113
ENDIF
IF(K.LE.3) THEN
F1C=XI*6.*RIA*(XCA(J,K)-XCI)
F2C=XI*6.*RIA*((XCA(J,K)+F1C/2.)-XCI)
F3C=XI*6.*RIA*((XCA(J,K)+F2C/2.)-XCI)
F4C=XI*6.*RIA*(XCA(J,K)+F3C-XCI)
F1B=XI*6.*RIB*(XCB(J,K)-XCBI)
F2B=XI*6.*RIB*((XCB(J,K)+F1B/2.)-XCBI)
F3B=XI*6.*RIB*((XCB(J,K)+F2B/2.)-XCBI)
F4B=XI*6.*RIB*(XCB(J,K)+F3B-XCBI)
XCB(J,K+1)=XCB(J,K)-(F1B+2.*F2B+2.*F3B+F4B)/6.
XCA(J,K+1)=XCA(J,K)-(F1C+2.*F2C+2.*F3C+F4C)/6.
ELSE
COEC1=55.*RATC(j,k)-59.*RATC(J,K-1)+37.*RATC(J,K-2)
& -9.*RATC(J,K-3)
COEB1=55.*RATB(j,k)-59.*RATB(J,K-1)+37.*RATB(J,K-2)
& -9.*RATB(J,K-3)
XCA(J,K+1)=XCA(J,K)-(XI/24.)*COEC1
XCB(J,K+1)=XCB(J,K)-(XI/24.)*COEB1
ENDIF
IF(YCT(JD,K).EQ.1) GOTO 140

```

C ***** CHANGE VALUES FOR BULK SUB *****

```

113 CCO = XCA(J,K+1)*CF
CBO = XCB(J,K+1)*CF
CCT=CCT1-(CB1-CBO)-(CC1-CCO)
IF(CCT.GT.CCT1) WRITE(*,*)CCT,CCT1=',CCT,CCT1
CCTT=CCT1-(CC1-CCO)

```


COO=CO1+(CCT1-CCTT)

C ***** NEW VALUE BASED ON DISSOCIATION OF WATER AND BORAN *****

CALL EQB(DISS,CCT,CHO)
 COO=1.D-14/CHO
 CCO=DISS*CCT/(DISS+CHO)
 CBO=CCT-CCO

135 XCA(J,K+1)=CCO/CF
 XCB(J,K+1)=CBO/CF

140 CONTINUE
 OPEN(5, FILE=FILE1,ACCESS='APPEND', STATUS='UNKNOWN')

C ***** PRITE CONCENTRATION PROFILES *****

IF(KPPR.NE.1) GO TO 350
 IF(TAUTOT.LT.TAUPR) GOTO 350
 JFLAG = 1
 ZA = FLOAT(NT)
 ZB = FLOAT(K-1)
 Z = ZB*CHT/ZA
 KOUNT = KOUNT + 1
 IF(KOUNT.NE.(KOUNT/10*10)) GO TO 350
 ppm=(CBO+CCO)/CFT*74.
 WRITE(*,200)

200 FORMAT(' Z',8X,'PPM',8X,'YCT',8X,'RIA')
 WRITE(*,201)Z,PPM,YCT(J,K),RIA

201 FORMAT(1X,E8.3,7(2X,E8.3))
 WRITE (5,35) Z, PPM, YCT(J,K),RIA, YCA(J,K), YCB(J,K)
 CLOSE (5)

350 CONTINUE

400 CONTINUE

C ***** PRINT BREAKTHROUGH CURVES *****

IF(KPBK.NE.1) GO TO 450
 TAUTIM = TAUTOT*PDA*QA/(FLOW2*CFT*60.)
 T = TAUTIM
 WRITE(*,137)

137 FORMAT('TIME(MIN)',12X,'CCT',14X,'PH')
 PPMBN=((CBO+CCO)/CFT)*74.
 PH=14+LOG10(COO)

WRITE(*,139) TAUTIM,PPMBN,PH

139 FORMAT(F9.1,8X,E8.3,10X,E8.3,8X,E13.5)

IF(KPRINT.NE.1) GO TO 450
 KPRINT = 0
 WRITE (5,29) TAUTIM, PPMBN, PH
 CLOSE (5)

450 CONTINUE

KPRINT=KPRINT+1

KK=KK+1

JK = J

IF(J.EQ.4) THEN

J = 1

```

ELSE
J = J + 1
ENDIF
IF(JFLAG.EQ.1) STOP
TAUTOT = TAUTOT + TAU
K=K+1
GO TO 1

```

C ***** PRINT OUT FORMATS *****

```

10 FORMAT('MIXED BEN SYSTEM PARAMETERS:')
11 FORMAT(' ')
12 FORMAT(' RESIN REGENERATION',3X,' YCO =',F5.3)
13 FORMAT(' RESIN PROPERTIES',5X,' PDA=',F6.4)
81 FORMAT(24X,'VD =', F6.4)
14 FORMAT(' RESIN CONSTANTS',6X,' QA =',E10.4)
82 FORMAT(24X,'TKCO=',F6.3)
15 FORMAT(' COLUMN PARAMETERS',4X,' CF =',E10.4,' FR =',E10.4)
83 FORMAT(24X,'DIA =',F6.2,5X,'CHT =',F6.1)
16 FORMAT(' IONIC CONSTANTS',6X,' DH =',E10.4,2X,'DB =',E10.4)
84 FORMAT(24X,'DO =',E10.4,' DC =', E10.4)
17 FORMAT(' FLUID PROPERTIES', 5X,' CP =',F7.5,5X,'DEN=',F6.4)
18 FORMAT(' ')
19 FORMAT(' CALCULATED PARAMETERS')
20 FORMAT(' ')
21 FORMAT(' INTEGRATION INCREMENTS : TAU=',F7.5,5X,'XI =',F7.5,
# 5X,'NT =',I6)
22 FORMAT(' TRANSFER COEFFICIENTS : REA=', E10.4)
88 FORMAT(24X,'KLA =', E10.4)
23 FORMAT(' SUPERFICIAL VELOCITY : VS =',F7.3)
99 FORMAT(' THE RATIO OF MASS TRANSFER COEFF. KM/KX IS: 'F6.3)
24 FORMAT(' ')
25 FORMAT(' BREAKTHROUGH CURVE RESULTS:')
26 FORMAT(' ')
27 FORMAT(' ',5X,'T(MIN)',10X,'CCO',12X,'PH')
28 FORMAT(' ')
29 FORMAT(' ',3(4X,E8.3),5X,F5.2)
30 FORMAT(' ')
31 FORMAT('CONCENTRATION PROFILES AFTER ',F6.0,'MINUTES')
32 FORMAT(' ')
33 FORMAT(' ',7X,'Z',10X,'PPM',10X,'YCT',10X,'RIA',10X,
1 'YCA',10X,'YCB')
34 FORMAT(' ')
35 FORMAT(' ',7(2X,E10.3))
138 STOP
END

```

C ***** SUBROUTINES *****

```

SUBROUTINE BULK(TKCO,COO,CCO,YT,DO,DC,RIA,RIB,CCI,CCBI,
1 DE,DISS,CCT,DB)
C TO CALCULATE 'RI' AND THE INTERFACE CONCENTRATION
C USING THE BULK PHASE NUETRALIZATION MODEL
IMPLICIT REAL*8 (A-H,O-Z)

```

```

A = DO/DC
Y = COO/(CCO)
IF(YT.LT.0.002) THEN
YP = SQRT((Y + 1./A)*(Y + 1.))
DE = 2.*A*(YP - Y - 1.)/(1. - A)
XCI = 0.0
XCBI=0.0
ELSE
S = TKCO*(1.-YT)/YT
XCI = SQRT(((A*Y+1.)*(Y+1.))/((A*S+1.)*(S+1.)))
DE = 2.*A*(S*XCI+XCI-Y-1.)/((1.-A)*(1.-XCI))
XCBI=(XCI**2.)*(1+S)/(1+Y)
END IF
CCI=XCI*(CCO)
CCBI=XCBI*CCT
RIA = (ABS(DE))**(2./3.)
IF(DE.EQ.0) THEN
RIB=0.
ELSE
RIB=(dB/(DC*(ABS(DE))))*RIA
END IF
DE=DE*DC
RETURN
END

```

```

C ***** SUB FOR CALCULATING EQUILIBRIUM BALANCE
C WATER AND ACID DISSOCIATION *****

```

```

SUBROUTINE EQB(DISS,CCT,CHO)
IMPLICIT REAL*8 (A-H,O-Z)
TOL=1.E-6
DALT=1.E-10
B=DISS
C=-(DISS*CCT+1.D-14)
D=-(1.D-14*DISS)
125 U=CHOO**3.+B*CHOO**2.+C*CHOO+D
V=3.*CHOO**2.+2*B*CHOO+C
CHO=CHOO-U/V
U2=(CHO-CHOO)/CHO
IF(ABS(U2).GT.TOL) THEN
CHOO=CHO
GO TO 125
ENDIF
RETURN
END

```

```

C ***** SUB FOR CALCULATING MASS BALANCE *****

```

```

SUBROUTINE MB(YTT,DISS,CHO,XCL,XCBL,XI,TAU,XCLN,XCBLN,TRATE)
IMPLICIT REAL*8 (A-H,O-Z)
LOAD = 1.0 - YTT
XTOTAL = (XCL+XCBL) - LOAD*XI*TAU
XCLN = DISS*XTOTAL/(DISS+CHO)

```

```

XCBLN= XTOTAL - XCLN
TRATE= LOAD/TAU
RETURN
END

```

C ***** SUB FOR CHANGING FLOW CONDITIONS *****

```

SUBROUTINE FLOW(NT,CHT,PDA,VD,DEN,DC,CP,XI,CFT,TIME2,QA,TAUC)
IMPLICIT REAL*8 (A-H,O-Z)
REAL KLA, NZ
VS=0.01
R=100.*PDA*VS*DEN/((1-VD)*CP)
S=(CP/100.)/(DEN*DC)
IF(R.LT.20) THEN
KLA = 1.85*VS*((VD/(1.-VD))**(1./3.))/
# (VD*(S**(2./3.))*(R**(2./3.)))
ELSE
KLA = 1.15*VS/(VD*(S**(2./3.))*(R**.5))
ENDIF
CHTD = KLA*(1-VD)*CHT/(VS*PDA)
NZ = CHTD/XI
TR = NZ/NT
TAUPR2 = KLA*CFT*(TIME2*60.-VD*CHT/VS)/(PDA*QA)
TAUC = TAUPR2/TR
RETURN
END

```

APPENDIX E

COMPUTER CODE FOR RADIAL FLOW

Sdebug

C * THIS PROGRAM IS TO BE USED FOR SOLVING ION EXCHANGE
C * CHROMATOGRAPHY UNDER RADIAL INWARD FLOW CONDITION.

\$INCLUDE:'COMMON2.FOR'

```
CHARACTER*20 FILE1
WRITE(*,*) 'ENTER THE OUTPUT FILE NAME'
READ(*,2000) FILE1
2000 FORMAT(A20)
WRITE(*,*) 'ENTER TIME AND DISTANCE INCREMENT TAU, RI='
READ (*,*) TAU,RI
WRITE(*,*) 'ENTER TIME ==>'
READ (*,*) TIME
WRITE(*,*) 'INPUT KPBK,KPPR AND SIGN VALUE'
READ (*,*) KPBK,KPPR,SIGN
OPEN(5,FILE=FILE1,ACCESS='APPEND',STATUS='UNKNOWN')
```

C ***** INITIAL CONDITIONS AND BED PROPERTIES *****

CALL INPUT

C ***** CALCULATED TOTAL NUMBER OF STEPS IN DISTANCE NT *****

C TIME STEP

```
NT=FLOAT(1./RI)
MT=NT+1
WRITE(*,*)'MT=',MT
VOL= ((3.1415927*(DIA1**2.-DIA2**2.)/4.)*CHT)/10.
TAUPR = (TIME*FR*60.)/(VOL*VD)
```

C ***** SET INITIAL FRACTIONS FOR THE RESIN PHASE *****

```
DO 100 MA=1,MT
YCA(1,MA)=YCO
YNC(1,MA)=YNO
100 CONTINUE
TMAXA=QA*(1.-FCR)*VOL*(1.-VD)/(FR*CFA*60.)
TAUMAX=(TMAXA*60)*FR/(VOL*VD)
WRITE(*,222)
WRITE(*,223) TMAXA
WRITE(*,224)
222 FORMAT(' PROGRAM RUN TIME IS BASED ON TOTAL RESIN CAPACITY')
223 FORMAT(' AND FLOW CONDITIONS. THE PROGRAM WILL RUN FOR',F9.1)
224 FORMAT(' MINUTES OF COLUMN OPERATION FOR CURRENT CONDITIONS.')
CALL MTC
```

C ***** INITIALIZE VALUES *****

```
J=1
JK=1
JD=1
JLA=J-1
KPRINT=1
JFLAG=0
```

```

TAUTOT=0.
CCA(J,MT)=0.
TOL=1.E-6

```

C *****LOOP TO INCREMENT TIME AND CHECK PROGRAM RESTRAINTS *****

```

1   CONTINUE
    IF (TAUTOT.GT.TAUMAX) GO TO 138
    IF(J.EQ.3) THEN
      JJD = 1
    ELSE
      JJD = J+1
    ENDIF
    XNC(J,1) = CFC/CFC
    XHC(J,1) = 1.0D-7/CFC
    XOC(J,1) = 1.0D-7/CFA
    XCA(J,1) = CFA/CFA
    CNC(J,1) = CFC
    CHC(J,1) = 1.0D-7
    COC(J,1) = 1.0D-7
    CCA(J,1) = CFA

```

C ***** INPUT THE INITIAL GUESS VALUES *****

```

    IF(JD.NE.1) GO TO 101
    DO 900 KA=2,MT
      XNC(J,KA)=XNC(J,1)
      XCA(J,KA)=XCA(J,1)
      XHC(J,KA)=XHC(J,1)
      XOC(J,KA)=XOC(J,1)
      CNC(J,KA)=XNC(J,KA)*CFC
      CCA(J,KA)=XCA(J,KA)*CFA
      CHC(J,KA)=XHC(J,KA)*CFC
      COC(J,KA)=XOC(J,KA)*CFA
900  CONTINUE
    IF(JD.EQ.1) GO TO 105
101  DO 102 KF=2,MT
      XNC(J,KF)=XNC(JLA,KF)
      XCA(J,KF)=XCA(JLA,KF)
      XHC(J,KF)=XHC(JLA,KF)
      XOC(J,KF)=XOC(JLA,KF)
      CNC(J,KF)=XNC(J,KF)*CFC
      CCA(J,KF)=XCA(J,KF)*CFA
      CHC(J,KF)=XHC(J,KF)*CFC
      COC(J,KF)=XOC(J,KF)*CFA
102  CONTINUE
105  CONTINUE

```

C ***** CALCULATION OF DISCRETIZATION EQUATION AND WATER DISS *****

```

    NS=1
500  IF(NS.GT.8) GO TO 599

```

C***** CAL.CONCENTRATION OF ANIONIC AND CATIONIC SPECIES *****

```

KNUM=1
CALL SOURCE(J,KNUM)
CALL DISEQ(J,KNUM,JLA)
KNUM=0
CALL SOURCE(J,KNUM)
CALL DISEQ(J,KNUM,JLA)
CALL FRAC(J,JJD)
CALL DISSO(J,NS)

```

C***** CHECK CONVERGENCE *****

```

DO 501 NNN=1,MT
XCAM(NS,NNN)=XCA(J,NNN)
XCAN(NS,NNN)=XNC(J,NNN)
XCIM(NS,NNN)=XCCI(J,NNN)
XNIN(NS,NNN)=XNI(J,NNN)
501 CONTINUE
IF (NS.EQ.1) GOTO 590
NUMQ=0
NCOUNT=FLOAT(MT/10)
DO 550 MCH=1,MT
IF(MCH.EQ.MCH/10*10) THEN
TESTXCA1(MCH)=(XCAM(NS,MCH)-XCAM(NS-1,MCH))/XCAM(NS,MCH)
TESTXCA2(MCH)=(XCAN(NS,MCH)-XCAN(NS-1,MCH))/XCAN(NS,MCH)
TESTXCI1(MCH)=(XCIM(NS,MCH)-XCIM(NS-1,MCH))/XCIM(NS,MCH)
TESTXCI2(MCH)=(XNIN(NS,MCH)-XNIN(NS-1,MCH))/XNIN(NS,MCH)
IF((TESTXCA1(MCH).LT.TOL).AND.(TESTXCA2(MCH).LT.TOL)
& .AND.(TESTXCI1(MCH).LT.TOL).AND.(TESTXCI2(MCH).LT.TOL)) THEN
NUMQ=NUMQ+1
ELSE
GOTO 550
ENDIF
ENDIF
550 CONTINUE
IF(NUMQ.NE.NCOUNT) THEN
GOTO 590
ELSE
GOTO 599
ENDIF
590 NS=NS+1
GOTO 500
599 CONTINUE

```

C***** RENEW THE VALUES OF CONCENTRATIONS AND RATES *****

```

KNUM=1
CALL SOURCE(J,KNUM)
CALL DISEQ(J,KNUM,JLA)
KNUM=0
CALL SOURCE(J,KNUM)
CALL DISEQ(J,KNUM,JLA)
CALL FRAC(J,JJD)
CALL DISSO(J,NS)

```



```

ELSE
J = J+1
JLA=J-1
ENDIF
JD=JD+1
IF(JFLAG.EQ.1) STOP
TAUTOT=TAUTOT+TAU
GO TO 1

```

C ***** PRINT OUT FORMAT *****

```

29  FORMAT(' ',6(2X,E12.5)//)
138 STOP
    END

```

C ***** SUBROUTINES *****

```

    SUBROUTINE DISEQ(J,KNUM,JLA)
C    TO CALCULATE THE DISCRETIZATION EQUATION BY FULLY IMPLICIT
C    METHOD.
$INCLUDE: 'COMMON2.FOR'
    CALL COEFF(J,KNUM,JLA)

```

C *** CALL MATRIX SUB TO OBTAIN SIMULTANEOUS SOLUTIONS OF
C CONCENTRATION AT EACH CONTROL POINT BY SOLVING MATRIX *****

```

    CALL MATRIX

```

C ***** SET THE VALUES OF CONCENTRATIONS *****

```

    IF(KNUM.EQ.1)THEN
    DO 701 IC3=1,MT
    IF (COAA(IC3).NE.1.0) THEN
    RIA(IC3)=CORI(IC3)
    XCA(J,IC3)=XCOMPC(IC3)
    CCA(J,IC3)=XCA(J,IC3)*CFA
    CCI(J,IC3)=CII(IC3)
    XCCI(J,IC3)=CCI(J,IC3)/CFA
    ELSE
    XCA(J,IC3) = XCOMPC(IC3)
    CCA(J,IC3) = XCA(J,IC3)*CFA
    CCI(J,IC3) = CCA(J,IC3)
    XCCI(J,IC3)= CCI(J,IC3)/CFA
    ENDIF
701 CONTINUE
    ELSE
    DO 702 IC4=1,MT
    IF (COAA(IC4).NE.1.0) THEN
    RIC(IC4)=CORI(IC4)
    XNC(J,IC4)=XCOMPC(IC4)
    CNC(J,IC4)=XNC(J,IC4)*CFC
    CNI(J,IC4)=CII(IC4)
    XNI(J,IC4)=CNI(J,IC4)/CFC
    ELSE

```

```

XNC(J,IC4) = XCOMPC(IC4)
CNC(J,IC4) = XNC(J,IC4)*CFC
CNI(J,IC4) = CNC(J,IC4)
XNI(J,IC4) = CNI(J,IC4)/CFC
ENDIF
702  CONTINUE
    ENDF
    RETURN
    END

C  ***** SOLVING DISCRETIZATION EQUATION BY MATRIX *****

    SUBROUTINE MATRIX
$INCLUDE: 'COMMON2.FOR'
    PX(1)=AECOEF(1)/APCOEF(1)
    QX(1)=BCOEF(1)/APCOEF(1)
    DO 800 IMA=2, MT
    COEF=APCOEF(IMA)-AWCOEF(IMA)*PX(IMA-1)
    PX(IMA)=AECOEF(IMA)/COEF
    QX(IMA)=(BCOEF(IMA)+AWCOEF(IMA)*QX(IMA-1))/COEF
800  CONTINUE
    XCOMPC(MT)=QX(MT)
    DO 801 JAMA=NT,1,-1
    XCOMPC(JAMA)=PX(JAMA)*XCOMPC(JAMA+1)+QX(JAMA)
801  CONTINUE
    RETURN
    END

C  ***** CALCULATION OF RI AND THE INTERFACE CONCENTRATION *****

    SUBROUTINE BULK
$INCLUDE: 'COMMON2.FOR'
    A=CODO/CODC
    Y=ABS(COCOO/COCCO)
    IF(YT.LT.0.0001) THEN
    YP=((Y+1./A)*(Y+1.))**0.5
    DE=2.*A*(YP-Y-1.)/(1./A)
    XCI=0.0
    ELSE
    S=COTK*(1.-YT)/YT
    XCI=SQRT(((A*Y+1.)*(Y+1.))/((A*S+1.)*(S+1.)))
    IF(XCI.EQ.1.) XCI=0.9995
    DE=2.*A*(S*XCI+XCI-Y-1.)/((1.-A)*(1.-XCI))
    END IF
    COCII=XCI*COCCO
    CODE=(ABS(DE))*CODC
    DRIA=(ABS(DE))**(2./3.)
    RETURN
    END

C  ***** THE SUBROUTINE 'SOURCE' IS USED TO CALCULATE INTERFACE
C  CONCENTRATIONS FROM INITIAL GUESS FOR DISEQ SUB *****

    SUBROUTINE SOURCE(J,KNUM)

```

\$INCLUDE: 'COMMON2.FOR'

C ***** ITERATION OF RESIN SURFACE CONCENTRATIONS AND BULK
 C CONCENTRATIONS BASID ON ION EXCHANGE MODEL AND COLUMN
 C MATERIAL BALANCE *****

```

IF(KNUM.EQ.1) THEN
DO 601 IC1=1,MT
YT=YCA(J,IC1)
COCF=CFA
COCOO=XOC(J,IC1)*CFA
COCCO=XCA(J,IC1)*CFA
COKL(IC1)=DKLA(IC1)
COTK = TKCO
COSR = SR1
COPD = PDA
CODC = DC
CODO = DO
COQ = QA
COFCR= FCA
IF(YT.LT.1.0) THEN
CALL BULK
CII(IC1)=COCII
CORI(IC1)=DRIA
DDE(IC1)=CODE
ELSE
YT=1.0
CORI(IC1)=1.0
CII(IC1)=CCA(J,IC1)
AAA(IC1)=1.0
ENDIF
601 CONTINUE
ELSE
DO 602 IC2 =1, MT
YT=YNC(J,IC2)
COCF=CFC
COCOO=XHC(J,IC2)*CFC
COCCO=XNC(J,IC2)*CFC
COKL(IC2)=DKLN(IC2)
COTK = TKNH
COSR = SR2
COPD = PDC
CODC = DN
CODO = DH
COQ = QC
COFCR= FCR
IF(YT.LT.1.0) THEN
CALL BULK
CII(IC2)=COCII
CORI(IC2)=DRIA
DDE(IC2)=CODE
ELSE
YT=1.0
CORI(IC2)=1.0

```

```

        CII(IC2)=CNC(J,IC2)
        AAC(IC2)=1.0
        ENDIF
602    CONTINUE
        ENDIF
        DO 230 KEE=1,MT
        IF(KNUM.EQ.1) THEN
        COAA(KEE)= AAA(KEE)
        ELSE
        COAA(KEE)= AAC(KEE)
        ENDIF
230    CONTINUE
        RETURN
        END

C *****
C     SUBROUTINE COEFF. CALCULATES COEFF. AND
C     BOUNDARY CONDITIONS FOR DISEQ.
C *****

        SUBROUTINE COEFF(J,KNUM,JLA)
$INCLUDE: 'COMMON2.FOR'

C ***** CALCULATION OF COEFFICIENTS *****

        PECLET =(DIA1-DIA2)/COPD
        QVT = VOL*COQ*(1-VD)/(FR*60.*COCF)
        DO 3 IG=2,MT
        COKL(IG)=(1./COKL(IG-1)+1./COKL(IG))**(-1.)
        CORI(IG)=(1./CORI(IG-1)+1./CORI(IG))**(-1.)
        BB(IG) = QVT*COKL(IG)*CORI(IG)*COSR*COFCR
        PR(IG) = (RP(IG-1)+RP(IG))/(DIA1-DIA2)
3        CONTINUE
        IF(JLA.EQ.0) GO TO 8
        DO 301 IQE=2,MT
        IF (KNUM.EQ.1) THEN
        CLAST(IQE)=XCA(JLA,IQE)
        ELSE
        CLAST(IQE)=XNC(JLA,IQE)
        ENDIF
301    CONTINUE
        GO TO 9
8        DO 5 IIT=2,MT
        CLAST(IIT)=0.
5        CONTINUE
9        CONTINUE
        DO 10 ITE=2,MT-1
        IF(COAA(ITE).EQ.1.0) THEN
        AECOEF(ITE) =2./PECLET/(RI*PR(ITE))
        AWCOEF(ITE)=(1.+1./(PR(ITE)*PECLET))+AECOEF(ITE)
        SPCOEF(ITE)=0.
        APO(ITE)=RI/TAU
        APCOEF(ITE)=AECOEF(ITE)+AWCOEF(ITE)+APO(ITE)
        BCOEF(ITE)=APO(ITE)*CLAST(ITE)

```

```

ELSE
  AECOEF(ITE)= 2./PECLET/RI/PR(ITE)
  AWCOEF(ITE)=AECOEF(ITE)+(SIGN*1.+1./(PECLET*PR(ITE)))
  APO(ITE) = RI/TAU
  SPCOEF(ITE) = -(RI*BB(ITE))
  APCOEF(ITE) = AWCOEF(ITE)+AECOEF(ITE)+APO(ITE)-SPCOEF(ITE)
  BCOEF(ITE) =RI*BB(ITE)*(CII(ITE)/COCF)+APO(ITE)*CLAST(ITE)
ENDIF
10  CONTINUE

C***** BOUNDARY CONDITIONS *****

C    CONSIDER I=1 BOUNDARY
  APCOEF(1)=1.0
  AECOEF(1)=0.0
  AWCOEF(1)=0.0
  BCOEF(1) =1.0
C    CONSIDER I=MT BOUNDARY
  AECOEF(MT)=0.0
  AWCOEF(MT)=2./(RI*PECLET*PR(MT))+(1.+1./(peclet*pr(mt)))
  APO(MT) = RI/TAU
  SPCOEF(MT)=- (RI*BB(MT))
  APCOEF(MT)=AECOEF(MT)+AWCOEF(MT)+APO(MT)-SPCOEF(MT)
  BCOEF(MT)=- (SPCOEF(MT))*(CII(MT)/COCF)+APO(MT)*CLAST(MT)
  RETURN
  END

C    ***** SUB FOR CHECKING WATER DISSOCIATION *****

  SUBROUTINE DISSO(J,NS)
$INCLUDE: 'COMMON2.FOR'
  DO 502 LL=2,MT
    BZ2=CNC(J,LL)-CCA(J,LL)
    CHC(J,LL)=(-BZ2+(BZ2**2.+4.0E-14)**0.5)/2.0
    COC(J,LL)=1.0E-14/CHC(J,LL)
    XHC(J,LL)=CHC(J,LL)/CFC
    XOC(J,LL)=COC(J,LL)/CFA
    PH(J,LL)=-DLOG10(CHC(J,LL))
    CHOT(NS,LL)=CHC(J,LL)
502  CONTINUE
  RETURN
  END

C    ***** SUB 'MTC' FOR CALCULATING MASS TRANSFOR COEFFICIENT *****

  SUBROUTINE MTC
$INCLUDE:'COMMON2.FOR'

C    ***** CALCULATION OF IONIC DIFFUDION COEFFICIENTS BASED ON
C    TEMPERATURE USING LIMITING IONIC CONDUCTIVITIES
C    (ROBINSON AND STOKES -- 1959) *****

  RTF = (8.931D-10)*(TMP+273.16)
  XLAMH = 221.7134 + 5.5296*TMP - 0.014445*TMP*TMP

```

```

XLAMN = 23.00498 + 1.06416*TMP + 0.0033196*TMP*TMP
XLAMO = 104.74113 + 3.807544*TMP
XLAMC = 39.6493 + 1.39176*TMP + 0.0033196*TMP*TMP
DN = RTF*XLAMN
DO = RTF*XLAMO
DC = RTF*XLAMC
DH = RTF*XLAMH

```

```

C ***** FUNCTION STATEMENTS FOR DETERMINING NON-IONIC MASS
C TRANSFER COEFFICIENTS BASED ON SYSTEM PARAMETERS *****

```

```

RR=0.
RR1=DIA1/2.
DO 2 M=1,MT
RP(M)=RR1-RR
AREA = 2.*3.1415927*CHT*RP(M)/10.
VS = FR/AREA
REC= PDC*100.*VS*DEN/((1.-VD)*CP)
REA= PDA*100.*VS*DEN/((1.-VD)*CP)
SCN= (CP/100.)/DEN/DN
SCA= (CP/100.)/DEN/DC
IF(REC.LT.20.) THEN
1 DKLN(M) = 1.85*VS*((VD/(1.-VD))**(1./3.))/
(VD*(SCN**(2./3.))*(REC**(2./3.)))
DKLA(M) = 1.85*VS*((VD/(1.-VD))**(1./3.))/
1 (VD*(SCA**(2./3.))*(REA**(2./3.)))
ELSE
DKLN(M) = 1.15*VS/(VD*(SCN**(2./3.))*(REC**0.5))
DKLA(M) = 1.15*VS/(VD*(SCA**(2./3.))*(REA**0.5))
ENDIF
WRITE(5,354)
WRITE(5,355)DKLN(M),DKLA(M)
354 FORMAT(6X,' KLN ',12X,' KLA ')
355 FORMAT(3X,E10.5,6X,E10.5)
RR=RR+RI*((DIA1-DIA2)/2.)
2 CONTINUE
THETA=(3.1415927*CHT*((DIA1**2.-DIA2**2.)/4.)*VD)/FR/60./10.
EITA=VD/(1.-VD)
SR1=6./PDA
SR2=6./PDC
RETURN
END

```

```

C *****
C SUBROUTINE FRAC
C *****

```

```

SUBROUTINE FRAC(J,JJD)
$INCLUDE:'COMMON2.FOR'
DO 500 IS=1,MT
XDIFC=XCA(J,IS)-XCCI(J,IS)
RATEA(IS)=SR1*DKLA(IS)*RIA(IS)*THETA*XDIFC
YCA(JJD,IS)=YCA(J,IS)+TAU*RATEA(IS)
IF(YCA(JJD,IS).GT.1.) THEN

```

```

YCA(JJD,IS)=1.
DLOAD1=YCA(JJD,IS)-YCA(J,IS)
XCADD =DLOAD1/(TAU*SR1*DKLA(IS)*RIA(IS)*THETA)+XCCI(J,IS)
XCA(J,IS+1)=XCA(J,IS+1)+(XCA(J,IS)-XCADD)
IF (XCA(J,IS+1).GT.1.) XCA(J,IS+1)=1.
CCA(J,IS+1)=XCA(J,IS+1)*CFA
ENDIF
500 CONTINUE
DO 501 IFA=1,MT
XDIFN=XNC(J,IFA)-XNI(J,IFA)
RATEC(IFA)=SR2*DKLN(IFA)*RIC(IFA)*THETA*XDIFN
YNC(JJD,IFA)=YNC(J,IFA)+TAU*RATEC(IFA)
IF(YNC(JJD,IFA).GT.1.) THEN
YNC(JJD,IFA)=1.0
DLOAD2 =YNC(JJD,IFA)-YNC(J,IFA)
XNCDD=DLOAD2/(TAU*SR2*DKLN(IFA)*RIC(IFA)*THETA)+XNI(J,IFA)
XNC(J,IFA+1)=XNC(J,IFA+1)+(XNC(J,IFA)-XNCDD)
IF (XCA(J,IS+1).GT.1.) XCA(J,IS+1)=1.
CNC(J,IFA+1)=XNC(J,IFA+1)*CFC
ENDIF
501 CONTINUE
RETURN
END

```

```

C *****
C SUBROUTINE INPUT
C *****

```

```

SUBROUTINE INPUT
$INCLUDE:'COMMON2.FOR'
YNO=1.0000D-3
YCO=1.0000D-3
QC=3.0728
QA=2.4334
PDC=0.076
PDA=0.063
DIA1=105.5*2.
DIA2=82.2*2.
CHT=54.6
FCR=0.442
FCA=0.558
TKCO=1.45
TKNH=1.55
CP=0.9
DEN=1.0
VD=0.45
FR=3.888D3
CF=1.2D-3/35.5
TMP=20.
DISS=1.0D-14
CFA=CF
CFC=CF
CFCT=CFC+1.0D-7
CFAT=CFA+1.0D-7

```

```

WRITE(5,10)
WRITE(5,12) YNO,YCO
WRITE(5,13) PDA,PDC
WRITE(5,14) QC, QA
WRITE(5,15) DIA1,DIA2,CHT
CALL MTC
WRITE(5,16) DN,DH,DC,DO
WRITE(5,17) CP,DEN,TMP
WRITE(5,19)
WRITE(5,21) TAU,RI

C ***** OUTPUT BREAKTHROUGH CURVE HEADINGS *****

      IF(KPBK.NE.1)GOTO 50
      WRITE(5,25)
      WRITE(5,27)
50     CONTINUE

C ***** OUTPUT CONCENTRATION PROFILE HEADINGS *****

      IF(KPPR.NE.1) GO TO 60
      WRITE(5,31) TIME
      WRITE(5,33)
      WRITE(5,43)
60     CONTINUE

10     FORMAT(' MIXED BED SYSTEM PARAMETERS://)
12     FORMAT(' RESIN REGENERATION',3X,' YNO=',E10.4,' YCO=',E10.4)
13     FORMAT(' RESIN PROPERTIES',5X,' PDA=',F8.4,' PDC=',F8.4)
14     FORMAT(' RESIN CONSTANTS',6X,' QC=',F8.4,' QA=',F8.4)
15     FORMAT(' COLUMN PARAMETERS',4X,' :DIA1=',F8.4,'DIA2=',F8.4/
1     22X,' :CHT=',F8.2)
16     FORMAT(' IONIC CONSTANTS',6X,' DN =',E10.4,' DH =',E10.4/
1     22X ' :DC=',E10.4,' DO=',E10.4)
17     FORMAT(' FLUID PROPERTIES',5X,' CP=',F8.5,5X,'DEN=',F8.4/
1     22X ' : TMP=',F8.2//)
19     FORMAT(' CALCULATED PARAMETERS://)
21     FORMAT(' INTEGRATION INCREMENTS: TAU=',F8.5,5X,'RI=',F7.5//)
25     FORMAT(' BREAKTHROUGH CURVE RESULTS://)
27     FORMAT(' ',5X,'T(MIN)',10X,'CCA',10X,'CNC',12X,'PH'//)
31     FORMAT('CONCENTRATION PROFILES AFTER',F6.0,'MINUTES//)
33     FORMAT(9X,'R',9X,'CCA',9X,'CNC',9X,'YCA',9X,'YNC',9X,'PH')
43     FORMAT(17X,' PPb',5X,' PPb')
      RETURN
      END

```


VITA

Jidong Lou

Candidate for the Degree of

Master of Science

Thesis: SIMULATIONS OF BORATE ION EXCHANGE AND RADIAL FLOW FOR
REACTOR WATER CLEAN UP SYSTEMS

Major Field: Chemical Engineering

Biographical:

Personal Data: Born in Changzhou, Jiangsu, The People's Republic of China(PRC),
July 2, 1955, the son of Chenyi Lou and Shangzhi Po.

Education: Graduated from BeiMa High School, Lishui, Jiangsu, PRC, in January,
1973; received Bachelor of Engineering Degree in Chemical Engineering
Mechanism from Jiangsu Institute of Chemical Technology at Changzhou in
May, 1982; completed requirements for the Master of Science degree at
Oklahoma State University in May, 1993.

Professional Experience: Employed as a teaching assistant, lecturer with Jiangsu
Institute of Chemical Technology, PRC, 1982-1991; employed as a part time
engineer for Yong-Hong Industrial Company, PRC, 1983-1984; employed as
a teaching assistant and a reseach assistant, School of Chemical Engineeing,
Oklahoma State University, September, 1991, to May, 1993.